STRUCTURAL STUDIES OF ACTINYL CO-ORDINATION COMPOUNDS

by

Mark Pennington

A thesis submitted to the University of Warwick in partial fulfilment of the requirements for the degree of Doctor of Philosophy

Department of Chemistry,
University of Warwick,
Coventry CV4 7AL

October 1987

Acknowledgements

I would like to thank my supervisor Dr. N.W. Alcock for his guidance in crystallography throughout the course of my work. My thanks also to Dr. D. Brown and Mr. R.A.P. Wiltshire for their help in the preparation of neptunium compounds in the brief time I was at A.E.R.E. Harwell. In addition I would also like to thank everyone in the Chemistry department for their help and encouragement throughout the period of my research.

This thesis has been written using the *troff* word processing program with the preprocessors *refer*, *tbl*, and *eqn* running under the UNIX† operating system and printed on an Agfa P400PS postscript printer. I would like to thank Mr. R. McMahon for help with the system, and the operators for their service during the last few years.

I am indebted to the S.E.R.C. for support under the CASE scheme and the Chemistry Division of A.E.R.E.

† UNIX is a trademark of A.T.&T. Bell Laboratories.

DECLARATION

The work described in this thesis is entirely original and my own, except where otherwise indicated.

Publications

Parts of the work contained in this thesis have been published, accepted, or submitted for publication in the scientific literature with the following references:

M.Pennington, N.W. Alcock, and D. Brown, *Inorganica Chimica Acta; Proceedings of the Second Conference on Lanthanides and Actinides* , Lisbon 1987.

N.W. Alcock, D.J. Flanders, M. Pennington, and D. Brown, *Acta Cryst.* , 1987, C43 , 1476.

N.W. Alcock, D.J. Flanders, M. Pennington, and D. Brown, *Acta Cryst.* , 1987, accepted for publication.

ABSTRACT

The work contained in this thesis describes the crystal and molecular structures of a number of uranium(VI) compounds, and the preparation of two of the neptunium(VI) analogues. Apparent from the results is the invariance of the uranyl U=O bond length to substitution of sulphur or nitrogen for oxygen as the equatorial donor atom. This area has been explored through the determination of the following crystal structures:

a) The dithiocarbamate complexes $[Et_4N][UO_2(C_5H_8NS_2)_3]$; $[Et_4N][UO_2(C_7H_{10}NS_2)_3]$; $[Et_4N][UO_2(C_5H_{10}NS_2)_3]$; and $[Me_4N][UO_2(C_5H_8NS_2)_3]$.

b) The pentane 2,4-dionate complexes $\{UO_2(C_5H_7COCHCOC_6H_5)_2(C_5H_5N)]$ and $UO_2(CH_3COCHCOOC(CH_3)_3)_2(C_5H_5N)]$.

c) The biapyridyl bis nitrato complex $\{UO_2(C_5H_5N)_2)(NO_3)_2$.

In addition, the structures are described of the 1,10-Phenanthroline complex of uranyl acetate, and two unexpected products, $[Ph_4As][(C_4N_2S_2)_2]$ and $[(Me_2C_4HN_2S)_2]$, obtained by ligand dimerisation whilst attempting to form U-S bonded species.

Table of Contents

Chapter 1: Introduction 1
1.1 The Actinide Elements 1
1.2 Bonding Mechanisms in the Uranyl and Neptunyl Ions 3
1.3 Effects of Oxidation State and Metal Type on the Bond Lengths in the Actinyl Complexes 3
1.4 The Nature and Geometry of the Actinyl Ion 6
1.5 The Linearity of the Uranyl Ion 7
1.6 Review of the Coordination Chemistry of Uranium 12
References 15
Chapter 2: The Crystal and Molecular Structures of Four Uranyl(VI) Complexes with N,N-Dialkyldithiocarbamate Ligands 18
2.1 Introduction 18
2.2 Experimental 19
2.3 Discussion 21
References 58
Chapter 3: Two Pyridine-Acetyl Acetone Complexes of Uranium(VI) 60
3.1 Introduction 60
3.2 Experimental 60
3.3 Discussion 62
References 78
Chapter 4: The Crystal and Molecular Structures of Dioxobis(pyridine)dinitratouranium(VI) 79
4.1 Introduction 79
4.2 Experimental 79
4.3 Discussion 80
References 87
Chapter 5: The Structure of a 1,10-Phenanthroline Complex of Uranyl Acetate 88
5.1 Intoduction 88
5.2 Experimental 88
5.3 Discussion 89
References 96
Chapter 6: Some Unexpected Side Reactions - Three Further Structures 97
6.1 Introduction 97
6.2 Experimental 97
6.3 Discussion 99
References 107
Chapter 7: Experimental Section 108
7.1 The Collection of X-Ray Diffraction Data 108

7.2 Techniques Used in Handling Neptunium - 237 113
References 116
Chapter 8: Conclusions and Further Areas of Study 117
8.1 Conclusions 117
8.2 Areas of Further Study 119
References 119
Appendix A: Structure Solution and Crystallographic Theory A1
A1.1 Diffraction of X-Rays A1
A1.2 Symmetry and Space Groups A1
A1.3 Data Reduction A6
A1.4 The Structure Factor and Patterson Function A8
A1.5 Structure Solution and Refinement A9
References A13
Appendix B: Final Structure Factor Tables B1

List of Tables

Table	Title	Page
Table 1.1	Oxidation States of the Lanthanides and Actinides	2
Table 2.1	Crystal Data and Data Collection Conditions	32
Table 2.1 cont.	Analytical and infra red Data	33
Table 2.2	Comparison of Salient Bond Lengths	34
Table 2.3	Atomic Coordinates for [1]	35
Table 2.4	Atomic Coordinates for [2]	36
Table 2.5	Atomic Coordinates for [3]	38
Table 2.6	Atomic Coordinates for [4]	40
Table 2.7	Bond Lengths and Angles for [1]	41
Table 2.8	Bond Lengths and Angles for [2]	43
Table 2.9	Bond Lengths and Angles for [3]	47
Table 2.10	Bond Lengths and Angles for [4]	50
Table 2.11	Deviations from Planes for [1]	52
Table 2.12	Deviations from Planes for [2]	53
Table 2.13	Deviations from Planes for [3]	55
Table 2.14	Deviations from Planes for [4]	57
Table 3.1	Crystal Data and Data Collection Conditions	69
Table 3.1 cont	Analytical and infra red data	70
Table 3.2	Atomic Coordinates for [5]	71
Table 3.3	Atomic Coordinates for [6]	72
Table 3.4	Comparison of Bond Lengths and Angles	73
Table 3.5	Bond Lengths for [5] & [6]	74
Table 3.6	Bond Angles for [5] & [6]	75
Table 3.7	Deviations from Mean Planes	77
Table 3.8	Comparison of Inter-Plane Angles	77
Table 4.1	Atomic Coordinates for [8]	84
Table 4.2	Bond Lengths and Angles for [8]	85
Table 4.3	Deviations from Mean Planes for [8]	86
Table 5.1	Atomic Coordinates for [9]	93
Table 5.2	Bond Lengths and Angles Around Uranium for [9]	94

Table 5.3	Deviations from Mean Planes	95
Table 6.1	Atomic Coordinates for [10]	104
Table 6.1 cont	Bond Lengths and Angles for [10]	105
Table 6.2	Atomic Coordinates,Bond Lengths & Angles for [11]	106
Table 8.1	Effect of E.C.N. and Donor atom on U=O Lengths	117
Table 8.2	Uranium - Ligand Bond Length Range	118
Table A1	The 14 Bravais Lattices and Conventional Unit Cells	A3
Table A2	Determination of Translation Elements of Symmetry	A7

List of Figures

Figure	Title	Page
Figure 1.1	The Valence Orbitals of Uranium	3
Figure 1.2	Polar Diagram for *spdf* Hybrid Orbital	3
Figure 1.3	Molecular Orbitals of the Uranyl(VI) Ion	4
Figure 1.4	MoO_2^{2+} Orbital Energy *vs.* Bond Angle	7
Figure 1.5	UO_2Orbital Energy *vs.* Bond Angle	8
Figure 1.6	Molecular Structure of Uranyl H_2dapp Salt	10
Figure 2.1	View of the Anion of [1]	23
Figure 2.2	Packing Diagram for [1]	24
Figure 2.3	View of the Anion of [2]	25
Figure 2.4	Packing Diagram for [2]	26
Figure 2.5	View of the Anion of [3]	27
Figure 2.6	Packing Diagram for [3]	28
Figure 2.7	View of Puckering in [3]	29
Figure 2.8	View of the Anion of [4]	30
Figure 2.9	Packing Diagram for [4]	31
Figure 3.1a	View of the Molecule of [5]	64
Figure 3.1b	View of Twisting in [5]	65
Figure 3.2	Packing Diagram for [5]	66
Figure 3.3	View of the Molecule of [6]	67
Figure 3.4	Packing Diagram for [6]	68
Figure 4.1	View of the Molecule of [8]	82
Figure 4.2	Packing Diagram for [8]	83
Figure 5.1	View of [9] as an Idealised Non-centrosymmetric Dimer	91
Figure 5.2	Packing Diagram for [9]	92
Figure 6.1	View of the Anion of [10]	100
Figure 6.2	Packing Diagram for [10]	101
Figure 6.3	View of the Molecule of [11]	102
Figure 6.4	Packing Diagram for [11]	103

Figure 7.1	The Four Circle of the Diffractometer	110
Figure 7.2	Pattern of Spots on Film from a Rotation Photograph	110
Figure 7.3	Plot of the Distribution Coefficient of Np(VI) in HCl	114
Figure A1	Diffraction of X-Rays from Crystal Planes	A2
Figure A2	Derivation of Miller Indicies For Any Plane of Reflection	A2
Figure A3	Possible Types of Lattice Centering	A4

CHAPTER 1

Introduction

1.1. The Actinide Elements

The actinides are the fourteen elements between actinium (Z=89) and rutherfordium (Z=103). In an analagous fashion to the *d*-series, and the 4*f*-lanthanide series, the actinides arise from the successive addition of electrons into the empty 5*f*-orbitals of the preceeding elements. All of the known isotopes of the actinides are radioactive. The terrestrial occurence of U and Th is due to the half-lives of ^{232}Th, ^{235}U and ^{238}U which are sufficiently long to have enabled them to exist since genesis. Protactinium can be found in nature, despite its short half-life (3.28×10^4 yrs), since it is a member of the ^{235}U decay chain. The remaining elements are produced synthetically since their half-lives are so short that any primordial deposits will have completely decayed.

The actinide elements and their electronic configurations are listed in the following table (Table 1.1). This table also illustrates the comparison with the lanthanides. As can be seen, whilst the lanthanide elements have a limited range of oxidation states, normally +3 in both aqueous solution and solid compounds, the actinides exist in a wide variety of oxidation states with neptunium and plutonium for example, having the range +3 to +7. However, the common oxidation state of americium and the remaining elements is +3 and this second half of the actinide series approaches the behaviour of the lanthanides, with the sole exception of nobelium (Z=102) for which the dipositive state appears to be extremely stable, a result of the filled *f*-shell electronic configuration ($5f^{14}$) of the No^{2+} ion.

The differences between the most stable dominant oxidation states of the actinides and lanthanides are attributable to two main factors. First, the sum of the first three ionisation enthalpies is comparatively low, so the lanthanides are highly electropositive, and bonding tends to be ionic. Secondly, the 5*f* electrons of the actinides are not as strongly shielded as the 4*f* electrons of the lanthanides, less energy is thus needed to promote the 5*f* electron to a 6*d*-orbital, which can then be used in bonding.

The work contained in this thesis describes the synthesis and structural aspects of some uranium(VI) coordination chemistry, and the synthesis of two of the neptunium analogues. Preparative work on neptunium was carried out at A.E.R.E. Harwell.

The element was first discovered in 1940 by McMillan and Abelson[1] as ^{239}Np:

$$30\% : {}^{238}\mathrm{U}(n,\gamma)\ {}^{239}\mathrm{U} \xrightarrow{\beta^-} {}^{239}\mathrm{Np} \xrightarrow{\beta^-} {}^{239}\mathrm{Pu}$$

The known isotopes of neptunium range from ^{228}Np to ^{243}Np, with half lives in the range 52s (^{228}Np) to 2.14×10^6 yrs (^{237}Np).[2] The next longest half lives are found for ^{235}Np ($t_{1/2}$=410d),

TABLE 1.1

Oxidation States of the Actinides and Lanthanides

(Most common oxidation states emboldened, least common in parentheses)

	Actinides			Lanthanides	
89 Ac	**3**	$6d\ 7s^2$	57 La	**3**	$5d\ 6s^2$
90 Th	(3),**4**	$6d^2\ 7s^2$	58 Ce	**3,4**	$4f\ 5d\ 6s^2$
91 Pa	(3),**4,5**	$5f^2\ 6d\ 7s^2$	59 Pr	**3**,(4)	$4f^3\ 6s^2$
92 U	**3,4,5,6**	$5f^3\ 6d\ 7s^2$	60 Nd	(2),**3**	$4f^4\ 6s^2$
93 Np	**3,4,5,6,7**	$5f^5\ 7s^2$	61 Pm	**3**	$4f^5\ 6s^2$
94 Pu	**3,4,5,6,7**	$5f^6\ 7s^2$	62 Sm	**2,3**	$4f^6\ 6s^2$
95 Am	(2),**3,4,5,6**	$5f^7\ 7s^2$	63 Eu	**2,3**	$4f^7\ 7s^2$
96 Cm	**3,4**	$5f^7\ 6d\ 7s^2$	64 Gd	**3**	$4f^7\ 5d\ 6s^2$
97 Bk	(2),**3,4**	$5f^9\ 7s^2$	65 Tb	**3**,(4)	$4f^9\ 6s^2$
98 Cf	**2,3**	$5f^{10}\ 7s^2$	66 Dy	**3**	$4f^{10}\ 6s^2$
99 Es	**2,3**	$5f^{11}\ 7s^2$	67 Ho	**3**	$4f^{11}\ 6s^2$
100 Fm	**2,3**	$5f^{12}\ 7s^2$	68 Er	**3**	$4f^{12}\ 6s^2$
101 Md	**2,3**	$5f^{13}\ 7s^2$	69 Tm	(2),**3**	$4f^{13}\ 6s^2$
102 No	**2,3**	$5f^{14}\ 7s^2$	70 Yb	**2,3**	$4f^{14}\ 6s^2$
103 Lr	**3**	$5f^{14}\ 6d\ 7s^2$	71 Lu	**3**	$4f^{14}\ 5d\ 6s^2$

and ^{236}Np ($t_{1/2}$=5000yrs) but the latter is a β emitter. This makes preparative work virtually impossible on all but the ^{237}Np isotope, which was used here. This isotope was first prepared by Waal and Seaborg[3] in 1942 by neutron bombardment of ^{238}U:

$$70\%: \quad ^{238}U(n,2n)\ ^{237}U \xrightarrow{\beta} {}^{237}Np$$

The isotope is also formed as one of the products in nuclear reactors[4]

$$30\%: \ ^{235}U(n,\gamma)\ ^{236}U(n,\gamma)\ ^{237}U \xrightarrow{\beta} {}^{237}Np$$

The most stable oxidation states of uranium and neptunium are (VI) and (V) respectively. Neptunium (VI), NpO_2^{2+}, does exist but can only be maintained by the presence of an oxidant in solution, and is readily reduced to the (V) state. However, complexes can be formed which maintain this +6 oxidation state when solid. The comparative stability of the uranyl and neptunyl ions is illustrated by their electrode potentials:[5]

$$UO_2^{2+} + e^- = UO_2^{+} \; ; \; E^o = 0.163 \text{ V} \qquad (1.2.1)$$

$$NpO_2^{2+} + e^- = NpO_2^{+} \; ; \; E^o = 1.236 \text{ V} \qquad (1.2.2)$$

The +5 state of neptunium is much more stable, and will only disproportionate at high acid concentrations (>5M $HClO_4$) to give the +4 and +6 oxidation states. The hydroxide species, $NpO_2(OH)$ is only formed when the acid concentration is reduced past pH 5.7. This is in contrast to the uranium(V) species which readily disproportionates[6] to U^{4+} and UO_2^{2+}, being most stable at pH 2.5.

$$2UO_2^{+} + 4H^+ \rightarrow U^{4+} + UO_2^{2+} + 2H_2O \qquad (1.2.3)$$

The oxygen atoms in all of the actinyl ions are non-basic, and as such do not attract protons, even at high acidities;[7] however, in aqueous solutions, both MO_2^{+} and MO_2^{2+} ions coordinate with water to form acidic hydrated species.

1.2. Bonding mechanisms in the uranyl and neptunyl ions.

If the equatorial coordination number is 5 or 6, then from symmetry considerations, it is possible for all the metal $5f$, $6d$ and $7s$ valence orbitals to participate in equatorial bonding, (Figure 1.1).[8] In the case of a distorted octahedron however, all the bonding orbitals except f_{xyz} can contribute.

Since π bonds are quite weak compared to the corresponding σ bonds, the strongest equatorial bonds will be formed with the eight f, d, and s orbitals that have electron density normal to the actinyl axis; viz the f_{xy^2}, f_{yz^2}, f_{xz^2}, f_{yz^2}, $d_{x^2-y^2}$, d_{xy}, d_{yz} and s orbitals. The remaining 5 orbitals, f_{xyz}, f_{z^3}, f_{xz^2}, d_{xz}, and d_{yz} orbitals which have a spatial distribution in some plane other than the equatorial may be involved in cases of staggered bonding.

Coulson and Lester[9] have suggested that the use of *spdf* hybrid orbitals is of importance in complexes where the equatorial coordination number is 6. The orbitals produced by such hybridisation would have lobes at 60° to one another in a planar arrangement, suitable for maximum overlap with the ligand orbitals. Furthermore, they suggest that the $6f$ rather than the $5f$ orbitals would be more favourable for such overlap because they protrude further into space, (Figure 1.2)

1.3 Effects of oxidation state and metal type on the bond lengths in the actinyl complexes.

It can be seen from Figure 1.3 that the ϕ_u orbital is not directed along the actinyl axis. Consequently an electron occupying this orbital is unlikely to have any effect on the length, strength, or geometry of the bonds in the actinyl ion, and should not therefore be responsible for any differences between UO_2^{2+} and NpO_2^{2+} ions which are in identical coordination environments. The δ_u orbital however lies along the actinyl axis and an electron occupying this orbital has the effect of lengthening the NpO_2 ion primary bonds by 0.09Å relative to those of NpO_2^{2+}. A lengthening of

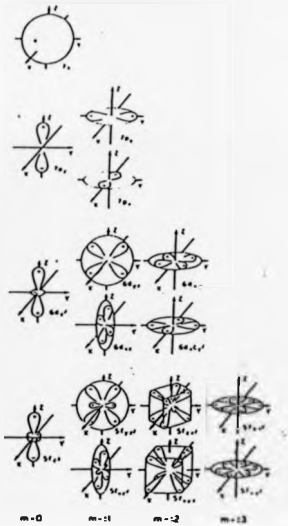

1.1 The valence orbitals of uranium (from ref.8)

1.2. Polar diagram for *spdf* hybrid orbital (from ref.9)

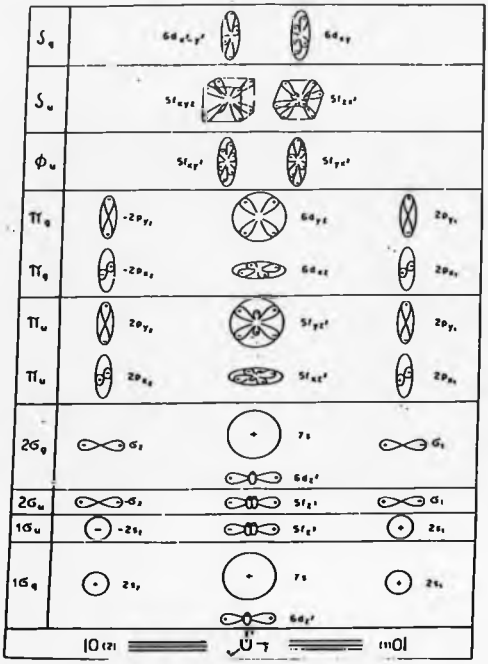

1.3 The molecular orbitals of the uranyl(VI) ion (from ref.8)

the secondary bonds also occurs in these circumstances and this is probably due to the repulsion of the partially filled ϕ_u orbital toward the equatorial ligands by the "extra" δ_u electron. This would increase the metal-ligand repulsion and therefore M-L bond length.

The actinide contraction, the decrease in ionic radius that is observed from uranium to americium,[10] is responsible for the major change in bond lengths between analagous uranium(VI) and neptunium (VI) complexes. Between protactinium (z=91) and uranium (z=92), the *5f* orbitals become lower in energy than the *6d* and *7s* orbitals with the increasing nuclear charge. As a consequence the *5f* orbitals start to fill. These orbitals do not shield themselves very well so the shells contract as the atomic number increases. A consequence of this is a stabilisation of the orbitals which bond with those of oxygen in the actinyl ions resulting in poorer overlap and a weakening of the M-O (MO_2^{2+}) bond with a reduction in its length along the actinide series. A similar change is observed in the secondary bonds around MO_2^{2+}. Structural changes can also occur in analagous actinide complexes as a result of this difference in ionic radius; for example the different crystal systems of the tribromides of neptunium and plutonium.[11]

The higher energy of the *5f* orbital compared with the *6d* orbital in protactinium explains the absence of a linear PaO_2^+ species comparable to that of the higher actinides. The only known oxo-ion is $[Pa{=}O]^{3+}$ which occurs, for example, in $(NEt_4)_2\,PaOCl_5$.[12]

1.4 The Nature and Geometry of the Actinyl Ion

The dioxo-cations MO_n^{z+} (M = U, n = 2; M = Np, n = 1, 2) can be considered to act as a single charged metal centre, having the characteristics of a "hard" Lewis acid.[13] As a result they will form complexes more readily with electronegative donor atoms (N, O, F^-, Cl^-) than with the larger more polarisable atoms which utilise π-bonds to a greater degree (S, P, Se, I^-). This "hard/soft - donor/acceptor" principle also implies that nitrogen would be less tightly bound to the metal than oxygen, since oxygen has the higher base strength.[14] U-O bonds will therefore be shorter than U-N bonds as is found for other "hard" acids eg Ti(IV), Fe(III), whereas "softer" ions (eg Cu(II), Co(II)) form M-O and M-N bonds which are of comparable length. Complexes involving donor S and Se atoms have been reviewed[15] and include $[Me_4N][UO_2(dtc)_3]$ (dtc=N,N-diethyldithiocarbamate), $UO_2(dtc)_2TPPO$ (TPPO= triphenylphosphine oxide), and $UO_2(dSec)_2TPAsO$ (dSec= diselenium carbamate; TPAsO= triphenylarsine oxide). Chapter 2 deacribes the synthesis and crystal structures of further dithiocarbamate complexes of uranium(VI).

1.5. The Linearity of the Uranyl Ion

The MO_2^{+} ion (O-M-O) is generally described as being linear and deviates little from linearity, one of the largest deviations for an ordered structure resulting in an O-U-O angle of 173.5(8)°.[16] Such a geometry is different from that encountered for other dioxocations[17] e.g. MoO_2^{+} where an O-M-O angle of 110° is found. This arises because the Mo_2^{+} ion contains a (d_{xy}) hybridised orbital set formed from the $4d$, $5s$, and $5p$ orbitals on the molybdenum which can interact with the $2p$ orbitals of the oxygen atoms in the dioxocation. Figure 1.4 shows the (net) potential energy curves obtained by considering each of the orbitals individually in the formation of the dioxocation, and then the effect of utilising the hybrid set. It can be seen that whilst the s and p orbitals favour a more linear geometry, it is the effect of the $4d$ orbital which produces a potential energy minimum with an O-Mo-O angle of 110°.

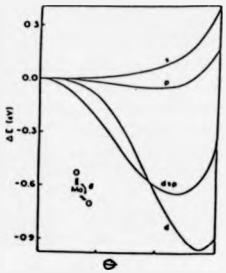

1.4. Relative total energy as a function of bond angle for Mo $4s$, $5s$, $5p$ (separately) and d_{xy} (all together) basis sets in the MoO_2^{+}. (from ref.17)

In the UO_2^{+} ion the $5f$, $6d$, $7s$ and $7p$ valence orbitals are higher in energy than, and thus less likely to interact with, the oxygen $2p$ orbitals. The similar potential energy curves (Figure 1.5) show that the fd_{xy} hybridised set which is formed is level in the region 110-118°. This indicates that it is not the addition of the f -orbital which is responsible for this *trans* -geometry, but the addition of the extra, non-valence, filled $6p$, orbital on uranium which forces the linear geometry.

This "linearity" imposes some geometrical constraints upon the type of polyhedra by which the uranyl ion can be accommodated. The dodecahedron or square antiprism, are the preferred coordination polyhedra of hexa-coordinate d^0-d^3 transition metals.[18]

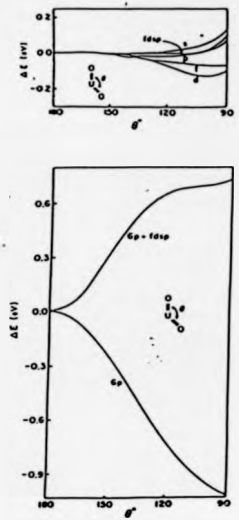

1.5 Relative total energy as a function of bond angle fo for U 5*f*, 6*d*, 7*s*, 7*p*, (separately) and *fdsp* (all together) basis sets in UO_2^{+} (top) and for U 6*p* and 6*p* + 5*f*,6*d*,7*s*,7*p* basis sets in UO_2^{2+} (bottom) (from ref. 17)

yet hexagonal bipyramid geometry is exhibited by those complexes involving six donor atoms coordinated to the uranyl group despite being energetically less favourable The few examples of complexes with this geometry which do not contain the actinyl ion arise as a result of steric constraints. The example of tetramethylammonium triacetato diphenyl plumbate(IV),[19] $[Me_4N][Pb(Ph)_2(CH_3COO)_3)]$, has the special combination of two bulky monodentate and three short bite bidentate ligands about the central metal atom. From this we can deduce that it must be the essential dimensional requirements of the linear uranyl group which stabilises the hexagonal

bipyramidal stereochemistry. No other geometry could accommodate such a linear moiety.

The M-O bond lengths within the MO_2^{2+} unit lie between 1.5Å and 2.1Å with mean values of 1.77Å and 1.74Å for uranium[20] and neptunium[21, 22] respectively. The dioxocation can accommodate between 4 and 6 donor atoms in the equatorial plane, and it is found that equatorial coordination number has little effect on M=O (MO_2^{2+}) bond lengths, mean U=O lengths are 1.809, 1.764, and 1.779Å for 4, 5, and 6 coordination respectively Furthermore, a recent review[20] suggests that contrary to the earlier analysis by Zachariasen[23] there is no obvious dependence of the M=O bond lengths on the type of ligands found in the coordination sphere, for example, with six oxygen atoms equatorially coordinated, U=O lengths range 1.65(4)[24, 25] to 1.909(46)[26] Most determinations have standard deviations of 0.003Å, so any trends in length will generally be masked by experimental uncertainties.

The arrangement of ligands in the equatorial plane becomes more puckered as the coordination number is increased. This puckering is reduced with a coordinating bidentate ligand with a small "bite" as in $NaUO_2(CH_3CO_2)_3$ which has a planar arrangement.[27] When the size of the donor atom is increased, either an exaggerated form of equatorial puckering will be found, or the equatorial coordination number will be reduced. An example of the first effect is seen in dithiocarbamate complexes e.g. $[Me_4N][UO_2(dtc)_3]$,[28] and those complexes described in Chapter 2. The second effect is observed on comparison of $[UO_2(CH_3CO_2)_2.(TPPO)_2$[29] with $UO_2(CH_3CS_2)_2.TPPO$[30] where substitution of the oxygen by sulphur reduces the equatorial coordination number from 6 to 5.

Constraints on the coordination geometry can arise in other ways; one example is in the structure of $[UO_2(H_2dapp)NO_3][UO_2(NO_3)_4]$ (Figure 1.6).[31] The ring systems are so strained that in spite of the small size of the nitrogen donors, no equatorial plane can be defined by them. Extreme distortion is found here.

The lengths of the M-L (L=ligand) bonds lie in the range 2.2 - 2.9Å and by comparison with the primary MO_2^{2+} are denoted secondary bonds. This allows the coordination geometry in these complexes to vary from a distorted octahedron, through a pentagonal bipyramidal arrangement to a hexagonal bipyramid. These are illustrated in Figures 1.7-9. If the cone angle subtended by the coordinating ligand is sufficiently large,[32] or if the donor atoms are sufficiently large, the complex will assume a distorted octahedral geometry. Examples are the structure of $NpO_2(OPPh_3)_2Cl_2$[33] and the anions of $Cs_3NpO_2Cl_4$[34] which accommodate four chlorine atoms in the equatorial plane. The ability of chlorine to coordinate in this way is determined by its large van der Waals' radius* of 1.75Å.[35]

*The van der Waals' radius of an atom is the distance at which the repulsive inter-atomic forces balance the attractive ones. The repulsive forces come into play as the electron clouds interpenetrate.

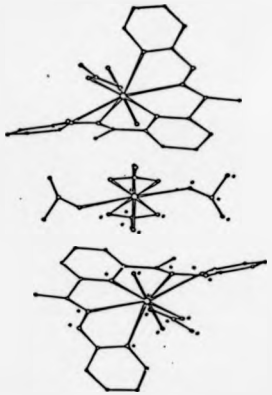

I.6. Molecular structure of $[UO_2(H_2dapp)NO_3]_2[UO_2(NO_3)_4]$

An equatorial coordination number of 5 is most common particularly with oxygen donors, with M-O (ligand) bond lengths in the range 2.35 - 2.40Å and the non bonded O...O separation 2.70 - 2.80Å, a value very close to the sum of the van der Waals radii (2.84Å). In some complexes particularly with hexacoordination in the equatorial plane, the O...O contact distance may be as low as 2.6Å, which indicates that simple addition of the two unconstrained van der Waals radii does not fully describe the limiting case.

The puckering of equatorial hexagons of monodentate groups (as in α-$UO_2(OH)_2$)[36] suggests that fitting six oxygen atoms in a plane about a UO_2^{2+} ion is quite difficult. If the liganda are small-bite, bidentates then the crowding is alleviated somewhat. In the sulphate ion, the average O...O distance of 2.38Å is greater than the expected L...L donor atom separation for hexa-equatorial coordination (2.35Å). Thus the sulphate ion cannot easily be accommodated in this geometry and is expected to assume an equatorial coordination number of 5.

This example could be used as a standard limiting value such that only ligands with a bidentate chelating bite less than 2.35Å can be comfortably accommodated within a hexagonal

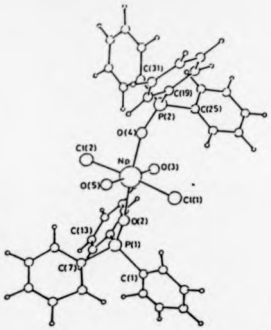

1.7. Distorted octahedral coordination geometry (from ref.29)

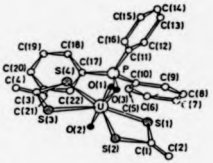

1.8. Pentagonal bipyramidal geometry (from ref.27)

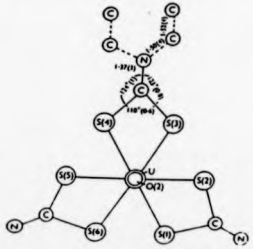

1.9. Hexagonal bipryamidal geometry around uranium. O(2) is below plane and not shown. (fro ref.25)

bipyramid. Typical bidentate ligands which fall in this category (including bite distances) are O_2^{2-} (1.48(6)Å), CO_3^{2-} (2.19(1)Å), $CH_3CO_2^-$ (2.17(2)Å), and NO_3^- (2.15(2)Å). These are seen in the following complexes: $Na_4UO_2(O_2)_3.9H_2O$,[37] $K_4UO_2(CO_3)_3$[38] $NaNpO_2(CH_3CO_2)_3$ and $RbNpO_2(NO_3)_3$.[39] Chapter 2 describes three uranyl complexes with dithiocarbamate ligands where the bite distance is substantially greater, yet hexagonal bipyramidal geometry is observed. This is presumably due to the longer U-S bond and puckering of the sulphur atoms which reduces steric crowding.

1.6. Review of the coordination chemistry of uranium

In 1967 Muetterties and Wright reviewed complexes which involved atoms with coordination numbers of seven or more,[40] and hence dealt with most of the known compounds of the actinides. Since then, there have been numerous other reviews covering such aspects as actinide fluoride complexes (1970), carbonates, nitrates, nitrites, sulphates, sulphites, selenates, selenites, tellurates, and tellurites (1973),[41] and chalcogenides (1972).[42]

Uranium and the other actinides are sufficiently large to discourage coordination numbers less than six. Five coordination is as yet unknown, and even hexa-coordination is rare. Where this is found, the metal atoms are usually in their highest oxidation states, a situation which corresponds to a minimum ionic radius for the element. Where uranium is incorporated into an octahedral hexacoordinate structure, a tetragonal compression results, with two short bonds perpendicular to a plane containing four longer ones. The octahedra are regular in other respects, the uranyl moiety ensuring that the bond angles are close to 90°. Examples of this distortion are seen in the structures of β-$UO_2(OH)_2$,[43] $CsUO_2Br_4$,[44] and UO_2MoO_4[45] all of which are polyhedra built around the uranyl group.

7-Coordination

Regardless of the nature of the five additional ligands, 7 coordinate polyhedra incorporating the uranyl group adopt the only configuration which will allow the trans O=U=O moiety to be linear. Numerous mononuclear pentagonal bipyramidal uranyl complexes exist. The structures of $[UO_2(H_2O)(CO(NH_2)_2)_4](NO_3)_2$ has been determined by neutron diffraction.[46] The nitrate groups are not coordinated to the U atom but are important to the scheme of hydrogen bonding that links the cation throughout the structure. In the complexes $UO_2(Et_2NCS_2)_2.L$; (L=Me_3NO, trimethyl-N-oxide; Ph_3PO, triphenyl phosphine oxide; and Ph_3AsO, triphenyl arsine oxide) the uranium atom exhibits pentagonal bipyramidal geometry. There is a variation of U-O(ligand)

bond lengths. Me_3NO approaches more closely (2.14(3)Å) than Ph_3PO (2.34(2)Å) or Ph_3AsO (2.30Å(2)), suggesting a greater donor ability for the former ligand.[47] The two U-O(uranyl) bond lengths (1.84(2) and 1.86(2)Å) are longer than those found in the arsine- and phosphine-oxide derivatives (mean value 1.70(3)Å), and the ν_3O-U-O is consequently lower: 892, 901, and 910, 905cm^{-1} for Me_3NO, Ph_3AsO and Ph_3PO products repectively. Similarly there is a decrease in the value of the νC-S and νC-N stretching modes for the complexes.

Crystallographic investigations of $UO_2(DSeC)_2.Ph_3PO$ and $UO_2(DSeC)_2Ph_3AsO$ (DSeC= have shown that each uranium is again in a pentagonal bipyramidal environment,[48] in which four selenium atoms and an oxygen atom occupy the corners of an irregular pentagon. The uranyl group is linear, (O-U-O angle 178(5)°). U-Se(mean) 2.98(2)Å U-O(ligand) 2.25(3)Å and U=O(uranyl) 1.76(2), 1.77(2)Å. Similar pentagonal bipyramidal species involving dithioacetic acid and dithiobenzoic acid have also been prepared and characterised structurally. All distances and angles in the molecule are comparable with the corresponding ones found in the dithiocarbamate complexes, indicating that the substitution of NEt_2 of the DTC by a methyl group in the chelated ligands has no detectable effect on the bonding the coordinated atoms.

A large number of pentagonal bipyramidal complexes of dioxouranium(VI) with 1,3-diketonates and related ligands have been reported,[49] but in the main the only investigation involves a study of ν_1 and ν_3 O-U-O stretching bands. Structural information on these compounds is limited. To date only two structures of compounds involving two pentane-2,4-dionato ligands and a monodentate ligand coordinated to the uranyl ion have been reported.[16, 50] (Chapter 3 describes a further two). Of these, dioxobispentane-2,4-dionatouranium(VI) is particularly worthy of note because of the large deviation from linearity of the uranyl ion(173.5(8)°). In both complexes the equatorial donor atoms form a slightly irregular pentagon.

A further example of uranium hepta-coordinated by oxygen atoms is seen in the structure of bis(hydroxyacetato)dioxouranium(VI).[51] In this, two of the glycolato groups are bidentate, whilst one is tridentate; the pentagonal bipyramids are linked through the glycolato groups forming infinite chains.

8-Coordination

There are several examples of complexes involving oxygen coordination with hexagonal bipyramidal geometries . One such structure which is noteworthy is that of the anion $[UO_2(NO_3)_4]^{2-}$.[52] In this, the uranyl group is linear (due to the centre of symmetry), and of the four equatorial nitrates, two are linked through only one donor atom. This is the only known example of monodentate coordination of nitrate to uranium. Puckering of the donor atoms is generally reduced with oxygen coordination, as seen in the structures of $Na_4[UO_2(O_2)_3]$[37] and $Na[UO_2(OAc)_3]$[27] where the equatorial oxygens are described as being coplanar (within

experimental error). However equatorial puckering can be found; e.g. in the anion $[UO_2(NO_3)_3]^-$, where the oxygen atoms lie 0.09Å above and below the plane.[53] This is probably due to a stereo-electronic hinderance between the lone pairs of electrons on the oxygen donors.

Six is the greatest number of ligands found coordinated equatorially to the uranyl group, and steric crowding limits the number of known species. Puckering is invariably required to accommodate the ligands. A good example of this is seen in the stucture of N,N-diethyldithiocarbamto-dioxouranium described by Bowman and Dori,[28] where deviations of about 0.2Å from the equatorial plane are reported for the sulphur atoms.

References

1. E. McMillan and P. Abelson, *Phys. Rev.*, vol. 57, p. 1185, 1940.
2. E.K. Hyde, I. Perlman, and G.T. Seaborg, *The Nuclear Properties of the Heavy Elements - Detailed Radioactivity Properties*, 2, p. xlvi, 1964.
3. A.C. Wahl and G.T. Seaborg, *Phys. Rev.*, vol. 73, p. 940, 1948.
4. W.W. Schultz and G.E. Benedict, "Neptunium-237: Production and Recovery," USAEC Report TID-25955, 1972.
5. J.R. Brand and J.W. Cobble, *Inorg. Chem.*, vol. 9, p. 912, 1970.
6. A. Ekstrom, *Inorg. Chem.*, vol. 13, p. 2237, 1974.
7. "The Actinides," in *Comprehensive Inorganic Chemistry, Vol 5*, ed. A.F. Trotman-Dickenson, Pergamon, New York, 1973.
8. L. Cattalini, U. Croatto, S. Degetto, and E. Tondello, *Inorg. Chim. Acta Reviews*, vol. 5, p. 19, 1971.
9. C.A. Coulson and G.R. Lester, *J. Chem. Soc.*, p. 3650, 1956.
10. V.I. Spitsyn and J.J. Katz, in *Proc. Mosc. Symp. Chem. Trans. Elem.*, p. 123, Pergammon Press, Oxford, 1976.
11. D. Brown and J. Edwards, *J. Chem. Soc. Dalton Trans.*, p. 1757, 1972.
12. D. Brown, C.T. Reynolds, and P.T. Mosley, *J. Chem. Soc. Dalton Trans.*, p. 857, 1972.
13. R.G. Pearson, *J. Am. Chem. Soc.*, vol. 85, p. 3533, 1963.
14. U. Casellato, M. Vidali, and P.A. Vigato, *Inorg. Chim. Acta*, vol. 18, p. 77, 1976.
15. U. Casellato, M. Vidali, and P.A. Vigato, *Coord. Chem. Rev.*, vol. 28, p. 231, 1979.
16. N.W. Alcock, D.J. Flanders, and D. Brown, *J. Chem. Soc. , Dalton Trans.*, p. 679, 1984.
17. K. Tatsumi and R. Hoffman, *Inorg. Chem.*, vol. 19, p. 2656, 1980.
18. D.L. Keppert, *J. Chem. Soc.*, p. 4736, 1965.
19. N.W. Alcock, *J. Chem. Soc. Dalton Trans.*, p. 1189, 1972.
20. R.G. Denning, "Properties of the UO_2^{n+} (n=1,2) Ions," in *Gmelin Handbuch URAN Suppl. Vol A6*, pp. 31-79, 1983.
21. M.M. Roberts, *Ph.D. Thesis, University of Warwick*, 1981.
22. D.J. Flanders, *Ph.D. Thesis, University of Warwick*, 1985.
23. W.H. Zachariasen, *Acta Cryst.*, vol. 7, p. 795, 1954.
24. H. Brusset, Nguyen Quy Dao, and F. Haffner, *J. Inorg. Nucl. Chem.*, vol. 36, p. 791, 1974.

25. C. Bois, Nguyen Quy Dao, and N. Rodier, *J. Inorg. Nucl. Chem.*, vol. 38, p. 755, 1976.
26. N. Armagan, *Acta Cryst. B.*, vol. 33, p. 2281, 1977.
27. W.H. Zachariasen and H.A. Plettinger, *Acta Cryst.*, vol. 12, p. 526, 1959.
28. K. Bowman and Z. Dori, *J. Chem. Soc. Chem. Commun.*, p. 636, 1968.
29. C. Panattoni, R. Graziani, G. Bandoli, B. Zarli, and G. Bombieri, *Inorg. Chem.*, vol. 8, p. 320, 1969.
30. G. Bombieri, U. Croatto, E. Forsellini, B. Zarli, and R. Graziani, *J. Chem. Soc. Dalton Trans.*, p. 560, 1972.
31. G. Bandoli, D.A. Clemente, G. Marangoni, G. Paolucci, *J. Chem. Soc. Chem. Commun.*, p. 235, 1978.
32. K.W. Bagnall, *Inorg. Chim. Acta*, vol. 94, p. 3, 1984.
33. N.W. Alcock, M.M. Roberts, and D. Brown, *J. Chem. Soc. Dalton Trans.*, p. 25, 1982.
34. N.W. Alcock, M.M. Roberts, and D. Brown, *Acta Cryst.*, vol. B38, p. 1805, 1982.
35. A. Bondi, *J. Phys. Chem.*, vol. 68, p. 441, 1964.
36. J.C. Taylor, *Acta Cryst.*, vol. B27, p. 1088, 1971.
37. N.W. Alcock, *J. Chem. Soc. (A)*, p. 1588, 1968.
38. A. Anderson, C. Chieh, D.E. Irish, and J.P.K. Tong, *Can. J. Chem.*, vol. 58, p. 1651, 1980.
39. N.W. Alcock, M.M. Roberts, and D. Brown, *J. Chem. Soc., Dalton Trans.*, p. 869, 1982.
40. E.L. Muetterties, C.M. Wright, *Quart. Rev. Chem. Soc.*, vol. 21, p. 109, 1967.
41. D. Brown, *Comprehensive Inorganic Chemistry*, vol. 5, p. 277, Pergamon Press, Oxford, 1973.
42. R.M. Dell N.J. Bridger, *MTP International Review of Science, Inorganic Chemistry (Series One)*, vol. 7, p. 211, Butterworth, London, 1972.
43. M.J. Bannister, J.C. Taylor, *Acta Cryst.*, vol. 26B, p. 1775, 1970.
44. Yu.N. Mikhailov, V.G. Kuznetsov, *Zh. Neorg. Khim.*, vol. 16, p. 2512, 1971.
45. V.N. Serezhkin, L.M. Kovba, V.K. Trunov, *Radiokhimiya*, vol. 13, p. 659, 1971.
46. N.K. Dalley, M.H. Meuller, S.H. Simonsen, *Inorg. Chem.*, vol. 11, p. 1840, 1972.
47. E. Forsellini, G. Bombieri, R. Graziani, and B.Zarli, *J. Inorg. Nucl. Chem. Lett.*, vol. 8, p. 461, 1972.
48. B. Zarli, R.Graziani, E.Fosellini, U. Croatto, G. Bombieri, *J. Chem. Soc. Chem. Commun.*, p. 1501, 1971.

49. K.W. Bagnall, *Gmelin Handbuch URAN Suppl., E1*, p. 40, 1979.

50. N.W. Alcock, D.J. Flanders, *Acta Cryst.*, vol. C43, p. 1480, 1987.

51. B.F. Mentzen, H. Sautereau, *Acta Cryst.*, vol. B36, p. 2051, 1980.

52. I.I. Kapshukov, Yu.F. Volkov, E.P. Moskvichev, I.A. Lebedev, G.N. Yakovlev, *Zh. Strukt. Khim.*, vol. 12, p. 94, 1971.

53. G.A. Barclay, T.M. Sabine, J.C. Taylor, *Acta Cryst.*, vol. 19, p. 205, 1965.

CHAPTER 2

The Crystal and Molecular Structures of Four Uranyl(VI) Complexes with N,N-Dialkyldithiocarbamate Ligands.

2.1.Introduction.

Complexes involving U-O and U-N bonds are more common than those which utilise U-S bonds. This is primarily a consequence of Pearson's Hard and Soft Acid and Base Principle,[1] but steric features may also play some role. The larger size of sulphur compared to oxygen results in an exaggerated puckering of the equatorial plane and therefore increased difficulty in accommodating S-donor ligands. Most of the complexes reported involve dithiocarbamates or other S-chelates which form a 4 membered ring.

Dithiocarbamate complexes of uranium(VI) were first mentioned by Delepine in 1908[2] and several dioxouranium(VI)bisdithiocarbamate complexes have been reported by Malatesta.[3] This work was extended to the preparation of more compounds of general formula $UO_2(R_2NCS_2)_2$[4] and to the compound $KUO_2(dtc)_3$[5] (dtc=N,N-diethyldithiocarbamate). A variety of dialkylammonium trisdithiocarbamate salts have been produced, (a) during early attempts to prepare the uranium(IV) salts, from uranium tetrachloride, the dialkylammonium salts of the reagents and dry solvents,[6] and (b) as a by-product in the reaction between uranyl nitrate and the sodium salt of the dithiocarbamate ligand from which the polymorphous $[Et_2NH_2][UO_2(dtc)_3]$ has been identified;[7] the cation in this case is derived from hydrolysis of the dithiocarbamate ligand. The brightly coloured solution formed when UO_2^{2+} is treated with dithiocarbamate ligands has been used in the colorimetric determination of uranium[8,9] and the quantitative precipitation of UO_2^{2+} with dithiocarbamates under acid conditions has been reported.[10,11]

There is a limited amount of structural data available for uranium(VI) dithiocarbamates. To date there has been only one crystal structure reported which involves six sulphur atoms of a dithiocarbamate ligand coordinated to UO_2^{2+} in the equatorial plane, and this only briefly.[12] This revealed the existence of a species in which three dithiocarbamate ligands were each coordinated through both sulphur atoms rather than the double salt $[UO_2(Et_2NCS_2)]^+[UO_2(Et_2NCS_2)_3]^-$ as was previously suggested for these complexes from polarographic studies.[13] A residual factor of 14% was reported for $[Me_4N][UO_2(dtc)_3]$ by Bowman and Dori due to their failure to refine the positions of the ethyl carbon atoms. A series of complexes of general formula $UO_2(DTC)_2.L$ (DTC=general dithiocarbamate; L=Ph_3PO, Ph_3AsO, Me_3NO) has been produced by reaction of L with the stoichiometric amount of $K[UO_2(DTC)_3]$ in acetone.[14,15,16,17] Unlike the

trisdithiocarbamate complexes, where puckering of the atoms in the equatorial plane is found the coordination of the sulphur atoms is virtually coplanar.

Most investigations into dithiocarbamate ligands involve infra red spectral studies of ν_sO-U-O,[18] and νC-S and νC-N[19,20] and reveal that the greater the ligand donation (*i.e.* the stronger the U-O(ligand) bond), the lower the stretching frequency of the uranyl group, (weaker U=O bond). In an attempt to increase the amount of structural information available for U-S species, the synthesis and structural determination of a further four dithiocarbamates of uranium (VI) was undertaken and is described here. Three of these tris(N-pyrrolidinedithiocarbamato) dioxouranium(VI) [1]; tris(N-piperidinedithocarbamato) dioxouranium(VI) [2]; and tris(N,N-dimethyldithiocarbamto) dioxouranium(VI) [3], were isolated as the tetraethylammonium salts. The fourth, tris(N,N-diethyldithiocarbamato) dioxouranium(VI) [4], was the same as that originally examined by Bowman and Dori. It was re-examined to confirm their results and improve the precision.

2.2 Experimental

2.2.1 *Preparation*

Compounds [1] - [3] were prepared by the method described by Graziani *et. al.*[21] The required amine (30mmol) was added dropwise with stirring to a cooled solution containing carbon disulphide (30mmol) and potassium hydroxide (30mmol) in water (8cm^3), producing the potassium salt of the dithiocarbamate ligand. After a period of 30 minutes the clear yellow solution obtained was added slowly to a solution of uranyl acetate dihydrate (10mmol) in water (150 cm^3). The colour became dark red immediately and then $K[UO_2(DTC)_3].H_2O$ precipitated as a dark red powder. The compound was collected and washed with ether. Metathesis with the stoichiometric amount of tetraethylammonium chloride yielded ruby red crystals of compounds [1] - [3] which were suitable for structure determination. Initial attempts to obtain [4] by this method did not lead to the desired product, but gave what appears to be an O_2-bridged species. This has not yet been fully characterised. However, an alternative route involving the addition of 100cm^3 of 0.01M uranyl nitrate to a solution containing sodium N,N-diethyldithiocarbamate (5g) and potassium nitrate (5g) was successful. Metathesis using tetramethylammonium chloride then gave red crystals of [4].

2.2.2 *Data Collection and Structure Refinements*

Data were collected with a Syntex $P2_1$ four circle diffractometer. Background intensities were measured at each end of the scan for 0.25 of the scan time. Three standard reflections which were monitored every 200 reflections, showed slight changes during the data collection; the data were rescaled for this. Unit cell dimensions and standard deviations were obtained by least squares fit to 15 high angle reflections ($25 \leq 2\theta \leq 29$). Observed reflections [$I/\sigma(I) \geq 3.0$] were corrected for Lorentz, polarisation and absorption effects, the last with ABSCOR[22] for [1] and by Gaussian methods [2]-[4]. The crystal data and data collection conditions for each compound are given in Table 2.1.

For compound [1], systematic absences $h0l; l \neq n$ and $0k0; k \neq 2n$ indicated the space group $P2_1/c$ and the position of the uranium atom was determined from a three dimensional Patterson map. The atomic coordinates of the non-hydrogen atoms were found by successive Fourier syntheses and all were refined anisotropically. Hydrogen atoms were inserted at calculated positions with isotropic temperature factors U=0.07Å^2.

Compound [2] showed no systematic absences in the data collection. Analysis of the E-statistics printed as part of the Patterson routine showed it to be centrosymmetric, with two independent uranium atoms in the asymmetric unit. The positions of the lighter non-hydrogen atoms were located and refined by successive Fourier maps using anisotropic temperature factors for all atoms. Hydrogens were inserted at fixed positions with isotropic temperature factors U=0.07Å^2.

Systematic absences for compound [3], $0kl; l \neq 2n$; $h0l; h \neq 2n$; and $hk0; k \neq 2n$ gave the space group as *Pcab* which was rotated to the standard *Pbca*. The Patterson map showed two uranium atoms. These were inserted and the positions of the lighter atoms determined by Fourier syntheses. Anisotropic temperature factors were used for the sulphur, oxygen, nitrogen, and α-carbon atoms. The remainder were refined isotropically. Hydrogens were inserted at fixed positions with isotropic temperature factors U=0.07Å^2.

Systematic absences for [4], $0kl; k+l \neq 2n$ $h0l; h \neq 2n$ gave a choice of two possible space groups: $Pna2_1$ and *Pnam*: density calculations were consistent with 4 molecules per cell. If the space group was *Pnam*, then the molecule would be planar, with the uranium and sulphur atoms lying on a mirror plane. In view of the steric interactions that this would introduce in the equatorial plane, this seemed unlikely and $Pna2_1$ was selected. The position of the uranium atom was determined from a three dimensional Patterson map. The positions of the lighter non-hydrogen atoms were determined from successive difference Fourier syntheses, being cautious to allow for atoms generated by false symmetry. Anisotropic temperature factors were used for all non-hydrogen atoms, which were inserted at calculated positions with isotropic temperature factors U=0.07Å^2. Refinement gave a final R=0.048. This successful refinement confirms the space

group selection. In addition, a centrosymmetric model with half-occupancy ligand molecules disordered about the mirror plane was also tested but could not be refined beyond R=0.12.

One of the independent cation molecules of [2] and [3] has occupancy 0.5 for its carbon atoms since these are disordered over two sites. A weighting scheme of the form $W = 1/\sigma^2(F) + g(F^2)$) was applied to all three complexes and shown to be satisfactory by weight analysis. Final *R* -factors and the weighting constants are given in Table 2.1.

Calculations were performed using the SHELXTL system[23] on a Data General DG30 Desk Top computer. Table 2.2 gives a comparison of the average values of salient bond lengths and angles. Final atomic coordinates are given in Tables 2.3 - 2.6. Bond lengths and angles are listed in Tables 2.7 - 2.10. Details of least squares planes are listed in Table 2.11. Views of the anions of [1] - [4], and their unit cells are shown in Figures 2.1 - 2.9. A further view of [3] (Figure 2.6) directed along the U - C - N line of one Me_2NCS_2 group is also included to show the puckering of the sulphur atoms in the equatorial plane.

2.3 Discussion

All four complexes exhibit hexagonal bipyramidal coordination about the central uranium atom, involving three bidentate dithiocarbamate ligands in the equatorial plane and two axial oxygen atoms; this being the only stereochemistry that can accommodate the short, linear uranyl group.

U-O(uranyl) bond lengths in the range 1.735(5) - 1.862(12)Å are as expected, and not dissimilar from the values found for other hexa-coordinated UO_2^{2+} species.[24] U-S bonds for each complex are respectively 2.911(2) - 3.021(2)Å [1]; 2.900(7) - 2.981(6)Å [2]; 2.895(6) - 2.962(6)Å [3]; and 2.902 - 2.960Å [4]. The bond lengths determined by Bowman and Dori lie below these ranges, U-O 1.69(5) and 1.72(4)Å, U-S 2.80(1)Å, presumably a result of their failure to fully refine the structure. Indeed some of their values (particularly the S-U-S bond angle) are clearly in error.

The uranyl bond angle varies from being essentially linear (179.5(5)°) to showing a slight deviation (177.2(5)°). This "linearity" seems to be controlled by the degree of puckering of the sulphurs in the equatorial plane. and a general trend which emerges for compounds [1] - [3] is that the greater the puckering, the closer the uranyl group approaches to linearity. This is illustrated in Table 2.2 where the maximum puckering of [1] is 0.31(5)Å with an O-U-O angle 178.3(3) compared to 0.56(5)Å deviation for [3] with mean O-U-O 179.0(8). The greater pucker in [3] compared to [2] may be attributed to a shorter U-S or U-O bond in the latter. Compound [4], however, does not fit this trend, and puckering above and below the equatorial plane of -0.30 (S2) to +0.32 (S3), *i.e.* 0.6Å occurrs with an O-U-O(uranyl) angle of 177.2(5). This greater

deviation may be associated with the presence of the smaller tetramethylammonium cation. In each compound, the dithiocarbamate ligand defines an "almost perfect" hexagon. Mean bite angles are slightly less than the ideal 60.0°, and range 58.7(1) - 59.1(2)° with intermolecular angles 61.5(1) - 62.1(2)°. Intramolecular S - S(bite) distances within each compound are similar and range 2.873(4) - 2.898(5)Å. S - S contacts between adjacent ligands are not much greater and range 2.991(4) - 3.029(6)Å. Both sets of distances are well within the sum of the van der Waals radii for two sulphur atoms. This may be a result of the puckering which alleviates equatorial strain, but causes the sulphur atoms to approach one another more closely in order to maintain the bite angle. Support for this theory is supplied by the corresponding values for dithiophosphinate complexes[25] where the bite angle is much larger (110.5(2)Å) than that encountered for the dithiocarbamate ligands. As a result, steric crowding in the equatorial plane prevents the coordination of three ligands and the sulphur atoms become less puckered (maximum value 0.15Å). The bite distance in these dithiophosphinate complexes approaches more closely the sum of the van der Waals radii for two sulphur atoms. The complexes are not coordinatively unsaturated, the fifth site of the pentagonal bipyramid is taken by molecules of alcohol, triphenylphosphine oxide or chloride atoms.

In [1], the α-carbon atoms are displaced with respect to the mean equatorial plane. C(15) is above (+0.08), C(25) is below (-0.04) whilst C(35) is virtually coplanar (-0.0006). The pyrrolidine rings are displaced in the same direction as the α-carbons with the exception of N(3)-C(33) which lies above the plane, with C(34) below. This is presumably a result of packing interactions. All the piperidine rings in compound [2] adopt the chair conformation with the chair out of plane displacement 0.54Å. The cation of the second molecule in the asymmetric unit is disordered over two sites. In the first molecule of the asymmetric unit of [3], all of the Me_2N-C moieties are directed below the equatorial plane and away from O(11), (Table 2.14). In the second molecule the units are either directed above, below, or twisted about the mean plane. In [4], the α-carbon atoms C(11) and C(21) both lie below the mean equatorial plane defined by the six sulphur atoms (0.25, 0.09Å respectively) whilst α-carbon C(31) lies 0.20Å above. The positions of the carbon atoms of the ethyl groups of these ligands with respect to this plane is influenced by the extent of the displacement of the sulphur atoms above or below the plane; *e.g.* S(2) lies further below this plane than S(1) does above, and carbon atoms C(11) - C(14) are all found below. Only C(15) of this ligand molecule is found above. A similar result is found for C(32) - C(35) which are found above with the exception of C(33). In the third dithiocarbamate ligand, the β carbon atoms C(22) and C(24) both lie below the plane, but the terminal C-atoms of the ethyl groups C(23) and C(25) are found above the plane.

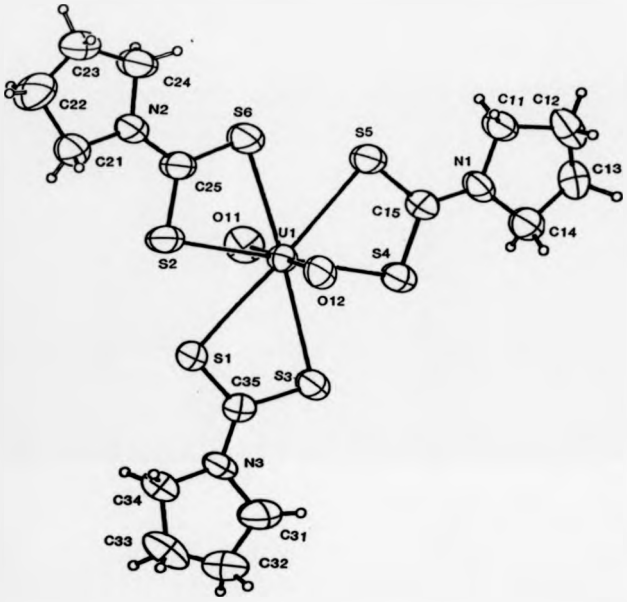

FIGURE 2.1 View of the anion of [1], showing atomic numbering scheme.

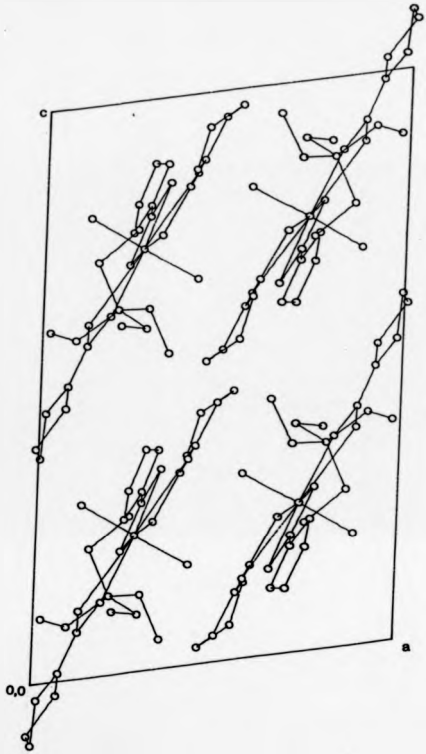

FIGURE 2.2 Packing diagram for [1]

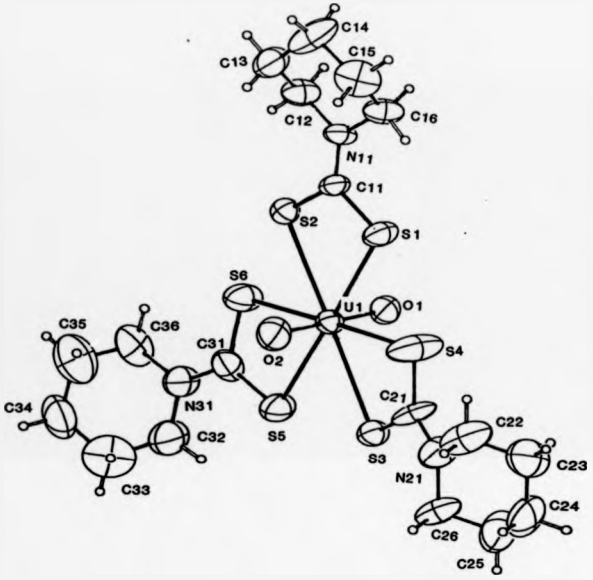

FIGURE 2.3 View of one anion of [2], showing atomic numbering scheme.

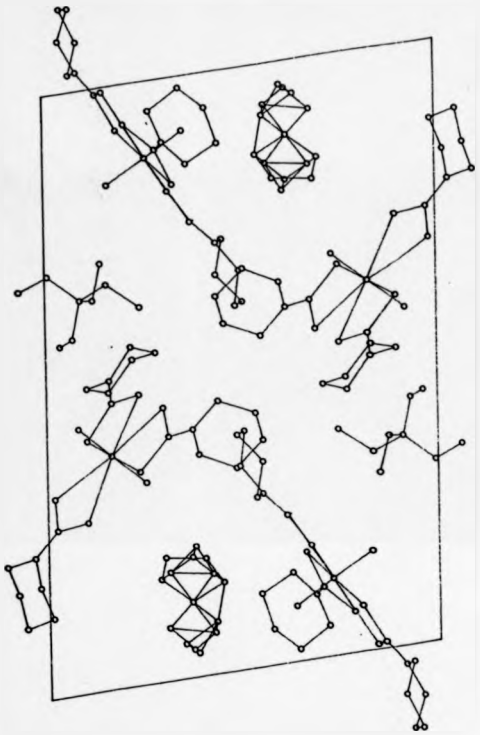

FIGURE 2.4 Packing diagram for [2]

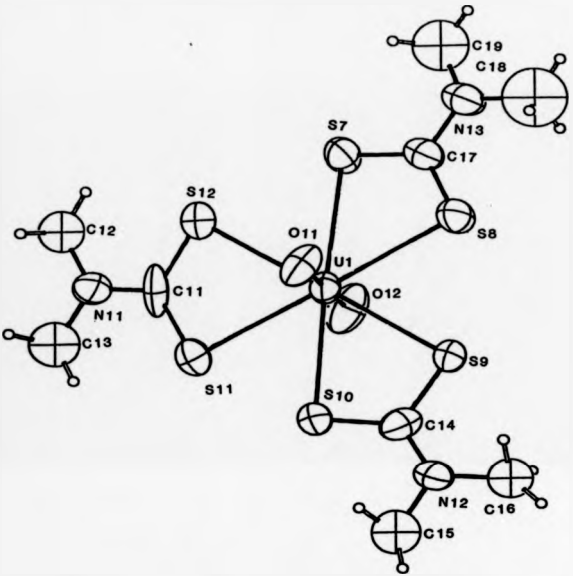

FIGURE 2.5 View of one anion of [3], showing the atomic numbering scheme.

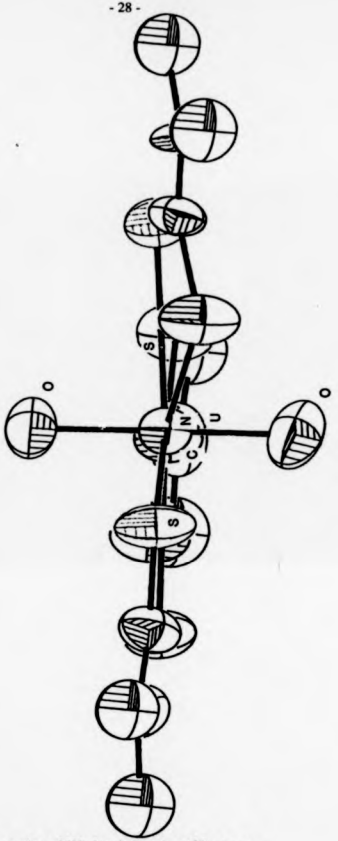

FIGURE 2.6 Side view of one anion of [3] showing pucker of S- atoms

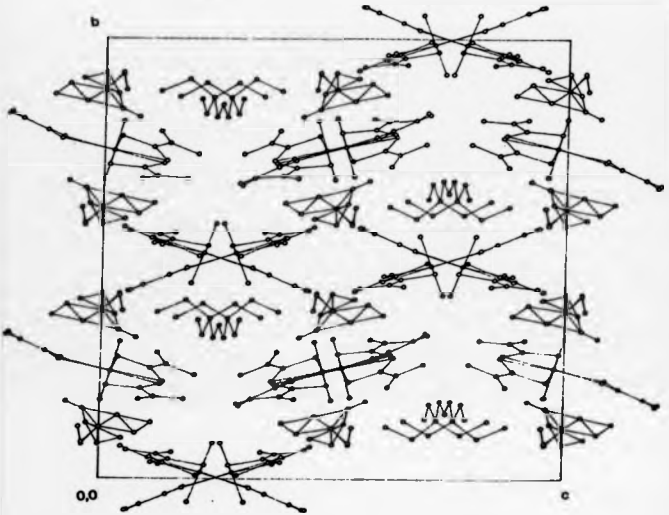

FIGURE 2.7 Packing diagram for [3]

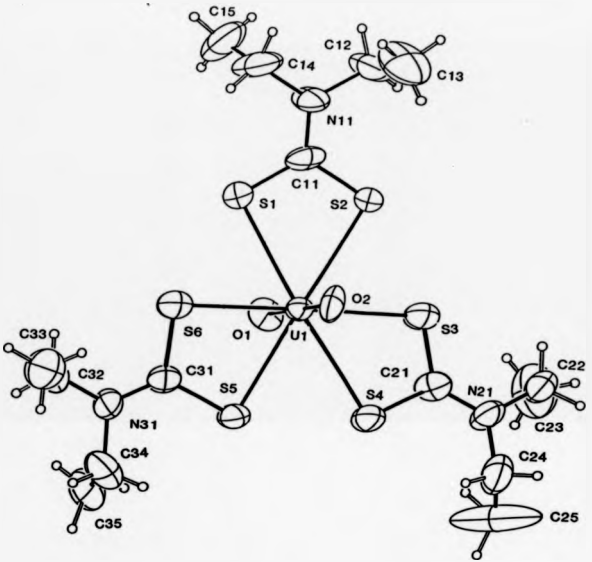

FIGURE 2.8 View of the anion of (4), showing atomic numbering scheme.

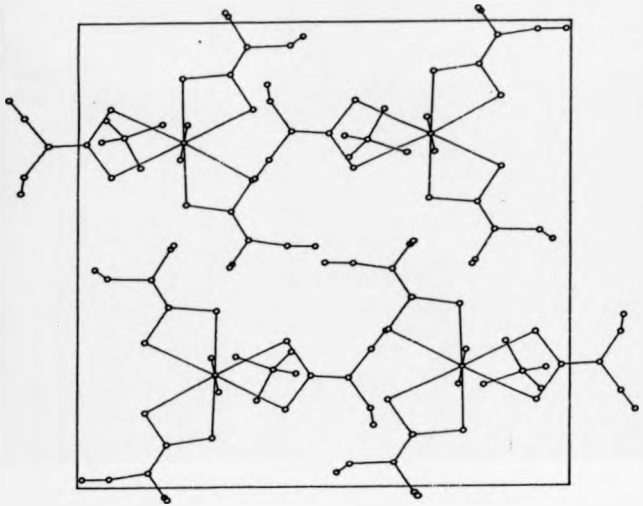

FIGURE 2.9 Packing diagram for [4].

TABLE 2.1

Crystal Data and Data Collection Conditions

Compound	[1]	[2]	[3]	[4]
Formula	$C_{23}H_{44}N_4O_2S_4U$	$C_{28}H_{38}N_4O_2S_4U$	$C_{17}H_{28}N_4O_2S_4U$	$C_{19}H_{42}N_4O_2S_4U$
M	838.36	881.10	760.91	788.54
D_c/g cm^{-3}	1.743	1.547	1.756	1.69
Z	4	4	16	4
Crystal System	Monoclinic	Triclinic	Orthorhombic	Orthorhombic
a/Å	17.322(4)	11.498(2)	20.613(5)	19.103(8)
b/Å	18.287(4)	16.938(4)	22.443(4)	17.228(6)
c/Å	10.227(3)	22.596(5)	24.879(5)	9.432(3)
α/°	90.00	81.33(2)	90.0	90.0
β/°	99.68(2)	85.08(2)	90.0	90.0
γ/°	89.96	77.89(2)	90.0	90.0
Systematic Absences	$h0l: l \neq 2n$ $0k0: k \neq 2n$	None	$0kl: l \neq 2n$ $h0l: h \neq 2n$ $hk0: h \neq 2n$	$0kl: k+l \neq 2n$ $h0l: h \neq 2n$
Space Group	$P2_1/c$	$P\bar{1}$	$Pbca$	$Pna2_1$
Crystal size/mm.	.38×.18×.17	.18×.32×.39	.13×.51×.32	.15×.45×.23
Max. transmission factor	0.64	0.63	0.82	0.53
Min. transmission factor	0.53	0.55	0.49	0.46
Temp./° C	16	16	16	16
Scan range about K_{α_1}-K_{α_2}/°	-1.1/+1.1	-1.0/+1.0	-1.0/+1.0	-1.10/+1.10
Reflections collected	6 037	10 279	9 548	3 192
Reflections observed [$I/\sigma(I) \geq 3.0$]	3 970	5 729	3 722	2 231
Weighting constant: g	0.0006	0.0018	0.0022	0.0018
R(final)	0.039	0.057	0.054	0.048
R_w (final)	0.039	0.061	0.057	0.050
max on final difference Fourier	1.89	2.02	1.26	1.79
min on final difference Fourier	0.67	-1.04	-1.06	-2.16
max δ/σ(final cycle)	0.90	0.688	0.623	0.273

TABLE 2.1 cont.

Analytical and infra red data

Compound	[1]	[2]	[3]	[4]
Formula	$C_{23}H_{46}N_4O_2S_4U$	$C_{28}H_{58}N_4O_2S_4U$	$C_{17}H_{38}N_4O_2S_4U$	$C_{19}H_{42}N_4O_2S_4U$
M	838.36	881.10	760.91	788.54
C (found)	32.17	35.21	26.25	28.68
(expected)	32.95	35.44	26.83	28.94
H (found)	5.16	5.56	4.97	5.26
(expected)	5.28	5.72	5.03	5.37
N (found)	6.82	6.28	7.57	6.32
(expected)	6.68	6.36	7.37	7.10
ν O-U-O	915	915	910	875
ν C-S	1000	1050	1000	1000
ν C-N	1490	1500	1500	1470

TABLE 2.2

Comparison of the averaged values for salient bond lengths(Å) angles(°), and out of plane puckering around the central uranium atom

Compound	[1]	[2]	[3]	[4]
U-O	1.755(5)	1.755(11)	1.768(13)	1.798(11)
U-S	2.947(2)	2.926(6)	2.935(7)	2.923(4)
S-S (Bite)	2.897(5)	2.873(1)	2.898(7)	2.887(6)
S-S (Intermolecular)	3.017(4)	2.991(2)	3.029(7)	3.014(5)
C_α-S	1.688(8)	1.702(20)	1.694(23)	1.707(6)
O-U-O	178.3(3)	179.2(5)	179.0(8)	177.2(5)
S-U-S (Bite)	58.7(1)	58.8(1)	59.1(2)	59.0(1)
S-U-S (Intermolecular)	61.5(1)	61.5(2)	61.9(2)	62.1(2)
S-C_α-S	117.4(8)	115.0(10)	118.6(13)	115.1(9)
S-Puckering(max)	0.31(5)	0.43(5)	0.56(5)	0.62(4)
Angle O-O line/ S_4 plane	89.0(4)	89.5(4)	88.0(4)	89.5(5)

TABLE 2.3

Atomic coordinates (×10⁴) for [I] (with standard deviations in parentheses).

ATOM	x	y	z	U
[illegible]	7249.3(3)	3861.7(2)	2355.5(3)	42(1)*
O(11)	3727(6)	3937(3)	1784(4)	65(2)*
O(12)	8756(6)	3783(3)	3657(4)	59(2)*
O(1)	7637.5(28)	5417.1(13)	2134.2(14)	65(1)*
O(2)	8746.1(29)	4356.2(13)	1178.2(15)	70(1)*
O(3)	6333.5(29)	5608.8(15)	3487.2(16)	79(1)*
O(4)	3622.9(28)	3565.3(12)	3613.3(14)	66(1)*
O(5)	6727.9(26)	3500.6(11)	3551.1(13)	63(1)*
O(6)	8136.4(29)	2814.7(13)	1138.2(15)	70(1)*
N(1)	3633(7)	1936(4)	3660(4)	57(3)*
N(2)	9237(8)	3581(4)	130(4)	60(3)*
N(4)	2082(7)	5043(4)	3619(4)	56(3)*
N(3)	7068(8)	6485(4)	3136(4)	61(3)*
C(11)	5850(10)	1163(4)	3678(6)	52(4)*
C(12)	3515(10)	778(5)	4356(6)	76(4)*
C(13)	4590(11)	1290(5)	4715(5)	73(4)*
C(14)	5853(10)	2042(5)	4543(5)	67(4)*
C(15)	6035(8)	2468(4)	3395(5)	53(3)*
C(21)	9834(12)	3956(5)	-285(6)	74(4)*
C(22)	9955(14)	3567(6)	-1067(7)	98(6)*
C(23)	10083(11)	2810(5)	-892(6)	78(4)*
C(24)	9285(9)	2666(5)	-244(5)	62(4)*
C(25)	8750(9)	3498(5)	811(5)	56(3)*
C(31)	5618(13)	6697(5)	3835(6)	90(5)*
C(32)	6579(15)	7439(6)	3869(7)	113(7)*
C(33)	7449(15)	7623(6)	3182(8)	119(7)*
C(34)	7550(11)	6981(5)	2692(5)	73(4)*
C(35)	7077(8)	5682(4)	2943(5)	51(3)*
C(41)	2984(12)	4391(7)	4008(7)	98(6)*
C(42)	2181(13)	3656(6)	3905(8)	98(6)*
C(43)	2972(12)	5738(6)	3668(8)	102(6)*
C(44)	3553(13)	5970(7)	4491(7)	99(6)*
C(45)	1482(13)	4879(7)	2754(7)	108(6)*
C(46)	2587(14)	4675(8)	2260(8)	112(6)*
C(47)	928(12)	5149(7)	4071(9)	116(7)*
C(48)	228(14)	5866(7)	3876(11)	137(8)*

* Equivalent isotropic U defined as one third of the trace of the orthogonalised U_{ij} tensor

TABLE 2.4

Atomic coordinates (×10⁴) for [2] (with standard deviations in parentheses).

atom	x	y	z	U
U(1)	526.4(6)	2647.6(4)	8718.8(2)	41(1)*
U(2)	2041.5(7)	1710.8(4)	3865.1(3)	49(1)*
S(1)	-1548(5)	1927(3)	9243(2)	61(2)*
S(2)	551(4)	1578(3)	9914(2)	50(2)*
S(3)	393(4)	3794(3)	7539(2)	53(2)*
S(4)	-1684(6)	3210(5)	8110(3)	112(3)*
S(5)	2624(5)	3341(4)	8216(2)	76(2)*
S(6)	2757(5)	2126(4)	9323(2)	74(2)*
S(7)	3512(6)	188(3)	3295(2)	83(2)*
S(8)	1240(5)	1065(3)	2825(2)	66(2)*
S(9)	-411(5)	2432(3)	3531(2)	72(2)*
S(10)	431(5)	3028(3)	4537(2)	69(2)*
S(11)	2996(5)	2421(3)	4814(2)	66(2)*
S(12)	4529(6)	1067(3)	4168(2)	85(3)*
O(1)	129(11)	3608(8)	9084(5)	69(5)*
O(2)	950(10)	1676(6)	8354(4)	52(5)*
O(3)	2488(11)	2589(7)	3344(4)	63(5)*
O(4)	1571(12)	843(7)	4393(4)	68(5)*
N(11)	-1389(12)	902(7)	10305(5)	48(5)*
N(21)	-1747(14)	4437(11)	7126(6)	77(7)*
N(31)	4400(14)	3101(10)	8940(6)	68(7)*
N(41)	2626(14)	-343(10)	2362(7)	78(7)*
N(51)	-1690(14)	3807(9)	4100(6)	70(7)*
N(61)	5228(15)	1657(10)	5113(7)	82(8)*
N(71)	1501(14)	927(9)	6506(5)	61(6)*
N(81)	9885(16)	3734(10)	1247(6)	83(8)*
C(11)	-853(16)	1395(9)	9894(6)	46(6)*
C(12)	-800(16)	448(11)	10864(7)	58(7)*
C(13)	-1533(20)	719(14)	11398(8)	76(10)*
C(14)	-2725(23)	494(14)	11414(7)	96(11)*
C(15)	-3357(18)	921(12)	10814(8)	85(10)*
C(16)	-2558(15)	700(10)	10282(7)	58(7)*
C(22)	-3051(21)	4587(14)	7169(8)	109(12)*
C(23)	-3586(23)	4439(16)	6598(10)	138(15)*
C(24)	-3116(27)	5081(15)	6106(9)	122(14)*
C(21)	-1089(19)	3824(11)	7546(7)	74(8)*
C(25)	-1745(23)	4903(17)	6052(9)	100(13)*
C(26)	-1250(21)	5014(13)	6608(7)	91(10)*
C(31)	3391(16)	2906(10)	8838(7)	60(8)*
C(32)	5012(21)	3697(14)	8519(8)	100(12)*
C(33)	5152(21)	4510(14)	8787(11)	110(12)*
C(34)	5729(23)	4200(15)	9411(10)	105(13)*
C(35)	5122(23)	3534(13)	9806(11)	120(13)*
C(36)	5043(18)	2760(12)	9488(9)	79(10)*

TABLE 2.4 cont.

Atomic coordinates (×10⁴) for [2] (with standard deviations in parentheses).

C(41)	2463(17)	246(10)	2772(7)	59(8)*
C(42)	1936(18)	-211(15)	1862(8)	80(10)*
C(43)	2622(25)	95(16)	1321(10)	109(14)*
C(44)	3817(23)	-575(18)	1224(9)	114(14)*
C(45)	4497(21)	-748(19)	1789(9)	113(14)*
C(46)	3810(22)	-1007(14)	2284(10)	106(12)*
C(51)	-684(17)	3158(11)	4045(7)	61(8)*
C(52)	-2621(18)	3972(12)	3666(7)	77(9)*
C(53)	-2829(20)	4983(12)	3371(8)	84(10)*
C(54)	-3073(25)	5581(13)	3778(11)	121(14)*
C(55)	-2078(20)	5387(14)	4228(9)	85(11)*
C(56)	-1959(21)	4441(13)	4516(9)	95(11)*
C(61)	4365(16)	1721(10)	4734(7)	51(7)*
C(62)	5075(21)	2219(14)	5618(10)	95(11)*
C(63)	5952(24)	2857(17)	5480(12)	117(14)*
C(64)	7155(21)	2308(13)	5427(9)	109(12)*
C(65)	7309(19)	1684(15)	4926(11)	130(13)*
C(66)	6407(20)	1093(13)	5041(9)	108(11)*
C(71)	2677(23)	1249(18)	6487(9)	126(14)*
C(72)	2986(25)	1461(18)	7079(10)	140(16)*
C(73)	1549(22)	68(12)	6967(9)	108(12)*
C(74)	2492(26)	-680(16)	6824(14)	191(20)*
C(75)	1366(22)	725(14)	5886(7)	100(11)*
C(76)	265(21)	381(14)	5798(8)	94(11)*
C(77)	461(23)	1605(15)	6718(9)	117(13)*
C(78)	397(32)	2483(19)	6259(11)	53(9)
C(81)	9400(46)	2925(27)	1691(18)	87(13)
C(82)	8787(46)	4535(30)	1498(20)	110(15)
C(83)	8504(61)	3076(40)	2038(26)	148(22)
C(84)	8089(37)	4082(23)	1945(16)	75(11)
C(85)	8414(50)	3550(33)	557(22)	92(17)
C(86)	8905(33)	4349(20)	862(14)	58(9)
C(87)	8468(47)	3940(32)	397(21)	85(15)
C(88)	10346(49)	4321(31)	684(21)	113(16)
C(89)	11118(43)	3143(28)	868(19)	94(14)
C(90)	11560(44)	3766(28)	460(18)	93(14)
C(91)	10374(33)	4282(21)	1664(14)	55(9)
C(92)	10541(47)	3148(30)	1791(19)	101(14)
C(93)	11033(47)	3819(31)	2151(21)	79(16)
C(94)	11547(47)	3761(30)	1986(20)	76(15)
Co(1)	5076(41)	2698(26)	2133(18)	73(11)
Co(2)	5254(44)	2810(28)	2697(19)	100(14)
Co(3)	4414(42)	2897(28)	2106(18)	90(13)
O(5)	5699(35)	2858(22)	1766(16)	135(12)

* Equivalent isotropic U defined as one third of the trace of the orthogonalised U_{ij} tensor.

TABLE 2.5

Atomic coordinates (×10⁴) for [3] (with standard deviations in parentheses).

x/a	y	z	U
O(1)	-267 0(4)	2539 0(3)	4791 1(3)	45(1)*
O(2)	7472 1(5)	-140 4(3)	2151.4(3)	46(1)*
S(1)	8157(4)	289(3)	3231(3)	78(3)*
S(2)	3900(3)	-304(3)	2234(3)	61(2)*
S(3)	6262(3)	-566(3)	1052(3)	77(3)*
S(4)	5606(3)	-489(3)	1071(3)	70(3)*
S(5)	5859(4)	-72(3)	2058(3)	71(3)*
S(6)	5734(4)	191(3)	3209(3)	77(3)*
S(7)	-1535(3)	2222(3)	4639(3)	64(2)*
S(8)	-337(3)	2772(3)	3678(3)	73(3)*
S(9)	460(3)	2830(3)	3735(3)	64(3)*
S(10)	1029.7(3)	2356(3)	4881(3)	67(2)*
S(11)	430(4)	3274(3)	5986(3)	66(3)*
S(12)	-582(4)	3253(3)	5860(3)	78(3)*
O(11)	-569(8)	5193(5)	4932(7)	70(6)*
O(12)	-73(10)	1876(6)	4597(7)	85(8)*
O(21)	7485(9)	-802(5)	2423(7)	66(6)*
O(22)	7534(10)	526(6)	1875(7)	66(7)*
N(11)	-297(16)	1836(7)	6768(8)	65(8)*
N(12)	1700(9)	3117(7)	3874(8)	62(8)*
N(13)	-2196(11)	2378(11)	3607(10)	97(11)*
N(21)	5512(10)	-475(7)	1040(8)	63(8)*
N(22)	7419(13)	583(8)	4136(8)	83(10)*
N(23)	9517(8)	-555(7)	1213(8)	49(7)*
C(11)	-266(13)	2885(8)	6222(9)	73(11)*
C(12)	-882(12)	1665(10)	7030(11)	76(8)
C(13)	276(14)	1715(11)	7083(12)	93(9)
C(14)	1155(12)	2926(9)	4152(10)	63(9)*
C(15)	2290(14)	3182(11)	4193(12)	91(10)
C(16)	1748(13)	3176(10)	3229(11)	74(8)
C(17)	-1634(12)	2463(10)	3947(11)	64(9)*
C(18)	-2203(22)	2641(15)	3014(16)	168(18)
C(19)	-2754(15)	2103(12)	3796(15)	119(12)
C(21)	6081(11)	-357(9)	1355(10)	68(9)*
C(22)	5517(14)	-727(10)	448(10)	77(8)
C(23)	4868(13)	-324(10)	1261(13)	87(9)
C(24)	7425(12)	353(9)	3574(9)	57(9)*
C(25)	6786(16)	709(12)	4411(14)	108(11)
C(26)	8037(15)	719(11)	4458(14)	98(10)
C(27)	8964(11)	-441(8)	1466(10)	55(9)*
C(28)	10138(13)	-682(10)	1538(12)	80(8)
C(29)	9575(15)	-650(10)	568(11)	87(9)

TABLE 2.5 cont

N(31)	4881(10)	1339(7)	2689(8)	69(6)
C(31)	4747(14)	1811(10)	2146(11)	79(8)
C(32)	4616(16)	1326(11)	1582(14)	104(10)
C(33)	4317(17)	1713(13)	2858(14)	104(11)
C(34)	3644(19)	1370(14)	2953(16)	138(14)
C(35)	5026(15)	924(10)	3222(13)	93(9)
C(36)	5185(18)	1199(12)	3886(16)	120(12)
C(37)	5408(16)	1782(12)	2616(13)	99(10)
C(38)	6072(19)	1496(12)	2486(16)	121(12)
N(41)	2308(14)	1158(11)	4986(13)	71(8)
C(40)	3254(45)	904(34)	5507(43)	181(39)
C(41)	2985(39)	779(28)	4948(36)	145(29)
C(42)	3187(56)	1253(38)	4750(47)	214(47)
C(43)	2240(33)	1780(24)	4286(28)	110(23)
C(45)	1351(54)	811(39)	4627(43)	163(40)
C(46)	1211(46)	1171(34)	4559(39)	168(36)
C(47)	2141(69)	1003(54)	5751(65)	242(64)
C(39)	2456(43)	1601(29)	4643(35)	115(24)
C(51)	2083(37)	762(27)	4628(31)	121(25)
C(52)	2062(35)	1423(29)	5383(33)	279(34)
C(54)	2111(53)	1270(43)	6077(47)	172(43)

* Equivalent isotropic U defined as one third of the trace of the orthogonalised U_{ij} tensor.

TABLE 2.6

Atomic coordinates (x10⁴) for [4] (standard deviations in parentheses)

atom	x	y	z	U
U(1)	2413.1(2)	7168.5(3)	2500.0	34(1)*
S(1)	3143(2)	5683(2)	2799(7)	51(2)*
S(2)	1676(2)	5704(2)	2068(5)	50(2)*
S(3)	1071(3)	7228(3)	1046(7)	57(2)*
S(4)	1618(2)	8597(3)	2384(8)	65(2)*
S(5)	3119(2)	8608(2)	3309(7)	60(2)*
S(6)	3792(2)	7145(3)	3931(6)	56(2)*
O(1)	2789(7)	7249(7)	834(11)	49(4)*
O(2)	2051(5)	7090(7)	4327(14)	55(4)*
N(11)	2357(7)	4395(7)	2633(45)	70(6)*
N(21)	309(8)	8526(9)	1312(18)	62(6)*
N(31)	4473(7)	8478(8)	4056(17)	55(5)*
N(1)	2533(7)	5956(7)	7604(52)	58(5)*
C(11)	2399(8)	5175(8)	2580(41)	55(5)*
C(12)	1699(10)	3950(10)	2566(35)	87(8)*
C(13)	1333(14)	3887(15)	3957(30)	107(12)*
C(14)	2964(13)	3945(11)	3120(29)	98(11)*
C(15)	3357(14)	3651(14)	1907(32)	117(14)*
C(21)	928(10)	8153(10)	1539(18)	48(6)*
C(22)	-275(10)	8131(11)	613(24)	67(8)*
C(23)	-211(14)	8188(18)	-933(28)	118(13)*
C(24)	182(11)	9317(13)	1869(29)	87(10)*
C(25)	187(25)	9901(16)	816(37)	207(27)*
C(31)	3878(8)	8134(10)	3818(22)	50(6)*
C(32)	5128(10)	8076(13)	4385(25)	75(8)*
C(33)	5207(13)	8029(14)	5899(27)	97(11)*
C(34)	4582(12)	9366(13)	3997(33)	105(12)*
C(35)	4686(11)	9638(13)	2517(34)	144(16)*
C(1)	2986	5580	8776	152(16)*
C(2)	1873(13)	6287(23)	8836(28)	153(18)*
C(3)	2831(21)	6715(21)	7214(35)	262(26)*
C(4)	2434(17)	5498(14)	6365(27)	129(17)*

*Equivalent isotropic U defined as one third of the trace of the orthogonalised U_{ij} tensor.

TABLE 2.7

Bond lengths (Å)
and angles (°) for [1] (standard deviations in parentheses).

a) Bond lengths

U(1)-O(11)	1.752(6)	U(1)-O(13)	1.758(6)
U(1)-S(1)	2.915(2)	U(1)-S(2)	2.934(3)
U(1)-S(3)	3.018(3)	U(1)-S(4)	2.923(3)
U(1)-S(5)	2.937(2)	U(1)-S(6)	2.952(3)
S(1)-S(3)	2.888(4)	S(1)-C(35)	1.672(9)
S(2)-S(6)	2.889(3)	S(2)-C(25)	1.681(9)
S(3)-C(35)	1.708(9)	S(4)-S(5)	2.891(4)
S(4)-C(15)	1.707(9)	S(5)-C(15)	1.693(9)
S(6)-C(25)	1.674(9)	N(1)-C(11)	1.464(10)
N(1)-C(14)	1.459(13)	N(1)-C(15)	1.346(11)
N(2)-C(21)	1.465(13)	N(2)-C(24)	1.463(11)
N(2)-C(25)	1.373(12)	N(4)-C(41)	1.546(13)
N(4)-C(43)	1.558(14)	N(4)-C(45)	1.550(14)
N(4)-C(47)	1.534(17)	N(3)-C(31)	1.466(15)
N(3)-C(34)	1.439(12)	N(3)-C(35)	1.365(11)
C(11)-C(12)	1.517(15)	C(12)-C(13)	1.508(15)
C(13)-C(14)	1.499(13)	C(21)-C(22)	1.551(16)
C(22)-C(23)	1.417(15)	C(23)-C(24)	1.518(16)
C(31)-C(32)	1.404(15)	C(32)-C(33)	1.398(20)
C(33)-C(34)	1.464(15)	C(41)-C(42)	1.538(16)
C(43)-C(44)	1.510(18)	C(45)-C(46)	1.573(20)
C(47)-C(48)	1.508(19)		

TABLE 2.7 cont.

b) Bond angles

O(11)-U(1)-O(12)	178.7(3)	O(11)-U(1)-S(1)	87.6(2)
O(12)-U(1)-S(1)	93.8(2)	O(11)-U(1)-S(2)	92.6(2)
O(12)-U(1)-S(2)	86.6(2)	S(1)-U(1)-S(2)	59.7(1)
O(11)-U(1)-S(3)	93.4(2)	O(12)-U(1)-S(3)	85.6(2)
S(1)-U(1)-S(3)	58.8(1)	S(2)-U(1)-S(3)	117.0(1)
O(11)-U(1)-S(4)	88.8(2)	O(12)-U(1)-S(4)	89.9(2)
S(1)-U(1)-S(4)	120.6(1)	S(2)-U(1)-S(4)	176.6(1)
S(2)-U(1)-S(4)	63.1(1)	O(11)-U(1)-S(5)	88.5(2)
O(12)-U(1)-S(5)	90.9(2)	S(1)-U(1)-S(5)	177.2(1)
S(2)-U(1)-S(5)	120.6(1)	S(3)-U(1)-S(5)	122.9(1)
S(4)-U(1)-S(5)	59.1(1)	O(11)-U(1)-S(6)	88.1(2)
O(12)-U(1)-S(6)	91.7(2)	S(1)-U(1)-S(6)	118.1(1)
S(2)-U(1)-S(6)	58.8(1)	S(3)-U(1)-S(6)	175.3(1)
S(4)-U(1)-S(6)	121.6(1)	S(5)-U(1)-S(6)	61.5(1)
U(1)-S(1)-S(3)	62.8(1)	U(1)-S(1)-C(35)	94.7(3)
S(3)-S(1)-C(35)	32.0(3)	U(1)-S(2)-S(6)	60.9(1)
U(1)-S(2)-C(25)	91.2(3)	S(6)-S(2)-C(25)	30.5(3)
U(1)-S(3)-S(1)	59.2(1)	U(1)-S(3)-C(35)	90.4(3)
S(1)-S(3)-C(35)	31.2(3)	U(1)-S(4)-S(5)	60.7(1)
U(1)-S(4)-C(15)	92.1(3)	S(5)-S(4)-C(15)	31.6(3)
U(1)-S(5)-S(4)	60.2(1)	U(1)-S(5)-C(15)	91.9(3)
S(4)-S(5)-C(15)	31.9(3)	U(1)-S(6)-S(2)	60.3(1)
U(1)-S(6)-C(25)	90.7(3)	S(2)-S(6)-C(25)	30.6(3)
C(11)-N(1)-C(14)	112.5(7)	C(11)-N(1)-C(15)	121.3(8)
C(14)-N(1)-C(15)	126.1(7)	C(21)-N(2)-C(24)	112.1(8)
C(21)-N(2)-C(25)	123.5(7)	C(24)-N(2)-C(25)	124.4(7)
C(41)-N(4)-C(45)	109.7(7)	C(41)-N(4)-C(45)	111.8(8)
C(43)-N(4)-C(45)	110.0(8)	C(41)-N(4)-C(47)	106.5(8)
C(43)-N(4)-C(47)	111.2(8)	C(45)-N(4)-C(47)	107.7(8)
C(31)-N(3)-C(34)	111.0(7)	C(31)-N(3)-C(35)	124.8(8)
C(34)-N(3)-C(35)	124.2(8)	N(1)-C(11)-C(12)	103.3(8)
C(11)-C(12)-C(13)	104.7(8)	C(12)-C(13)-C(14)	105.1(9)
N(1)-C(14)-C(13)	103.3(7)	S(4)-C(15)-S(5)	116.5(5)
S(4)-C(15)-N(1)	120.3(7)	S(5)-C(15)-N(1)	123.2(6)
N(2)-C(21)-C(22)	101.5(8)	C(21)-C(22)-C(23)	106.3(9)
C(22)-C(23)-C(24)	106.6(10)	N(2)-C(24)-C(23)	103.6(7)
S(2)-C(25)-S(6)	118.9(6)	S(2)-C(25)-N(2)	119.5(7)
S(6)-C(25)-N(2)	121.6(6)	N(3)-C(31)-C(32)	105.7(10)
C(31)-C(32)-C(33)	108.8(11)	C(32)-C(33)-C(34)	111.6(10)
N(3)-C(34)-C(33)	102.3(9)	S(1)-C(35)-S(3)	116.8(5)
S(1)-C(35)-N(3)	120.2(7)	S(3)-C(35)-N(3)	123.0(7)
N(4)-C(41)-C(42)	114.2(9)	N(4)-C(43)-C(44)	114.4(10)
N(4)-C(45)-C(46)	111.6(9)	N(4)-C(47)-C(48)	112.3(12)

TABLE 2.8

Bond lengths (Å) and angles (°) for [2]
(standard deviations in parentheses).

a) Bond lengths

U(1)-S(1)	2.913(5)	U(1)-S(2)	2.929(4)
U(1)-S(3)	2.948(4)	U(1)-S(4)	2.900(6)
U(1)-S(5)	2.904(6)	U(1)-S(6)	2.913(6)
U(1)-O(1)	1.734(12)	U(1)-O(2)	1.750(10)
U(2)-S(7)	2.946(5)	U(2)-S(8)	2.958(5)
U(2)-S(9)	2.922(5)	U(2)-S(10)	2.926(5)
U(2)-S(11)	2.922(5)	U(2)-S(12)	2.926(6)
U(2)-O(3)	1.765(10)	U(2)-O(4)	1.773(11)
S(1)-S(2)	2.873(7)	S(1)-C(11)	1.737(14)
S(2)-C(11)	1.700(19)	S(3)-S(4)	2.856(8)
S(3)-C(21)	1.693(23)	S(4)-C(21)	1.647(18)
S(5)-S(6)	2.863(6)	S(5)-C(31)	1.695(17)
S(6)-C(31)	1.718(17)	S(7)-S(8)	2.888(8)
S(7)-C(41)	1.739(20)	S(8)-C(41)	1.675(17)
S(9)-S(10)	2.876(8)	S(9)-C(51)	1.681(17)
S(10)-C(51)	1.728(19)	S(11)-S(12)	2.891(7)
S(11)-C(61)	1.714(16)	S(12)-C(61)	1.704(17)
N(11)-C(11)	1.297(19)	N(11)-C(12)	1.488(19)
N(11)-C(16)	1.445(24)	N(21)-C(22)	1.466(29)
N(21)-C(21)	1.376(21)	N(21)-C(26)	1.497(23)
N(31)-C(31)	1.302(26)	N(31)-C(32)	1.458(26)
N(31)-C(36)	1.465(24)	N(41)-C(41)	1.354(23)
N(41)-C(42)	1.401(25)	N(41)-C(46)	1.526(26)
N(51)-C(51)	1.360(22)	N(51)-C(52)	1.471(25)
N(51)-C(56)	1.411(25)	N(61)-C(61)	1.344(25)
N(61)-C(62)	1.500(29)	N(61)-C(66)	1.452(25)
N(71)-C(71)	1.524(33)	N(71)-C(73)	1.530(21)
N(71)-C(75)	1.506(23)	N(71)-C(77)	1.497(25)
N(81)-C(81)	1.621(46)	N(81)-C(82)	1.679(47)
N(81)-C(86)	1.541(35)	N(81)-C(88)	1.556(48)
N(81)-C(89)	1.748(45)	N(81)-C(91)	1.552(41)
N(81)-C(92)	1.554(45)	C(12)-C(13)	1.471(24)
C(13)-C(14)	1.475(36)	C(14)-C(15)	1.579(26)
C(15)-C(16)	1.483(25)	C(22)-C(23)	1.512(34)
C(23)-C(24)	1.454(32)	C(24)-C(25)	1.548(40)
C(25)-C(26)	1.468(31)	C(32)-C(33)	1.498(34)
C(33)-C(34)	1.575(34)	C(34)-C(35)	1.486(33)
C(35)-C(36)	1.482(32)	C(42)-C(43)	1.465(38)
C(43)-C(44)	1.546(35)	C(44)-C(45)	1.514(32)
C(45)-C(46)	1.368(32)	C(52)-C(53)	1.440(24)
C(53)-C(54)	1.446(31)	C(54)-C(55)	1.547(36)
C(55)-C(56)	1.459(27)	C(62)-C(63)	1.517(38)
C(63)-C(64)	1.461(33)	C(64)-C(65)	1.555(34)
C(65)-C(66)	1.486(33)	C(71)-C(72)	1.510(35)
C(73)-C(74)	1.445(31)	C(75)-C(76)	1.504(37)
C(77)-C(78)	1.548(32)	C(81)-C(83)	1.243(78)

TABLE 2.8 cont.

a)Bond lengths

C(81)-C(84)	2.167(54)	C(81)-C(92)	1.465(79)
C(82)-C(84)	1.428(68)	C(82)-C(86)	1.494(56)
C(82)-C(91)	1.843(64)	C(83)-C(84)	1.479(66)
C(85)-C(86)	1.688(69)	C(85)-C(87)	0.655(67)
C(86)-C(87)	1.467(66)	C(86)-C(88)	1.665(66)
C(88)-C(89)	1.816(58)	C(88)-C(90)	1.557(66)
C(89)-C(90)	1.361(61)	C(89)-C(92)	2.134(68)
C(91)-C(92)	1.664(54)	C(91)-C(93)	1.481(56)
C(91)-C(94)	1.587(59)	C(92)-C(93)	1.603(77)
C(92)-C(94)	1.745(79)	C(93)-C(94)	0.669(70)
Co(1)-Co(2)	1.349(63)	Co(1)-Co(3)	1.310(69)
Co(1)-O(5)	1.082(56)	Co(2)-O(5)	2.116(56)

b) Bond angles

S(1)-U(1)-S(2)	58.9(1)	S(1)-U(1)-S(3)	119.5(1)
S(2)-U(1)-S(3)	176.9(1)	S(1)-U(1)-S(4)	61.3(2)
S(2)-U(1)-S(4)	119.6(2)	S(3)-U(1)-S(4)	58.4(2)
S(1)-U(1)-S(5)	178.8(1)	S(2)-U(1)-S(5)	119.9(1)
S(3)-U(1)-S(5)	61.7(1)	S(4)-U(1)-S(5)	120.8(2)
S(1)-U(1)-S(6)	119.8(1)	S(2)-U(1)-S(6)	61.3(1)
S(3)-U(1)-S(6)	120.6(1)	S(4)-U(1)-S(6)	178.6(2)
S(5)-U(1)-S(6)	59.0(1)	S(1)-U(1)-O(1)	92.5(4)
S(2)-U(1)-O(1)	86.3(3)	S(3)-U(1)-O(1)	91.2(3)
S(4)-U(1)-O(1)	89.0(4)	S(5)-U(1)-O(1)	87.7(4)
S(6)-U(1)-O(1)	90.1(4)	S(1)-U(1)-O(2)	88.1(4)
S(2)-U(1)-O(2)	93.5(3)	S(3)-U(1)-O(2)	89.0(3)
S(4)-U(1)-O(2)	91.8(4)	S(5)-U(1)-O(2)	91.7(4)
S(6)-U(1)-O(2)	89.1(4)	O(1)-U(1)-O(2)	179.1(5)
S(7)-U(2)-S(8)	58.4(1)	S(7)-U(2)-S(9)	119.9(2)
S(8)-U(2)-S(9)	62.2(1)	S(7)-U(2)-S(10)	172.8(1)
S(8)-U(2)-S(10)	121.1(1)	S(9)-U(2)-S(10)	58.9(1)
S(7)-U(2)-S(11)	119.8(2)	S(8)-U(2)-S(11)	174.6(1)
S(9)-U(2)-S(11)	120.2(1)	S(10)-U(2)-S(11)	61.5(1)
S(7)-U(2)-S(12)	60.9(2)	S(8)-U(2)-S(12)	118.1(1)
S(9)-U(2)-S(12)	177.3(1)	S(10)-U(2)-S(12)	120.7(2)
S(11)-U(2)-S(12)	59.2(1)	S(7)-U(2)-O(3)	95.6(3)
S(8)-U(2)-O(3)	86.3(4)	S(9)-U(2)-O(3)	88.6(4)
S(10)-U(2)-O(3)	92.3(3)	S(11)-U(2)-O(3)	88.9(4)
S(12)-U(2)-O(3)	88.7(4)	S(7)-U(2)-O(4)	85.3(4)
S(8)-U(2)-O(4)	93.9(4)	S(9)-U(2)-O(4)	90.6(4)
S(10)-U(2)-O(4)	86.8(4)	S(11)-U(2)-O(4)	90.9(4)
S(12)-U(2)-O(4)	92.0(4)	O(3)-U(2)-O(4)	179.0(5)

TABLE 2.8 cont.

U(1)-S(1)-S(2)	60.8(1)	U(1)-S(1)-C(11)	93.7(6)
S(2)-S(1)-C(11)	32.9(6)	U(1)-S(2)-S(1)	60.3(1)
U(1)-S(2)-C(11)	93.9(4)	S(1)-S(2)-C(11)	33.7(4)
U(1)-S(3)-S(4)	59.9(1)	U(1)-S(3)-C(21)	90.6(5)
S(4)-S(3)-C(21)	30.8(5)	U(1)-S(4)-S(3)	61.6(2)
U(1)-S(4)-C(21)	93.2(8)	S(3)-S(4)-C(21)	31.7(7)
U(1)-S(5)-S(6)	60.7(2)	U(1)-S(5)-C(31)	92.9(7)
S(6)-S(5)-C(31)	33.2(6)	U(1)-S(6)-S(5)	60.4(2)
U(1)-S(6)-C(31)	92.1(6)	S(5)-S(6)-C(31)	32.7(6)
U(2)-S(7)-S(8)	61.8(1)	U(2)-S(7)-C(41)	92.8(5)
S(8)-S(7)-C(41)	31.8(5)	U(2)-S(8)-S(7)	60.6(1)
U(2)-S(8)-C(41)	93.8(6)	S(7)-S(8)-C(41)	33.2(6)
U(2)-S(9)-S(10)	60.6(2)	U(2)-S(9)-C(51)	93.3(7)
S(10)-S(9)-C(51)	33.0(6)	U(2)-S(10)-S(9)	60.5(1)
U(2)-S(10)-C(51)	92.1(6)	S(9)-S(10)-C(51)	32.0(5)
U(2)-S(11)-S(12)	60.4(2)	U(2)-S(11)-C(61)	92.5(6)
S(12)-S(11)-C(61)	32.2(6)	U(2)-S(12)-S(11)	60.3(2)
U(2)-S(12)-C(61)	92.6(6)	S(11)-S(12)-C(61)	32.4(6)
C(11)-N(11)-C(12)	121.2(15)	C(11)-N(11)-C(16)	126.5(13)
C(12)-N(11)-C(16)	112.3(12)	C(22)-N(21)-C(21)	120.5(15)
C(22)-N(21)-C(26)	114.0(14)	C(21)-N(21)-C(26)	125.5(17)
C(31)-N(31)-C(32)	123.1(15)	C(31)-N(31)-C(36)	124.8(15)
C(32)-N(31)-C(36)	112.1(16)	C(41)-N(41)-C(42)	123.5(15)
C(41)-N(41)-C(46)	121.1(17)	C(42)-N(41)-C(46)	112.3(16)
C(51)-N(51)-C(52)	120.9(14)	C(51)-N(51)-C(56)	127.7(17)
C(52)-N(51)-C(56)	111.2(15)	C(61)-N(61)-C(62)	122.3(15)
C(61)-N(61)-C(66)	123.0(16)	C(62)-N(61)-C(66)	114.6(17)
C(71)-N(71)-C(73)	109.0(15)	C(71)-N(71)-C(75)	106.7(15)
C(73)-N(71)-C(75)	111.1(14)	C(71)-N(71)-C(77)	112.9(17)
C(73)-N(71)-C(77)	105.0(14)	C(75)-N(71)-C(77)	112.3(15)
C(81)-N(81)-C(82)	91.6(23)	C(81)-N(81)-C(86)	112.4(25)
C(82)-N(81)-C(86)	55.1(20)	C(81)-N(81)-C(88)	163.4(28)
C(82)-N(81)-C(88)	99.1(24)	C(86)-N(81)-C(88)	65.0(24)
C(81)-N(81)-C(89)	103.0(21)	C(82)-N(81)-C(89)	165.4(23)
C(86)-N(81)-C(89)	117.1(20)	C(88)-N(81)-C(89)	66.6(22)
C(81)-N(81)-C(91)	105.2(22)	C(82)-N(81)-C(91)	69.4(23)
C(86)-N(81)-C(91)	111.6(19)	C(88)-N(81)-C(91)	90.5(25)
C(89)-N(81)-C(91)	106.5(24)	C(81)-N(81)-C(92)	54.9(27)
C(82)-N(81)-C(92)	108.9(24)	C(86)-N(81)-C(92)	161.5(24)
C(88)-N(81)-C(92)	131.3(31)	C(89)-N(81)-C(92)	80.6(23)
C(91)-N(81)-C(92)	64.8(22)	S(1)-C(11)-S(2)	113.4(8)
S(1)-C(11)-N(11)	121.8(14)	S(2)-C(11)-N(11)	125.6(12)
N(11)-C(12)-C(13)	111.8(13)	C(12)-C(13)-C(14)	111.6(17)
C(13)-C(14)-C(15)	110.7(16)	C(14)-C(15)-C(16)	111.8(15)
N(11)-C(16)-C(15)	113.2(15)	N(21)-C(22)-C(23)	110.3(17)
C(22)-C(23)-C(24)	108.5(23)	C(23)-C(24)-C(25)	109.6(19)
S(3)-C(21)-S(4)	117.5(10)	S(3)-C(21)-N(21)	118.5(14)
S(4)-C(21)-N(21)	123.5(16)	C(24)-C(25)-C(26)	111.6(18)
N(21)-C(26)-C(25)	109.6(19)	S(5)-C(31)-S(6)	114.1(11)
S(5)-C(31)-N(31)	124.4(12)	S(6)-C(31)-N(31)	121.5(12)
N(31)-C(32)-C(33)	111.2(16)	C(32)-C(33)-C(34)	110.3(17)
C(33)-C(34)-C(35)	112.2(22)	C(34)-C(35)-C(36)	110.5(19)
N(31)-C(36)-C(35)	110.1(15)	S(7)-C(41)-S(8)	115.0(10)
S(7)-C(41)-N(41)	121.9(13)	S(8)-C(41)-N(41)	123.1(14)

TABLE 2.8 cont.

N(41)-C(42)-C(43)	109.7(19)	C(42)-C(43)-C(44)	112.5(18)
C(43)-C(44)-C(45)	109.1(19)	C(44)-C(45)-C(46)	111.6(22)
N(41)-C(46)-C(45)	113.8(17)	S(9)-C(51)-S(10)	115.8(10)
S(9)-C(51)-N(51)	125.3(14)	S(10)-C(51)-N(51)	119.7(13)
N(51)-C(52)-C(53)	111.7(18)	C(52)-C(53)-C(54)	113.8(16)
C(53)-C(54)-C(55)	109.8(18)	C(54)-C(55)-C(56)	108.4(20)
N(51)-C(56)-C(55)	112.5(17)	S(11)-C(61)-S(12)	115.5(11)
S(11)-C(61)-N(61)	122.1(12)	S(12)-C(61)-N(61)	122.3(12)
N(61)-C(62)-C(63)	106.8(18)	C(62)-C(63)-C(64)	108.8(19)
C(63)-C(64)-C(65)	112.7(21)	C(64)-C(65)-C(66)	109.1(18)
N(61)-C(66)-C(65)	109.6(16)	N(71)-C(71)-C(72)	114.5(18)
N(71)-C(73)-C(74)	112.8(18)	N(71)-C(75)-C(76)	116.4(16)
N(71)-C(77)-C(78)	105.9(18)	N(81)-C(81)-C(83)	122.6(39)
N(81)-C(81)-C(84)	81.4(19)	C(83)-C(81)-C(84)	41.2(31)
N(81)-C(81)-C(92)	60.2(25)	C(83)-C(81)-C(92)	123.8(51)
C(84)-C(81)-C(92)	103.9(31)	N(81)-C(82)-C(84)	107.5(30)
N(81)-C(82)-C(86)	57.7(21)	C(84)-C(82)-C(86)	122.1(43)
N(81)-C(82)-C(91)	52.8(18)	C(84)-C(82)-C(91)	112.2(31)
C(86)-C(82)-C(91)	99.5(30)	C(81)-C(83)-C(84)	105.2(48)
C(81)-C(84)-C(82)	79.5(27)	C(81)-C(84)-C(83)	33.6(29)
C(82)-C(84)-C(83)	113.2(39)	C(86)-C(85)-C(87)	59.4(65)
N(81)-C(86)-C(82)	67.2(22)	N(81)-C(86)-C(85)	108.2(23)
C(82)-C(86)-C(85)	129.4(33)	N(81)-C(86)-C(87)	117.8(26)
C(82)-C(86)-C(87)	147.7(39)	C(85)-C(86)-C(87)	22.6(23)
N(81)-C(86)-C(88)	57.9(20)	C(82)-C(86)-C(88)	102.4(34)
C(85)-C(86)-C(88)	111.3(30)	C(87)-C(86)-C(88)	106.2(32)
C(85)-C(87)-C(86)	98.8(70)	N(81)-C(88)-C(86)	57.8(21)
N(81)-C(88)-C(89)	61.6(21)	C(86)-C(88)-C(89)	107.1(33)
N(81)-C(88)-C(90)	107.5(30)	C(86)-C(88)-C(90)	147.4(42)
C(89)-C(88)-C(90)	46.8(24)	N(81)-C(89)-C(88)	51.9(19)
N(81)-C(89)-C(90)	107.5(30)	C(88)-C(89)-C(90)	56.5(28)
N(81)-C(89)-C(92)	45.9(16)	C(88)-C(89)-C(92)	91.3(25)
C(90)-C(89)-C(92)	132.1(38)	C(88)-C(90)-C(89)	76.7(33)
N(81)-C(91)-C(82)	58.6(21)	N(81)-C(91)-C(92)	57.7(21)
C(82)-C(91)-C(92)	97.1(30)	N(81)-C(91)-C(93)	120.8(30)
C(82)-C(91)-C(93)	135.8(34)	C(92)-C(91)-C(93)	62.4(30)
N(81)-C(91)-C(94)	115.4(26)	C(82)-C(91)-C(94)	157.2(31)
C(92)-C(91)-C(94)	64.9(28)	C(93)-C(91)-C(94)	24.9(28)
N(81)-C(92)-C(81)	64.9(27)	N(81)-C(92)-C(89)	53.5(18)
C(81)-C(92)-C(89)	92.1(32)	N(81)-C(92)-C(91)	57.5(19)
C(81)-C(92)-C(91)	107.2(33)	C(89)-C(92)-C(91)	87.1(24)
N(81)-C(92)-C(93)	108.2(30)	C(81)-C(92)-C(93)	138.6(40)
C(89)-C(92)-C(93)	117.1(35)	C(91)-C(92)-C(93)	50.7(25)
N(81)-C(92)-C(94)	107.8(30)	C(81)-C(92)-C(94)	159.3(38)
C(89)-C(92)-C(94)	97.7(30)	C(91)-C(92)-C(94)	55.4(25)
C(93)-C(92)-C(94)	22.5(25)	C(91)-C(93)-C(92)	66.9(31)
C(91)-C(93)-C(94)	93.4(61)	C(92)-C(93)-C(94)	90.7(69)
C(91)-C(94)-C(92)	59.7(27)	C(91)-C(94)-C(93)	61.8(56)
C(92)-C(94)-C(93)	66.7(67)	Co(2)-Co(1)-Co(3)	113.9(39)
Co(2)-Co(1)-O(5)	120.7(51)	Co(3)-Co(1)-O(5)	120.8(46)
Co(1)-Co(2)-O(5)	26.1(25)	Co(1)-Co(3)-O(5)	26.5(23)
Co(1)-O(5)-Co(2)	33.3(32)	Co(1)-O(5)-Co(3)	32.7(30)
Co(2)-O(5)-Co(3)	64.1(21)		

TABLE 2.9

Bond lengths (Å) and angles (°) for [3]
(standard deviations in parentheses).

a) Bond lengths

U(1)-S(7)	2.944(7)	U(1)-S(8)	2.963(7)
U(1)-S(9)	2.897(6)	U(1)-S(10)	2.912(7)
U(1)-S(11)	2.960(6)	U(1)-S(12)	2.917(7)
U(1)-O(11)	1.761(14)	U(1)-O(12)	1.763(15)
U(2)-S(1)	2.935(7)	U(2)-S(2)	2.976(7)
U(2)-S(3)	2.936(7)	U(2)-S(4)	2.919(7)
U(2)-S(5)	2.926(7)	U(2)-S(6)	2.937(7)
U(2)-O(21)	1.761(14)	U(2)-O(22)	1.776(16)
S(1)-C(24)	1.752(23)	S(2)-S(3)	2.885(9)
S(2)-C(27)	1.765(25)	S(3)-C(27)	1.683(25)
S(4)-S(5)	2.876(10)	S(4)-C(21)	1.656(24)
S(5)-C(21)	1.715(25)	S(6)-C(24)	1.694(25)
S(7)-S(8)	2.882(9)	S(7)-C(17)	1.666(25)
S(8)-C(17)	1.653(25)	S(9)-S(10)	2.885(9)
S(9)-C(14)	1.728(25)	S(10)-C(14)	1.652(24)
S(11)-C(11)	1.667(30)	S(12)-C(11)	1.724(30)
N(11)-C(11)	1.375(28)	N(11)-C(12)	1.408(32)
N(11)-C(13)	1.409(34)	N(12)-C(14)	1.369(30)
N(12)-C(15)	1.420(34)	N(12)-C(16)	1.459(30)
N(13)-C(17)	1.394(33)	N(13)-C(18)	1.482(43)
N(13)-C(19)	1.415(38)	N(21)-C(21)	1.400(30)
N(21)-C(22)	1.471(29)	N(21)-C(23)	1.482(34)
N(22)-C(24)	1.383(27)	N(22)-C(25)	1.477(41)
N(22)-C(26)	1.504(39)	N(23)-C(27)	1.304(28)
N(23)-C(28)	1.477(32)	N(23)-C(29)	1.472(31)
N(31)-C(31)	1.492(32)	N(31)-C(33)	1.536(39)
N(31)-C(35)	1.607(34)	N(31)-C(37)	1.557(37)
C(31)-C(32)	1.512(39)	C(33)-C(34)	1.643(51)
C(35)-C(36)	1.488(45)	C(37)-C(38)	1.571(50)
N(41)-C(41)	1.686(82)	N(41)-C(42)	1.747(117)
N(41)-C(45)	1.956(112)	N(41)-C(47)	1.793(146)
N(41)-C(50)	1.380(77)	N(41)-C(51)	1.328(76)
N(41)-C(52)	1.220(77)	C(40)-C(41)	1.406(124)
C(40)-C(42)	1.933(139)	C(41)-C(42)	1.287(120)
C(41)-C(51)	1.999(111)	C(42)-C(50)	1.611(137)
C(43)-C(50)	1.022(98)	C(45)-C(46)	1.146(136)
C(45)-C(51)	1.100(135)	C(46)-C(51)	2.047(119)
C(47)-C(52)	1.341(153)	C(47)-C(54)	0.991(177)
C(50)-C(51)	2.180(100)	C(50)-C(52)	1.903(105)
C(52)-C(54)	1.607(129)		

TABLE 2.9 cont.

b) Bond angles

[illegible]	58.4(2)	S(7)-U(1)-S(9)	117.6(2)
[illegible]	61.3(2)	S(7)-U(1)-S(10)	177.3(2)
[illegible]	119.1(2)	S(9)-U(1)-S(10)	59.5(2)
[illegible]	120.1(2)	S(8)-U(1)-S(11)	178.2(2)
[illegible]	119.9(2)	S(10)-U(1)-S(11)	62.5(2)
[illegible]	62.8(2)	S(9)-U(1)-S(12)	119.5(2)
[illegible]	179.6(2)	S(10)-U(1)-S(12)	119.9(2)
[illegible]	59.4(2)	S(7)-U(1)-O(11)	90.4(6)
S(8)-U(1)-O(11)	83.9(6)	S(9)-U(1)-O(11)	97.2(5)
S(10)-U(1)-O(11)	90.2(6)	S(11)-U(1)-O(11)	97.2(5)
S(12)-U(1)-O(11)	83.5(5)	S(7)-U(1)-O(12)	87.8(7)
S(8)-U(1)-O(12)	95.8(6)	S(9)-U(1)-O(12)	64.4(6)
S(10)-U(1)-O(12)	91.7(7)	S(11)-U(1)-O(12)	83.8(6)
S(12)-U(1)-O(12)	94.9(6)	O(11)-U(1)-O(12)	178.6(8)
S(-U(2)-S(2)	60.9(2)	S(1)-U(2)-S(3)	117.3(2)
S(2)-U(2)-S( )	58.4(2)	S(1)-U(2)-S(4)	179.3(2)
S(2)-U(2)-S( )	118.5(2)	S(3)-U(2)-S(4)	62.1(2)
S( )-U(2)-S(5)	121.7(2)	S(2)-U(2)-S(5)	175.4(2)
S(3)-U(2)-S(5)	120.0(2)	S(4)-U(2)-S(5)	59.0(2)
S(1)-U(2)-S(6)	60.0(2)	S(2)-U(2)-S(6)	120.0(2)
S(3)-U(2)-S(6)	174.5(2)	S(4)-U(2)-S(6)	120.7(2)
S(5)-U(2)-S(6)	62.0(2)	S(1)-U(2)-O(21)	91.7(5)
S(2)-U(2)-O(21)	85.9(6)	S(3)-U(2)-O(21)	98.4(5)
S(4)-U(2)-O(21)	88.4(5)	S(5)-U(2)-O(21)	90.1(6)
S(6)-U(2)-O(21)	86.7(5)	S(1)-U(2)-O(22)	88.7(6)
S(2)-U(2)-O(22)	94.5(7)	S(3)-U(2)-O(22)	81.7(6)
S(4)-U(2)-O(22)	91.2(6)	S(5)-U(2)-O(22)	85.4(7)
S(6)-U(2)-O(22)	93.3(6)	O(21)-U(2)-O(22)	179.5(10)
U(2)-S(1)-C(24)	98.6(8)	U(2)-S(2)-S(3)	60.1(2)
U(2)-S(2)-C(27)	92.3(8)	S(3)-S(2)-C(27)	32.3(7)
U(2)-S(3)-S(2)	61.5(2)	U(2)-S(3)-C(27)	95.5(8)
S(2)-S(3)-C(27)	34.0(8)	U(2)-S(4)-S(5)	60.7(2)
U(2)-S(4)-C(21)	92.6(8)	S(5)-S(4)-C(21)	32.0(8)
U(2)-S(5)-S(4)	60.4(2)	U(2)-S(5)-C(21)	91.1(8)
S(4)-S(5)-C(21)	38.8(8)	U(2)-S(6)-C(24)	91.3(8)
U(1)-S(7)-S(8)	61.1(2)	U(1)-S(7)-C(17)	90.7(9)
S(8)-S(7)-C(17)	29.6(9)	U(1)-S(8)-S(7)	60.5(2)
U(1)-S(8)-C(17)	90.3(9)	S(7)-S(8)-C(17)	29.9(9)
U(1)-S(9)-S(10)	60.5(2)	U(1)-S(9)-C(14)	91.2(8)
S(10)-S(9)-C(14)	30.7(8)	U(1)-S(10)-S(9)	60.0(2)
U(1)-S(10)-C(14)	92.2(9)	S(9)-S(10)-C(14)	32.3(9)
U(1)-S(11)-C(11)	90.3(8)	U(1)-S(12)-C(11)	90.6(8)
C(11)-N(11)-C(12)	123.3(22)	C(11)-N(11)-C(13)	120.2(22)
C(12)-N(11)-C(13)	116.4(20)	C(14)-N(12)-C(15)	120.9(20)
C(14)-N(12)-C(16)	122.8(19)	C(15)-N(12)-C(16)	115.5(20)
C(17)-N(13)-C(18)	116.0(25)	C(17)-N(13)-C(19)	125.8(24)
C(18)-N(13)-C(19)	118.0(26)	C(21)-N(21)-C(22)	122.6(20)

TABLE 2.9 cont.

C(21)-N(21)-C(23)	122.6(19)	C(22)-N(21)-C(23)	114.7(20)
C(24)-N(22)-C(25)	118.5(23)	C(24)-N(22)-C(26)	121.5(23)
C(25)-N(22)-C(26)	120.0(21)	C(27)-N(23)-C(28)	124.0(19)
C(27)-N(23)-C(29)	122.3(20)	C(28)-N(23)-C(29)	113.7(19)
S(11)-C(11)-S(12)	118.4(12)	S(11)-C(11)-N(11)	123.1(21)
S(12)-C(11)-N(11)	118.4(21)	S(9)-C(14)-S(10)	117.0(14)
S(9)-C(14)-N(12)	118.8(17)	S(10)-C(14)-N(12)	123.7(18)
S(7)-C(17)-S(8)	120.5(15)	S(7)-C(17)-N(13)	117.1(18)
S(8)-C(17)-N(13)	122.3(19)	S(4)-C(21)-S(5)	117.1(14)
S(4)-C(21)-N(21)	121.3(16)	S(5)-C(21)-N(21)	121.5(17)
S(1)-C(24)-S(6)	117.8(12)	S(1)-C(24)-N(22)	120.0(19)
S(2)-C(24)-N(22)	122.1(20)	S(2)-C(27)-S(3)	113.7(13)
S(3)-C(27)-N(23)	122.2(17)	S(3)-C(27)-N(23)	124.0(17)
C(31)-N(31)-C(35)	113.1(21)	C(31)-N(31)-C(35)	106.9(18)
C(31)-N(31)-C(37)	110.3(20)	C(31)-N(31)-C(37)	115.5(19)
C(35)-N(31)-C(37)	97.1(20)	C(35)-N(31)-C(37)	113.0(20)
N(31)-C(31)-C(32)	115.8(20)	N(31)-C(33)-C(34)	116.9(24)
N(31)-C(35)-C(36)	112.4(21)	N(31)-C(37)-C(38)	107.9(23)
C(41)-N(41)-C(42)	44.0(41)	C(41)-N(41)-C(45)	113.2(41)
C(42)-N(41)-C(45)	133.4(47)	C(41)-N(41)-C(47)	95.0(53)
C(42)-N(41)-C(47)	120.0(59)	C(45)-N(41)-C(47)	38.5(54)
C(41)-N(41)-C(50)	103.5(47)	C(42)-N(41)-C(50)	60.7(50)
C(45)-N(41)-C(50)	107.6(47)	C(47)-N(41)-C(50)	138.4(55)
C(41)-N(41)-C(51)	82.2(43)	C(42)-N(41)-C(51)	103.7(49)
C(45)-N(41)-C(51)	32.5(44)	C(47)-N(41)-C(51)	112.0(55)
C(50)-N(41)-C(51)	107.3(46)	C(41)-N(41)-C(52)	133.1(48)
C(42)-N(41)-C(52)	122.7(50)	C(45)-N(41)-C(52)	102.0(47)
C(47)-N(41)-C(52)	48.4(56)	C(50)-N(41)-C(52)	93.9(50)
C(51)-N(41)-C(52)	133.5(52)	C(41)-C(40)-C(42)	41.7(49)
N(41)-C(41)-C(40)	99.1(58)	N(41)-C(41)-C(42)	70.5(62)
C(40)-C(41)-C(42)	91.6(75)	N(41)-C(41)-C(51)	41.1(29)
C(42)-C(41)-C(51)	134.0(68)	C(42)-C(41)-C(51)	92.9(68)
N(41)-C(42)-C(40)	79.6(58)	N(41)-C(42)-C(41)	65.5(60)
C(40)-C(42)-C(41)	46.6(56)	N(41)-C(42)-C(50)	48.3(45)
C(40)-C(42)-C(50)	120.1(72)	C(41)-C(42)-C(50)	112.4(90)

TABLE 2.10

Bond lengths (Å) and angles (°) for [4]
(standard deviations in parentheses)

a) Bond lengths

U(1)-S(1)	2.928(4)	U(1)-S(2)	2.918(4)
U(1)-S(3)	2.909(5)	U(1)-S(4)	2.902(4)
U(1)-S(5)	2.924(4)	U(1)-S(6)	2.960(5)
U(1)-O(1)	1.734(11)	U(1)-O(2)	1.862(12)
S(1)-S(2)	2.886(6)	S(1)-C(11)	1.681(16)
S(2)-C(11)	1.724(18)	S(3)-S(4)	2.866(7)
S(3)-C(21)	1.681(18)	S(4)-C(21)	1.710(19)
S(5)-S(6)	2.898(6)	S(5)-C(31)	1.732(17)
S(6)-C(31)	1.714(17)	N(11)-C(11)	1.348(18)
N(11)-C(12)	1.473(23)	N(11)-C(14)	1.469(30)
N(21)-C(21)	1.362(24)	N(21)-C(22)	1.465(25)
N(21)-C(24)	1.488(28)	N(31)-C(31)	1.382(21)
N(31)-C(32)	1.464(24)	N(31)-C(34)	1.532(26)
N(1)-C(1)	1.465(47)	N(1)-C(2)	1.444(34)
N(1)-C(3)	1.473(48)	N(1)-C(4)	1.423(48)
C(12)-C(13)	1.491(41)	C(14)-C(15)	1.460(39)
C(22)-C(23)	1.467(35)	C(24)-C(25)	1.414(40)
C(32)-C(33)	1.439(35)	C(34)-C(35)	1.509(43)
C(2)-C(3)	2.120(48)		

b) Bond angles

S(1)-U(1)-S(2)	59.2(1)	S(1)-U(1)-S(3)	119.7(1)
S(2)-U(1)-S(3)	62.6(1)	S(1)-U(1)-S(4)	175.3(2)
S(2)-U(1)-S(4)	118.2(1)	S(3)-U(1)-S(4)	59.1(1)
S(1)-U(1)-S(5)	119.8(1)	S(2)-U(1)-S(5)	172.9(2)
S(3)-U(1)-S(5)	119.9(1)	S(4)-U(1)-S(5)	62.2(1)
S(1)-U(1)-S(6)	61.4(1)	S(2)-U(1)-S(6)	118.8(1)
S(3)-U(1)-S(6)	178.4(1)	S(4)-U(1)-S(6)	119.9(1)
S(5)-U(1)-S(6)	58.8(1)	S(1)-U(1)-O(1)	87.7(4)
S(2)-U(1)-O(1)	98.2(4)	S(3)-U(1)-O(1)	86.3(4)
S(4)-U(1)-O(1)	96.7(4)	S(5)-U(1)-O(1)	88.7(4)
S(6)-U(1)-O(1)	92.6(4)	S(1)-U(1)-O(2)	91.4(4)
S(2)-U(1)-O(2)	83.5(4)	S(3)-U(1)-O(2)	96.4(3)
S(4)-U(1)-O(2)	84.3(4)	S(5)-U(1)-O(2)	89.5(4)
S(6)-U(1)-O(2)	84.7(3)	O(1)-U(1)-O(2)	177.2(5)

TABLE 2.10 cont.

b) Bond angles

U(1)-S(1)-S(2)	60.2(1)	U(1)-S(1)-C(11)	92.3(5)
S(2)-S(1)-C(11)	32.5(6)	U(1)-S(2)-S(1)	60.6(1)
U(1)-S(2)-C(11)	91.8(5)	S(1)-S(2)-C(11)	31.6(5)
U(1)-S(3)-S(4)	60.3(1)	U(1)-S(3)-C(21)	92.7(6)
S(4)-S(3)-C(21)	32.6(6)	U(1)-S(4)-S(3)	60.6(1)
U(1)-S(4)-C(21)	92.4(6)	S(3)-S(4)-C(21)	32.0(6)
U(1)-S(5)-S(6)	61.2(1)	U(1)-S(5)-C(31)	93.3(6)
S(6)-S(5)-C(31)	32.8(6)	U(1)-S(6)-S(5)	60.0(1)
U(1)-S(6)-C(31)	92.5(6)	S(5)-S(6)-C(31)	33.2(6)
C(11)-N(11)-C(12)	124.6(13)	C(11)-N(11)-C(14)	119.5(17)
C(12)-N(11)-C(14)	114.4(16)	C(21)-N(21)-C(22)	120.8(16)
C(21)-N(21)-C(24)	121.4(16)	C(22)-N(21)-C(24)	117.5(15)
C(31)-N(31)-C(32)	124.6(15)	C(31)-N(31)-C(34)	118.7(15)
C(32)-N(31)-C(34)	116.7(15)	C(1)-N(1)-C(2)	112.7(33)
C(1)-N(1)-C(3)	113.1(24)	C(2)-N(1)-C(3)	93.3(23)
C(1)-N(1)-C(4)	116.1(17)	C(2)-N(1)-C(4)	109.5(24)
C(3)-N(1)-C(4)	109.8(34)	S(1)-C(11)-S(2)	115.9(8)
S(1)-C(11)-N(11)	124.3(13)	S(2)-C(11)-N(11)	119.4(14)
N(11)-C(12)-C(13)	113.6(27)	N(11)-C(14)-C(15)	110.1(26)
S(3)-C(21)-S(4)	115.3(11)	S(3)-C(21)-N(21)	123.1(14)
S(4)-C(21)-N(21)	121.6(14)	N(21)-C(22)-C(23)	110.6(18)
N(21)-C(24)-C(25)	113.9(23)	S(5)-C(31)-S(6)	114.0(9)
S(5)-C(31)-N(31)	124.4(13)	S(6)-C(31)-N(31)	121.6(13)
N(31)-C(32)-C(33)	109.1(18)	N(31)-C(34)-C(35)	110.0(20)
N(1)-C(2)-C(3)	43.9(14)	N(1)-C(3)-C(2)	42.8(16)

TABLE 2.11

Deviations from planes (defined by starred atoms) and inter-plane angles for complex [1]

Deviations (Å)

Plane 1

S(1)* -0.17; S(2)* 0.11; S(3)* 0.14 S(4)* -0.06; S(5)* 0.01; S(6)* -0.03

Plane 2

S(1)* 0.00; S(3)* 0.00; C(35)* 0.00; N(3)* 0.00

Plane 3

S(4)* 0.00; S(5)* 0.00; C(15)* 0.00; N(1)* 0.00

Plane 4

S(2)* 0.00; S(6)* 0.00; C(25)* 0.01; N(2)* 0.00

Angles between planes(°)

Plane	Angle	Plane	Angle
1:2	6.3	2:3	6.0
1:3	6.3	2:4	4.2
1:4	6.3	3:4	9.4

Angle between O-O line and planes

Plane	Angle	Plane	Angle
1	89.0	2	83.0
3	83.9	4	82.7

TABLE 2.12

Deviations from planes (defined by starred atoms) and inter-plane angles for molecule 1 of complex [2]

Deviations (Å)

Plane 1

S(1)* -0.12; S(2)* 0.12; S(3)* -0.05; S(4)* 0.08; S(5)* 0.06; S(6)* -0.10

Plane 2

S(1)* 0.00; S(2)* 0.00; C(11)* 0.00; N(11)* 0.00

Plane 3

S(3)* 0.01; S(4)* 0.02; C(21)* -0.02; N(21)* 0.02

Plane 4

S(5)* 0.00; S(6)* 0.00; C(31)* -0.01; N(31)* 0.02

Angles between planes(°)

Plane	Angle	Plane	Angle
1:2	5.5	2:3	15.1
1:3	10.4	2:4	9.8
1:4	15.0	3:4	22.6

Angle between O-O line and planes

Plane	Angle	Plane	Angle
1	89.1	2	6.3
3	9.5	4	15.5

TABLE 2.12 cont.

Deviations from planes (defined by starred atoms) and inter-plane angles for molecule 2 of complex [2]

Deviations (Å)

Plane 1

S(7)* -0.25; S(8)* 0.18; S(9)* 0.20; S(10)* -0.15; S(11)* 0.08; S(12)* 0.12

Plane 2

S(7)* 0.00; S(8)* 0.00; C(41)* 0.00 N(41)* 0.00

Plane 3

S(9)* 0.00; S(10)* 0.00; C(51)* 0.00; N(51)* 0.00

Plane 4

S(11)* 0.00; S(12)* 0.00 C(61)* 0.02; N(61)* 0.00

Angles between planes(°)

Plane	Angle	Plane	Angle
1:2	8.9	2:3	1.9
1:3	7.7	2:4	7.5
1:4	3.8	3:4	5.8

Angle between O-O line and planes

Plane	Angle	Plane	Angle
1	89.4	2	9.5
3	8.3	4	5.4

TABLE 2.13

Deviations from planes (defined by starred atoms) and inter-plane angles for molecule 1 of complex [3]

Deviations (Å)

Plane 1

S(1)* 0.16; S(2)* -0.28; S(3) 0.28 S(4)* -0.17; S(5)* 0.05; S(6) -0.05

Plane 2

S(1)* 0.00; S(6)* 0.00; C(24)* 0.00; N(22)* 0.00

Plane 3

S(2)* 0.01; S(3)* 0.01; C(27)* -0.02; N(23)* -0.01

Plane 4

S(4)* 0.00; S(5)* 0.00; C(21)* 0.00; N(21)* 0.00

Angles between planes(°)

Plane	Angle	Plane	Angle
1:2	8.0	2:3	19.5
1:3	11.6	2:4	1.8
1:4	6.8	3:4	18.0

Angle between O-O line and planes

Plane	Angle	Plane	Angle
1	87.3	2	6.5
3	13.0	4	5.0

TABLE 2.13 cont.

Deviations from planes (defined by starred atoms) and inter-plane angles for molecule 2 of complex [3]

Deviations (Å)

Plane 1

S(7)* -0.23; S(8)* 0.22; S(9)* -0.23 S(10)* 0.24; S(11)* -0.24; S(12)*0.24

Plane 2

S(7)* 0.0; S(8)* 0.00; C(17)* 0.01; N(13)* 0.00

Plane 3

S(9)* 0.01; S(10)* 0.01; C(14)* -0.04; N(12) 0.02

Plane 4

S(11)* 0.00; S(12)* 0.00; C(11)* -0.02; N(11)* 0.01

Angles between planes(°)

Plane	Angle	Plane	Angle
1:2	10.5	2:3	13.9
1:3	9.3	2:4	19.7
1:4	15.1	3:4	24.3

Angle between O-O line and planes

Plane	Angle	Plane	Angle
1	68.3	2	7.0
3	12.5	4	5.5

TABLE 2.14

Deviations from planes (defined by starred atoms) and inter-plane angles for complex [4]

Deviations (Å)

Plane 1

S(1)* 0.19; S(2)* -0.30; S(3)* 0.32 S(4)* -0.24; S(5)* 0.12; S(6)* -0.10

Plane 2

S(1)* -0.01; S(2)* -0.01; N(11)* -0.01; C(11)* 0.04

Plane 3

S(3)* 0.00; S(4)* 0.00; N(21)* 0.00; C(21) 0.00

Plane 4

S(5)* 0.00; S(6)* 0.00; N(31)* 0.00; C(31)* 0.01

Angles between planes(°)

Plane	Angle	Plane	Angle
1:2	13.9	2:3	25.3
1:3	14.5	2:4	1.0
1:4	13.2	3:4	25.0

Angle between O-O line and planes

Plane	Angle	Plane	Angle
1	89.5	2	77.5
3	75.5	4	77.2

References

1. R.G. Pearson, *J. Am. Chem. Soc.*, vol. 85, p. 3533, 1963.
2. M.Delepine, *Bull. Soc. Chim. Fr.*, vol. 3, p. 643, 1908.
3. L. Malatesta, *Gazz. Chim. Ital.*, vol. 69, p. 408, 1939.
4. R.G. Jones, E. Bindschalder, G.A. Martin Jr., J.R. Thirtle, H. Gilman, *J. Amer. Chem. Soc.*, p. 4971, 1957.
5. R.A. Zingaro, *J. Amer. Chem. Soc.*, vol. 78, p. 3568, 1956.
6. H Albers S. Lange, *Chem. Ber.*, vol. 85, p. 278, 1952.
7. S. Bonatti, M. Frazini, *Atti. Accad. Nazl. Lincei Rend. Classe Sci. Fis. Mat. Nat*, vol. 41, p. 264, 1966.
8. C.J. Rodden, *Analytical Chemistry of the Manhatten Project*, p. pp1070, 1950.
9. E.B. Sandell, *Colorimetric Determination of Trace Metals*,, p. pp603, 1950.
10. K. Gleu, R. Schwab, *Angew. Chem.*, vol. 62, p. 320, 1950.
11. I.D. Muzyka, E.D. Romanenko, N.N. Tananaeva, *Russ. J. Inorg. Chem.*, vol. 11, p. 648, 1966.
12. K. Bowman, Z. Dori, *Chem. Commun.*, p. 636, 1956.
13. P. Zanello, A. Cinquanti, G. Mazzocchin, *Inorg. Chim. Acta.*, vol. 21, p. 195, 1977.
14. R. Graziani, B. Zarli, A. Cassol, G. Bombieri, E. Forsellini, E. Tondello, *Inorg. Chem.*, vol. 9, p. 2116, 1970.
15. A. Cassol, B. Zarli, E. Tondello, *Annu. Meet. Chim. Inorg.*, p. 121, 1968.
16. T.M. Siddal, C.F. Voisin, *J. Inorg. Nucl. Chem.*, vol. 34, p. 2078, 1972.
17. E. Forsellini, G. Bombieri, R.Graziani, B. Zarli, *Inorg. Nucl. Chem. Lett.*, vol. 8, p. 461, 1972.
18. S.M. Sinitsyna, N.M. Sinitsyn, *Russ. J. Inorg. Chem.*, vol. 10, p. 499, 1965.
19. J.Chatt, L.A. Duncanson, M.L. Venanzi, *Nature*, vol. 177, p. 1042, 1965.
20. J. Chatt, L.A. Duncanson, M.L. Venanzi, *Suomen Kemistilehti*, vol. B29, p. 75, 1956.
21. R. Graziani, B. Zarli, A. Cassol, G. Bombieri, E. Forsellini, E. Tondello, *Inorg. Chem.*, vol. 9, p. 2116, 1970.
22. N.W. Alcock, *Crystallographic Computing*, pp. p271-278, Copenhagen, Munksgaard.
23. G.M. Sheldrick, *SHELXTL User Manual*, Nicolet Instrument Co., 1981.
24. R.G. Denning, "Properties of the UO_2^+ (n=1,2) Ions," *Gmelin supl. vol. A6*, 1983.

25. A.E. Storey, F.Zonnevijle, A.A. Pinkerton, *Inorg. Chim. Acta*, vol. 75, p. 103, 1983.

CHAPTER 3

Two pyridine - acetylacetonate complexes of uranium(VI)

3.1. Introduction

The synthesis and structure of dioxobis(pentane-2,4-dionato)pyridineuranium(VI) has previously been reported.[1] This is notable amongst complexes involving the uranyl ion for the large deviation from linearity of the O-U-O bond angle, 173.5(8)°. A large number of other complexes of dioxouranium (VI) with β-diketones have been reported[2] but in the main these concentrate on the infra red spectral assignment of ν_1 and ν_3O-U-O. The only other uranyl complex of pentane-2,4-dione which has been characterised structurally is that of aquadioxobis(pentane-2,4-dionato)uranium(VI).[3,4] This present chapter describes the synthesis and structural characterisation of a further two such complexes: dioxobis(1,3-diphenylpropane-1,3-dionato)pyridineuranium(VI) [5], and dioxobis(t-butoxypentane-2,4-dionato)pyridineuranium(VI) [6]. From these it becomes apparent that contrary to earlier hypotheses[1], pyridine-uranyl repulsions do not determine the extent of the linearity of the uranyl group. $UO_2(acac)_2.H_2O$ is one of the earliest reported compounds of uranium and its preparation in 1904[5] was followed by the pyridine analogue in 1927.[6] Infra red data were obtained later.[7,8]

β-Dicarbonyl compounds are very versatile and exhibit a great variety of coordination modes besides the usual bidentate behaviour of mono-anions.[9,10] Acetylacetone can coordinate to the uranyl group through one oxygen as in $UO_2(acac)_2(acacH)$[11] where the diketone acts as a neutral donor. This is obtained by evaporating a suspension of $UO_2(acac)_2.H_2O$ in acetylacetone.[12] Other complexes which involve this mode of bonding include $UO_2(NO_3)_2.2HL$ (HL=1-phenyl-3-(2-pyridyl) propane-1,3-dione)[13]

There is even less data available on the neptunyl analogues, structural information being restricted to $NpO_2(acac)_2.py$[14] In an attempt to remedy this, the neptunium analogues of [5] and [6] were prepared.

3.2. Experimental

3.2.1 *Preparation*

Compounds [5] and [6] were prepared by adaptation of the method described by Hager.[7] This involved addition of a methanolic solution of uranyl nitrate (0.56g; 1.42mmol) to a methanolic solution containing two equivalents of ligand (0.25g; 2.8mmol). Dropwise addition of the stoichiometric amount of pyridine (0.20cm³: 2.4mmol) caused turbidity of the solution, and crystals deposited on standing. These were recrystallised from methanol. The neptunyl

analogues were prepared by essentially the same method using 0.25mmol of freshly prepared neptunyl (VI) nitrate, and reducing the quantities of the other reagents to the same proportions. The neptunium crystals were mounted in a glove box and encapsulated in a Lindeman capillary for radiation protection. Several crystals were examined to obtain a suitable single crystal, but all were found to be twinned or failed to give a satisfactory diffraction pattern.

3.2.2. *Data Collection and Structure Refinement*

Data on [5] and [6] were collected with a Syntex $P2_1$ four circle diffractometer. Background intensities were measured at each end of the scan for 0.25 of the scan time. Three standard reflections, monitored every 200 reflections, showed slight changes during data collection and the data were rescaled for this. Unit cell dimensions and standard deviations were obtained by least squares fit to 15 reflections ($25 \leq 2\theta \leq 29$). Observed reflections [$I/\sigma(I) \geq 3.0$] were corrected for Lorentz, polarisation and absorption effects, the last with ABSCOR.[15] Details for each compound are given in Table 3.1

For compound [5], systematic absences $0k0: k \neq 2n$, $hk0: h+k \neq 2n$ gave the space group as $P2_1/n$ and the position of the uranium atom was determined from a three dimensional Patterson map. The atomic coordinates of the lighter non-hydrogen atoms were found by successive Fourier syntheses and all were refined anisotropically. Hydrogen atoms were inserted at calculated positions with fixed isotropic temperature factors U=0.07Å^2.

Systematic absences for [6] indicated an A-centred cell, with a choice of three possible space groups; $A2_1ma$, $Am2a$, and $Amma$ as non-standard settings of $Cmc2_1$, $Ama2$, and $Cmcm$ respectively. $Cmcm$ was initially selected, and the cell rotated to conform. Patterson maps were calculated and structure solution attempted in each possible space group but this was successful only in $Cmc2_1$. Refinement of a $\delta f''$ multiplier showed that the correct hand had been chosen. The x and z-coordinates of the uranium atom were held fixed to define the origin. Anisotropic temperature factors were used for all atoms except hydrogens which were inserted at fixed positions and not refined (U=0.07Å^2). An attempt to include the hydrogen atoms for the methyl groups was unsuccessful as the refined perameters did not converge. The large thermal parameters for the corresponding carbon atoms suggest that these groups are slightly disordered, though no alternative positions were detectable on the Fourier synthesis. The thermal parameters and implausible bond distance from C(4) suggest that it may also be disordered between two positions which are not far separated from each other.

Final refinement of F was by cascaded least squares methods. A weighting scheme of the form $W=1/(\sigma^2(F)+g(F^2)$ was applied. The relatively large residual peaks on the final Fourier anthesis for [6] were in the neighbourhood of the metal ions. Calculations were performed using the SHELXTL[16] system on a Data General DG30 apart from the absorption correction on a

Burroughs B6800. Scattering factors in the analytical form and anomalous dispersion factors were taken from the International Tables.[17]

Infra red spectra of the complexes were taken with a Perkin Elmer 180 Spectrophotometer using Nujol mulls between KBr discs in the region 1000-400cm^{-1}, and between silicon plates for the region 500-150cm^{-1}. These confirmed the spectra previously reported for $UO_2(acac)_2$ py with slight shifts in ν_2 and ν_3 (Table 3.1).

Final atomic coordinates are given in Tables 3.2-3.3. Bond lengths and angles around the uranium atom for [5] and [6] are listed in Table 3.4, and compared with those values found for $UO_2(acac)_2$ py [7]. Full bond lengths and angles are given in Tables 3.5-6. Information on deviations from planes is given in Table 3.7. Figure 3.1 shows the molecule and numbering scheme for [5]. The packing diagram for [5] can be seen in Figure 3.2. Figure 3.3 shows the molecule and numbering scheme for [6] with the packing diagram in Figure 3.4.

3.3. Discussion

The complexes exhibit pentagonal-bipyramidal geometry about the uranyl (VI) atom, involving two bidentate β-diketonate ligands and a pyridine molecule. Thus they have similar geometries to [7], and aquadioxobis(pentane-2,4-dionato)uranium(VI)[14] the only other uranyl β-diketonates to have been studied structurally. In none of our complexes was the magnitude of the distortion of the actinyl bond angle as great as the 173.5(8)° found in [7], though that in [6] approaches it (175.8(8)°)

The packing diagram of [5] (Figure 3.2) appears to be dominated by a face-to-face alignment of the phenyl rings, while for [6], the relatively low density correlates with the molecules being held apart by contacts between the methyl groups. In complex [5], the groups containing the β-carbon atoms are oriented such that C(034) lies below (0.08(5)Å) the equatorial plane. In parallel with this distortion, the C(41) - C(46) ring lies completely above this plane (though not symmetrically), with deviations in the range 0.20 - 0.62(5)Å. The β carbon (C(012)) of the other ligand lies above the plane (0.15(5)Å) and the C(11) - C(16) ring is positioned below the plane (0.11 - 0.51(5)Å). Again this displacement is not symmetrical. These rings are twisted outwards away from one another (see Figure 3.1 and Table 4) with pairs C(15), C(16) and C(45), C(46) having maximum displacements below and above the plane repectively. The pyridine ligand slots into the cavity with a substantial out of plane twist; (C(51),C(52),C(53) are directed below the plane, and C(54), C(55) above).

The other phenyl rings on the ligands are twisted inwards towards one another, and are displaced above and below the equatorial plane. Deviations for C(21) - C(26) lie in the range 0.23(5)Å below (C(25)) and 0.50(5)Å above (C(22)). Similarly for C(31) - C(36), deviations are in the range 0.43(5)Å below (C(32)) and 0.76(5)Å above (C(35)).

In complex [6], primed atoms are related to unprimed ones by a mirror plane. The β carbon (C(3)) in this complex lies below the equatorial plane by 0.37(5)Å. C(2) and O(5) are both displaced below the plane (0.35 and 0.17(5)Å respectively) C(5) is found above the plane (0.23(5)Å), and the orientation of the *t*-butyl group with respect to the plane is such that C(6) is above (1.65(5)Å), C(7) is virtually co-planar (0.09(5)Å), and C(8) is directed below the plane (0.93(5)Å).

The ligand dimensions in each complex are as expected, (apart from the possible disorder in [6]), as are the U-O distances to the chelating ligands. The U-N distances are longer than U-O (eq) as predicted from the covalent radii; they are significantly longer than that found in complex [7]. The pyridine ring in complex [5] is twisted out of the equatorial plane, forming an angle with this plane of 36.9(2)°, whilst in complex [6], it lies parallel to the uranyl group(90.0° twist), (in [7], the out of plane twist is 48.7(10)°). These twists presumably reduce interference with the diketonate groups, but must have the effect of increasing repulsions between the *o*-hydrogen atoms on the pyridine and the actinyl oxygen atoms.

It is surprising to find that neither of the O-M-O groups in complexes [5] or [6] show substantial non-linearity compared to that found in [7]. The pyridine - uranyl repulsions were believed to be responsible for the non-linear O-U-O group in this complex; however study of the pyridine-H to actinyl-O distances shows that this steric influence is less in [7] than in the other complexes, yet the distortion of the actinyl bond is greatest (Table 3.6). Furthermore there is no apparent correlation between O-M-O bond angles and M-O(axial) bond lengths which could account for this. The one parameter which does show a correlation with the distortion is the U-N distance. It may therefore be that direct O-N repulsion in the actinyl coordination sphere is responsible for the bent O-U-O group in [7]. In their turn, the M-N distances show an inverse correlation with the M-O(equatorial) distances, implying that the acac groups in [5]-[6] are rather more strongly held than in [7], leading to steric pressure and slight weakening of the M-N bond.

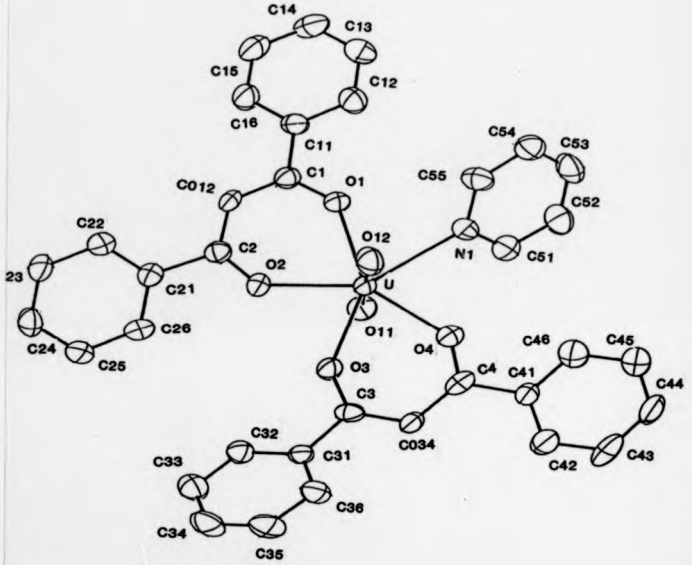

FIGURE 3.1 (a) The $C_{21}H_{31}NO_4U$ [5] molecule showing the atomic numbering scheme

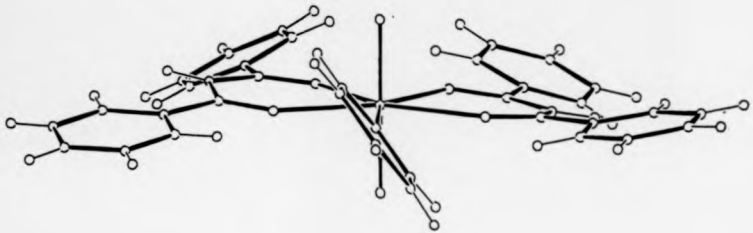

FIGURE 3.1 (b) side-on view of [5] showing deviations out of plane

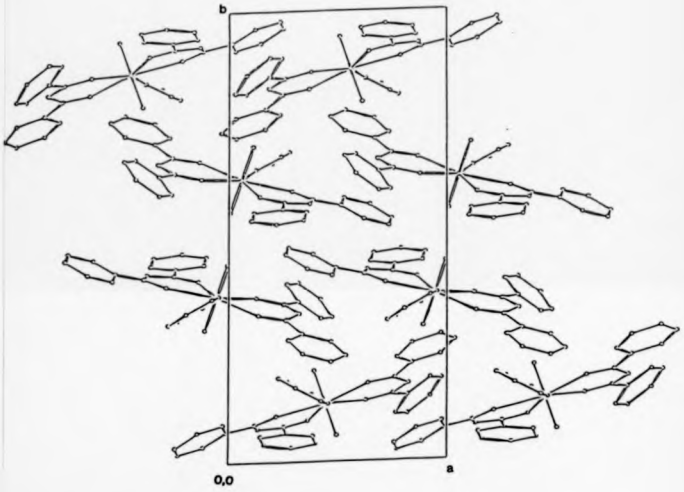

FIGURE 3.2 Packing diagram for [5].

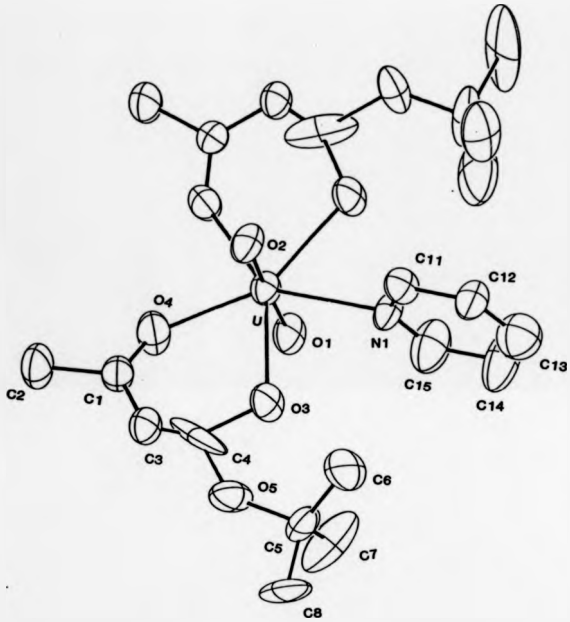

FIGURE 3.3 view of the $C_{33}H_{37}NO_6U$ [6] molecule showing the atomic numbering scheme

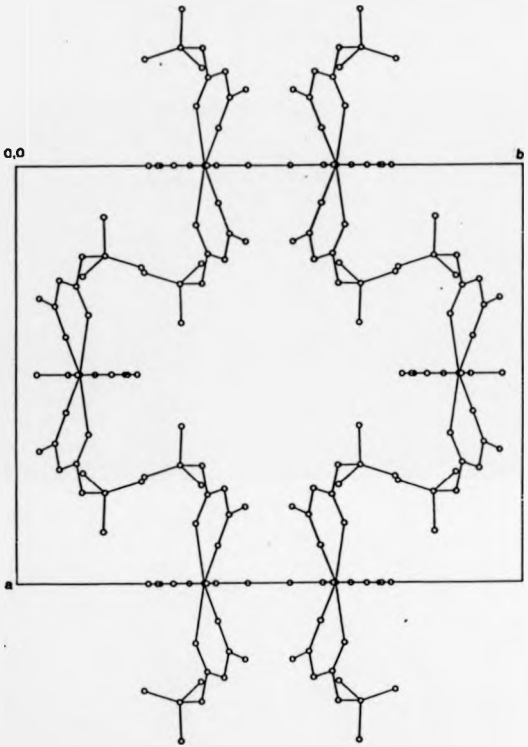

FIGURE 3.4 Packing diagram for [6]

TABLE 3.1

Crystal Data and Data Collection Conditions

Compound	**[5]**	**[6]**
Formula	$C_{21}H_{31}NO_6U$	$C_{35}H_{27}NO_6U$
M_r	795.6	663.5
Z	4	4
Crystal System	Monoclinic	Orthorhombic
a/Å	10.158(2)	15.939(9)
b/Å	21.937(8)	19.532(8)
c/Å	13.888(4)	9.777(6)
β/°	103.49(1)	
Systematic Absences	$0k\,0: k \neq 2n$	$hkl: h+k \neq 2n$
	$h\,0\,l: h+k \neq 2n$	$hol: l \neq 2n$
Space Group	$P2_1/n$	$Cmc2_1$
Crystal size/mm.	.15×.10×.28	.13×.04×.29
Max. transmission factor	0.57	0.74
Min. transmission factor	0.28	0.65
2θ(max)	50	50
Scan range about K_{α_1}-K_{α_2}/°	-1.05/+0.9	-.9/+1.0
Reflections collected	5 776	1 551
Reflections observed $[I/\sigma(I) \geq 3.0]$	3 269	1 178
Weighting constant: g	0.00016	0.00150
R(final)	0.036	0.048
Rw(final)	0.033	0.048
max on final difference Fourier	0.74	
min on final difference Fourier	-0.56	-1.49
max δ/σ(final cycle)	0.142	0.058

TABLE 3.1 cont.

Analytical and infra-red data

Compound	**[5]**	**[6]**
Formula	$C_{35}H_{71}NO_8U$	$C_{21}H_{31}NO_8U$
M_r	795.6	663.5
C (found)	50.63	37.65
(expected)	52.84	38.01
H (found)	2.68	4.99
(expected)	3.40	5.77
N (found)	1.24	1.98
(expected)	1.76	2.11
ν U=O	913	890
ν C=O	1720	1700
ν U-N	1480	1480

TABLE 3.2

Atomic coordinates (×10⁴) for [5], with standard deviations in parentheses.

	x	y	z	U
U(1)	561(1)	6293(1)	7937(1)	46(1)*
O(11)	58(5)	5568(3)	8237(4)	62(2)*
O(12)	1091(6)	7021(3)	7685(4)	66(2)*
O(1)	2855(5)	6020(3)	8525(4)	60(2)*
C(1)	3826(7)	5824(3)	8174(5)	44(3)*
C(11)	5112(7)	5686(3)	8901(5)	46(3)*
C(12)	5261(9)	5858(4)	9875(5)	67(4)*
C(13)	6415(9)	5696(4)	10572(6)	78(4)*
C(14)	7431(8)	5376(4)	10323(6)	67(4)*
C(15)	7384(9)	5223(4)	9376(7)	83(4)*
C(16)	6158(8)	5378(4)	8663(6)	75(4)*
C(812)	3693(7)	5736(4)	7159(5)	51(3)*
C(2)	2508(8)	5781(3)	6450(5)	46(3)*
O(2)	1385(5)	5910(3)	6653(4)	75(3)*
C(21)	2424(7)	5631(3)	5385(5)	47(3)*
C(22)	3551(8)	5556(4)	5006(5)	63(3)*
C(23)	3488(9)	5378(4)	4024(6)	67(4)*
C(24)	2143(9)	5297(4)	3419(6)	61(3)*
C(25)	1022(8)	5385(4)	3779(5)	62(3)*
C(26)	1146(7)	5559(4)	4755(5)	57(3)*
O(3)	-1258(5)	6339(3)	6571(4)	61(2)*
C(3)	-2491(7)	6484(3)	6345(5)	47(3)*
C(31)	-3168(7)	6439(3)	5256(5)	43(3)*
C(32)	-2635(8)	6833(4)	4681(5)	55(3)*
C(33)	-3167(9)	6812(4)	3667(6)	66(3)*
C(34)	-4208(9)	6394(4)	3234(6)	78(4)*
C(35)	-4724(9)	6797(4)	3794(6)	75(4)*
C(36)	-4238(8)	6818(4)	4815(5)	59(3)*
C(834)	-3289(7)	6703(3)	7816(5)	49(3)*
C(4)	-2584(7)	6838(3)	8000(5)	44(3)*
O(4)	-1341(5)	6728(3)	8390(4)	60(2)*
C(41)	-3362(8)	7154(3)	8640(5)	46(3)*
C(42)	-4693(8)	7337(4)	8306(6)	65(4)*
C(43)	-5357(9)	7658(4)	8904(7)	77(4)*
C(44)	-4694(9)	7786(4)	9858(7)	82(4)*
C(45)	-3379(9)	7599(4)	10225(7)	89(5)*
C(46)	-2712(9)	7282(4)	9618(6)	69(4)*
H(1)	1212(6)	6583(3)	9809(4)	52(2)*
C(51)	465(8)	6284(4)	10394(5)	63(3)*
C(52)	773(10)	6341(4)	11414(6)	83(4)*
C(53)	1953(10)	6644(4)	11845(6)	72(4)*
C(54)	2749(9)	6879(4)	11266(6)	67(4)*
C(55)	2352(8)	6798(4)	10250(6)	62(3)*

*Equivalent isotropic U defined as one third of the trace of the orthogonalised U_{ij} tensor

TABLE 3.3

Atomic coordinates (×10⁴) for [6], with standard deviations in parentheses.

	x	y	z	U
O(1)	0	6280(1)	7500	58(1)*
O(1)	0	7149(3)	7077(18)	66(7)*
O(2)	0	5417(7)	8038(18)	63(6)*
O(3)	-1429(9)	6447(7)	8331(12)	65(4)*
O(4)	-981(9)	6084(10)	5774(16)	87(6)*
C(1)	-1636(12)	5766(9)	5699(19)	55(6)*
C(2)	-1822(14)	5470(13)	4322(25)	90(9)*
C(3)	-2257(14)	5877(9)	6664(18)	58(6)*
C(4)	-2116(13)	6213(7)	7454(71)	121(16)*
O(5)	-2823(10)	6326(7)	8573(15)	78(5)*
C(5)	-2838(18)	6760(13)	9798(25)	100(11)*
C(6)	-2553(33)	7471(14)	9442(34)	149(15)*
C(7)	-3765(24)	6735(29)	10857(45)	223(24)*
C(8)	-2548(22)	6337(14)	10966(29)	113(13)*
N(1)	0	6571(11)	10896(25)	68(8)*
C(11)	0	6846(15)	11821(29)	59(9)*
C(12)	0	6229(13)	12489(124)	72(10)*
C(13)	0	6886(15)	12850(46)	101(11)
C(14)	0	7387(18)	11870(35)	119(19)*
C(15)	0	7201(17)	10396(36)	103(17)*

*Equivalent isotropic U defined as one third of the trace of the orthogonalised U_{ij} tensor

TABLE 3.4

Selected bond lengths (Å) and bond angles (°) around the metal atoms with standard deviations in parentheses. †

a) Bond lengths	**[5]**	**[6]**	**[7]**
M-O(11)	1.751(5)	1.746(18)	1.83(1)
M-O(12)	1.747(6)	1.771(14)	
M-O(1)	2.360(5)	2.440(14)	2.34(1)
M-O(2)	2.299(6)	2.281(15)	2.44(1)
M-O(3)	2.317(4)	"	"
M-O(4)	2.367(5)	"	"
M-N(1)	2.575(6)	2.595(24)	2.47(1)

b) Bond Angles	**[5]**	**[6]**	**[7]**
O(11)-M-O(12)	177.9(2)	175.8(8)	173.5(8)
O(11)-M-O(1)	90.3(2)	87.1(4)	89.1(5)
O(11)-M-O(2)	91.8(2)	93.1(6)	89.6(6)
O(11)-M-N(1)	86.7(2)	91.1(7)	93.2(5)
O(11)-M-O(4)	90.1(2)	"	"
O(11)-M-O(3)	90.8(2)	"	"
O(12)-M-N(1)	91.2(2)	84.7(7)	"
O(12)-M-O(1)	88.6(2)	91.4(4)	"
O(12)-M-O(2)	89.6(3)	90.2(6)	"
O(12)-M-O(4)	89.7(2)	"	"
O(12)-M-O(3)	91.1(2)	"	"
O(1)- M-O(2)	70.5(2)	71.9(5)	71.1(4)
O(3)- M-O(4)	70.1(2)	"	"

† The atomic numbering refers to [5], and the values for [6] relate to corresponding atoms. Compound [7] is included as a comparison.

TABLE 3.5

Full bond lengths (Å)

For compound [5]

U(1)-O(11)	1.750(5)	U(1)-O(12)	1.746(6)
U(1)-O(1)	2.367(5)	U(1)-O(2)	2.294(6)
U(1)-O(3)	2.329(4)	U(1)-O(4)	2.363(5)
U(1)-N(1)	2.575(6)	O(1)-C(1)	1.270(10)
C(1)-C(11)	1.492(9)	C(1)-C(12)	1.399(10)
C(11)-C(12)	1.374(11)	C(11)-C(16)	1.363(12)
C(12)-C(13)	1.383(11)	C(13)-C(14)	1.356(13)
C(14)-C(15)	1.336(13)	C(15)-C(16)	1.390(11)
C(012)-C(2)	1.377(9)	C(2)-O(2)	1.267(10)
C(2)-C(21)	1.498(10)	C(21)-C(22)	1.374(12)
C(21)-C(26)	1.402(9)	C(22)-C(23)	1.394(11)
C(23)-C(24)	1.379(11)	C(24)-C(25)	1.356(13)
C(25)-C(26)	1.387(11)	O(3)-C(3)	1.269(9)
C(3)-C(31)	1.518(9)	C(3)-C(034)	1.391(11)
C(31)-C(32)	1.385(11)	C(31)-C(36)	1.398(10)
C(32)-C(33)	1.391(10)	C(33)-C(34)	1.371(12)
C(34)-C(35)	1.363(13)	C(35)-C(36)	1.395(11)
C(034)-C(4)	1.403(9)	C(4)-O(4)	1.280(8)
C(4)-C(41)	1.488(11)	C(41)-C(42)	1.386(11)
C(41)-C(46)	1.398(10)	C(42)-C(43)	1.367(13)
C(43)-C(44)	1.378(12)	C(44)-C(45)	1.381(12)
C(45)-C(46)	1.382(14)	N(1)-C(51)	1.321(11)
N(1)-C(55)	1.339(10)	C(51)-C(52)	1.386(11)
C(52)-C(53)	1.383(13)	C(53)-C(54)	1.363(14)
C(54)-C(55)	1.392(12)		

For compound [6]

U(1)-O(1)	1.746(18)	U(1)-O(2)	1.771(14)
U(1)-O(3)	2.440(14)	U(1)-O(4)	2.281(15)
U(1)-N(1)	2.595(24)	U(1)-O(3a)	2.439(14)
U(1)-O(4a)	2.281(15)	O(3)-C(4)	1.466(47)
O(4)-C(1)	1.245(24)	C(1)-C(2)	1.511(31)
C(1)-C(3)	1.379(28)	C(3)-C(4)	1.637(55)
C(4)-O(5)	1.584(53)	O(5)-C(5)	1.468(29)
C(5)-C(6)	1.495(40)	C(5)-C(7)	1.512(47)
C(5)-C(8)	1.686(39)	N(1)-C(11)	1.371(36)
N(1)-C(15)	1.266(39)	C(11)-C(12)	1.479(121)
C(12)-C(13)	1.332(54)	C(13)-C(14)	1.378(51)
C(14)-C(15)	1.486(49)		

TABLE 3.6

Full bond angles (°) for compound [5]

O(11)-U(1)-O(12)	177.9(2)	O(11)-U(1)-O(1)	90.3(2)
O(12)-U(1)-O(1)	88.7(2)	O(11)-U(1)-O(2)	91.6(2)
O(12)-U(1)-O(2)	89.7(3)	O(1)-U(1)-O(2)	70.8(2)
O(11)-U(1)-O(3)	90.8(2)	O(12)-U(1)-O(3)	91.1(2)
O(1)-U(1)-O(3)	145.9(2)	O(2)-U(1)-O(3)	75.0(2)
O(11)-U(1)-O(4)	90.3(2)	O(12)-U(1)-O(4)	89.6(2)
O(1)-U(1)-O(4)	144.2(2)	O(2)-U(1)-O(4)	144.9(2)
O(3)-U(1)-O(4)	69.9(2)	O(11)-U(1)-N(1)	86.9(2)
O(12)-U(1)-N(1)	91.1(2)	O(1)-U(1)-N(1)	71.8(2)
O(2)-U(1)-N(1)	142.6(2)	O(3)-U(1)-N(1)	142.3(2)
O(4)-U(1)-N(1)	72.5(2)	U(1)-O(1)-C(1)	138.0(4)
O(1)-C(1)-C(11)	116.5(6)	O(1)-C(1)-C(012)	121.8(6)
C(11)-C(1)-C(012)	121.7(7)	C(1)-C(11)-C(12)	119.9(7)
C(1)-C(11)-C(16)	123.3(7)	C(12)-C(11)-C(16)	116.8(7)
C(11)-C(12)-C(13)	120.9(8)	C(12)-C(13)-C(14)	121.5(8)
C(13)-C(14)-C(15)	118.1(7)	C(14)-C(15)-C(16)	121.3(9)
C(11)-C(16)-C(15)	121.5(8)	C(1)-C(012)-C(2)	125.6(7)
C(012)-C(2)-O(2)	122.8(7)	C(012)-C(2)-C(21)	122.5(7)
O(2)-C(2)-C(21)	114.5(6)	U(1)-O(2)-C(2)	139.5(4)
C(2)-C(21)-C(22)	122.5(6)	C(2)-C(21)-C(26)	118.6(7)
C(22)-C(21)-C(26)	118.8(7)	C(21)-C(22)-C(23)	119.7(7)
C(22)-C(23)-C(24)	120.7(8)	C(23)-C(24)-C(25)	120.1(7)
C(24)-C(25)-C(26)	120.0(7)	C(21)-C(26)-C(25)	120.5(7)
U(1)-O(3)-C(3)	140.4(5)	O(3)-C(3)-C(31)	115.6(7)
O(3)-C(3)-C(034)	124.2(6)	C(31)-C(3)-C(034)	120.1(6)
C(3)-C(31)-C(32)	117.9(6)	C(3)-C(31)-C(36)	122.1(7)
C(32)-C(31)-C(36)	119.8(6)	C(31)-C(32)-C(33)	119.4(7)
C(32)-C(33)-C(34)	120.6(8)	C(33)-C(34)-C(35)	120.3(7)
C(34)-C(35)-C(36)	120.3(8)	C(31)-C(36)-C(35)	119.6(8)
C(3)-C(034)-C(4)	122.3(6)	C(034)-C(4)-O(4)	124.0(7)
C(034)-C(4)-C(41)	119.8(6)	O(4)-C(4)-C(41)	116.2(6)
U(1)-O(4)-C(4)	138.7(5)	C(4)-C(41)-C(42)	122.9(7)
C(4)-C(41)-C(46)	118.4(7)	C(42)-C(41)-C(46)	118.7(8)
C(41)-C(42)-C(43)	121.3(7)	C(42)-C(43)-C(44)	119.5(8)
C(43)-C(44)-C(45)	120.8(9)	C(44)-C(45)-C(46)	119.5(8)
C(41)-C(46)-C(45)	120.2(8)	U(1)-N(1)-C(51)	120.2(5)
U(1)-N(1)-C(55)	123.0(5)	C(51)-N(1)-C(55)	116.5(6)
N(1)-C(51)-C(52)	124.5(8)	C(51)-C(52)-C(53)	117.4(9)
C(52)-C(53)-C(54)	119.9(8)	C(53)-C(54)-C(55)	118.0(8)
N(1)-C(55)-C(54)	123.6(8)		

TABLE 3.6 cont.

Full bond angles (°) for complex [6]

O(1)-U(1)-O(2)	175.8(8)	O(1)-U(1)-O(3)	87.1(4)
O(2)-U(1)-O(3)	91.4(4)	O(1)-U(1)-O(4)	93.1(6)
O(2)-U(1)-O(4)	90.2(6)	O(3)-U(1)-O(4)	71.9(5)
O(1)-U(1)-N(1)	91.1(7)	O(2)-U(1)-N(1)	84.7(7)
O(3)-U(1)-N(1)	69.3(3)	O(4)-U(1)-N(1)	140.7(4)
O(1)-U(1)-O(3a)	87.1(4)	O(2)-U(1)-O(3a)	91.4(4)
O(3)-U(1)-O(3a)	138.8(6)	O(4)-U(1)-O(3a)	150.8(5)
N(1)-U(1)-O(3a)	69.3(3)	O(1)-U(1)-O(4a)	93.2(6)
O(2)-U(1)-O(4a)	90.1(6)	O(3)-U(1)-O(4a)	150.8(5)
O(4)-U(1)-O(4a)	78.1(7)	N(1)-U(1)-O(4a)	140.7(4)
U(1)-O(3)-C(4)	117.6(20)	U(1)-O(4)-C(1)	135.6(13)
O(4)-C(1)-C(2)	112.8(17)	O(4)-C(1)-C(3)	126.1(18)
C(2)-C(1)-C(3)	121.5(18)	C(1)-C(3)-C(4)	115.9(27)
O(3)-C(4)-C(3)	142.5(24)	O(3)-C(4)-O(5)	94.8(36)
C(3)-C(4)-O(5)	116.8(21)	C(4)-O(5)-C(5)	130.6(20)
O(5)-C(5)-C(6)	110.1(21)	O(5)-C(5)-C(7)	97.2(25)
C(6)-C(5)-C(7)	118.7(33)	O(5)-C(5)-C(8)	106.2(20)
C(6)-C(5)-C(8)	120.4(27)	C(7)-C(5)-C(8)	109.6(27)
U(1)-N(1)-C(11)	119.8(17)	U(1)-N(1)-C(15)	116.3(21)
C(11)-N(1)-C(15)	124.7(27)	N(1)-C(11)-C(12)	117.7(27)
C(11)-C(12)-C(13)	119.3(66)	C(12)-C(13)-C(14)	120.3(61)
C(13)-C(14)-C(15)	120.2(32)	N(1)-C(15)-C(14)	117.9(30)

TABLE 3.7

Deviations (Å) from mean planes (defined by starred atoms; e.s.d.'s +/- 0.05Å)

Complex [5]

O(1)* -0.03; C(1)* 0.01; C(2)* 0.10; O(2)* -0.07; U(1)* -0.02; O(3)* -0.03; C(3)* -0.06; O(4)* 0.09; C(4)* 0.04; N(1)* -0.04; C(012) 0.15; C(034) -0.08; C(11) -0.11; C(12) -0.07; C(13) -0.26; C(14) -0.49; C(15) -0.51; C(16) -0.31; C(21) 0.15; C(22) 0.50; C(23) 0.45; C(24) 0.08; C(25) -0.23; C(26) -0.18; C(31) 0.02; C(32) -0.43; C(33) -0.28; C(34) 0.31; C(35) 0.76; C(36) 0.60; C(41) 0.20; C(42) 0.26; C(43) 0.47; C(44) 0.62; C(45) 0.54; C(46) 0.33

Complex [6]

O(3)* 0.13; C(4)* -0.01; C(1)* -0.20; O(4)* 0.16; U(1)* 0.01; O(3')* 0.13; C(4')* -0.01; C(1')* -0.22; O(4')* 0.16; N(1)* -0.22; C(2) -0.35; C(3) -0.37; C(5) 0.23; C(6) 1.65; C(7) 0.09; C(8) -0.93; O(5) -0.17;

TABLE 3.8

Comparison of M-N bond lengths (Å), O-M-O bond angles (°), inter-plane angles, and proximity of (pyridine) H - O (uranyl) atoms †

compound	[5]	[6]	[7]
M-N /Å	2.569(6)	2.595(2)	2.47(1)
O(11)-M-O(12) /°	177.9(2)	175.8(8)	173.5(8)
equatorial/pyridyl angle/°	36.9(2)	90.0(0)	48.7(10)
O(11)-H(51)	2.14	2.677	3.179
O(12)-H(55)	3.145	2.634	-

† Atomic numbering as for Table 5

References

1. N.W. Alcock, D.J. Flanders, and D. Brown, *J. Chem. Soc. Dalton Trans.*,, p. 679, 1984.
2. K.W. Bagnall, *Gmelin Handbuch Suppl Vol E.1*, p. 1, 1979.
3. E. Frasson, G. Bombieri, and C. Panattoni, *Coord. Chem. Revs.*, vol. 1, p. 145, 1966.
4. N.W. Alcock and D.J. Flanders, *Acta Cryst.*, vol. C43, p. 1480, 1987.
5. W. Blitz and J.A. Clinch, *Z. Anorg. Allgem. Chem.*, vol. 40, p. 218, 1904.
6. K. Hager, *Z. Anorg. Allgem. Chem.*, vol. 162, p. 82, 1927.
7. L. Sacconi, G. Caroti, and P. Paoletti, *J. Chem. Soc*, p. 4257, 1958.
8. L. Sacconi, G. Caroti, and P.Paoletti, *J. Inorg. Nucl. Chem.*, vol. 8, p. 93, 1958.
9. R.M. Pike, *Coord. Chem. Rev.*, vol. 2, p. 162, 1967.
10. S. Kawaguchi, *Coord. Chem. Rev.*, vol. 70, p. 51, 1986.
11. J.M. Haigh and D.A. Thornton, *Inorg. Nucl. Chem. Lett.*, vol. 6, p. 231, 1970.
12. A.E. Comyns, B.M. Gatehouse, and E. Wait, *J. Chem. Soc*, p. 4655, 1958.
13. L. Sacconi and G. Giannoni, *J. Chem. Soc.*, p. 2368, 1954.
14. N.W. Alcock, D.J. Flanders, M. Pennington, and D. Brown, *Acta Cryst.*, vol. C43, p. 1476, 1987.
15. N.W. Alcock, *Crystallographic Computing*, pp. p271-278, Copenhagen, Munksgaard.
16. G.M. Sheldrick, *SHELXTL User Manual*, Nicolet Instrument Co., 1983.
17. *International Tables For X-Ray Crystallography*, IV, Kynoch Press, Birmingham, 1974.

CHAPTER 4

The crystal and molecular structure of dioxobis(pyridine)dinitratouranium (VI)

4.1 Introduction

Relatively few uranyl complexes are known which contain a U-N bond; they include $UO_2Cl_2.2NH_3$[1] $[UO_2(C_5H_5N)_2]Cl_2$[2] and the title complex $[UO_2(C_5H_5N)_2](NO_3)_2$, [8]. The aqua-analogue, aquadioxobis(nitrato)pyridineuranium(VI), was first prepared by Barr and Horton.[3] The bis(pyridine) complex, [8], is prepared from this by replacement of the water molecule by pyridine. A detailed infra red study of the aqua complex with both pyridine and substituted pyridines shows a decrease in $\nu(UO_2^{2+})$ from 930cm^{-1} (pyridine) to 924cm^{-1} (α-picoline) to 921cm^{-1} (α-benzylpyridine). Study of the nitrate stretching bands (~ 1275cm^{-1}) indicated that there was no change in strength of the U-O(NO_3) bond in this series of compounds. This also shows that the substituents in α-picoline and -benzylpyridine do not influence the uranyl ion through the pyridine ring, but do so directly, since there is no change in the frequency of the ONO_2^- vibrations. The substitution of water for pyridine to give [8] leads to a slight increase in $\nu(ONO_2^-)$ splitting, indicative of an increase in the U-O(NO_3) bond strength.[4]

4.2 Experimental

4.2.1 *Preparation*

The complex was prepared by the method described by Barr and Horton. Pyridine (0.40g; 5.1mmole) was added to a stirred solution of uranyl nitrate (2g; 5.1mmole) in ethanol, causing precipitation of the aquopyridine complex. This was filtered and washed with ether, and vacuum dried. This product was then dissolved in pyridine and reprecipitated as $UO_2(py)_2(NO_3)_2$ by cooling after the addition of an equal volume of ether. The bright yellow crystals were washed with ether and dried. The crystals were found to lose pyridine on standing.

4.2.2 *Data Collection*

Freshly prepared crystals were used because of the problem caused by the loss of pyridine. To minimise this problem further, the mounted crystals were encapsulated in a Lindemann capillary in an atmosphere saturated with pyridine. Data were collected with a Syntex $P2_1$ automatic four-circle diffractometer. Maximum 2θ was 50°, scan range of +/- 1.1° (2θ) around K_{α_1}-K_{α_2}, scan speed 5-29.3° min^{-1} depending on the intensity of a 2s prescan. Background intensities were measured at each end of the scan for 0.25 of the scan time. Three standard reflections,

monitored every 200 reflections, showed slight changes during data collection; the data was rescaled to correct for this. Unit cell dimensions and standard deviations were obtained by least squares fit to 15 high angle reflections, ($25 \leq 2\theta \leq 29$). The crystal was recentered on 8 of these reflections every 100 reflections to maintain the unit cell parameters. Of the 1 414 reflections collected, 826 were considered to be observed, ($I/\sigma(I) \geq 3.0$), and were corrected for Lorentz, polarisation and absorption effects, the last by Gaussian methods. The crystal dimensions were 0.41 x 0.49 x 0.57mm, giving rise to maximum and minimum transmission factors of 0.112 and 0.031 respectively.

4.2.3 *Crystal Data*

Dioxobis(pyridine)dinitratouranium(VI); **[8]**: $C_{10}H_{10}N_4O_8U$, M = 552.24, monoclinic, space group $P2_1/a$, a= 16.456(3), b = 7.861(3), c = 5.719(1)Å, β = 95.12(2)°, U = 736.8(4)Å^3, Z = 2, D_c = 2.48 g cm^{-3}, μ(Mo - K_α) = 104.9 cm^{-1}, F(000) = 496

4.2.4 *Structure Solution*

Systematic absences h0l:h≠2n and 0k0:k≠2n gave the space group as $P2_1/a$, which was used in the refinement rather than rotating to the standard $P2_1/c$. The position of the uranium atom was found by the Patterson routine of SHELXTL[5] and the remaining lighter atoms by successive Fourier syntheses. Anisotropic temperature factors were used for all except the hydrogen atoms which were inserted at fixed positions (U=0.07Å^2) and not refined. Final refinement on F was by cascaded least squares methods. A weighting scheme of the form $W = 1/(\sigma^2(F) + g(F^2))$ was applied with g=0.00090. Calculations were carried out on a Data General DG30 using the SHELXTL system. Final R=0.075, wR=0.086. All of the relatively large residuals on the final difference map lay close to the uranium atom. Largest positive and negative peaks on a final difference Fourier synthesis were at heights of 4.26 and -3.69 el Å^{-3} Scattering factors in the analytical form and anomalous dispersion factors were taken from the International Tables.[6] Atomic coordinates are given in Table 4.1. Bond lengths and angles around the uranium atom are listed in Table 4.2. Table 4.3 contains details of the least squares planes. A full list of bond lengths and angles is given in Table 4.4

4.3 Discussion

Crystal decomposition resulted in a relatively poor data set, giving poor final refinement as indicated by the R- factors. In addition, the large size of the crystal introduced errors into its measurement for absorption correction purposes. As a result it would be unwise to draw too many conclusions from the structure, and only the general features are discussed below.

The complex exhibits the usual centrosymmetric hexagonal-bipyramidal geometry about the central uranium atom which is coordinated to two nitrogen atoms and four oxygen atoms in

the equatorial plane as shown in Figure 4.1. The packing diagram, Figure 4.2, indicates a face to face alignment of the aromatic rings. U-O(uranyl) distances (1.751(15)Å are similar to those in other hexagonal bipyramidal complexes (1.78(3)Å).[7] The uranyl group is constrained by symmetry to be linear. The nitrate group lies in the equatorial plane, but is twisted slightly such that the angle O(1)-U(1)-O(2) is 85.2(6)° whilst O(1)-U(1)-O(4) is 90.4(6)°. This twist is further illustrated by the angle of 79.5(5)° between the O(1)-O(1A) uranyl line and the plane of the nitrate ligand, rather than 90° if it lay in the equatorial plane. The U-N(pyridine) bond, 2.543(15)Å, is similar to other U-N distances (2.578(13)Å)[8] and not dissimilar from the values encountered in Chapter 3 (e.g. 2.569(6)Å). The pyridine molecule is also twisted slightly such that C(1) is directed away from O(1). The plane of the pyridine molecule forms an angle of 11.7(3)° with the plane of the nitrate group, and 2.0(5)° with the O-O(uranyl) line. There would appear to be no intramolecular contacts between pyridine-H and uranyl-O (contact distances 2.73(5)Å).

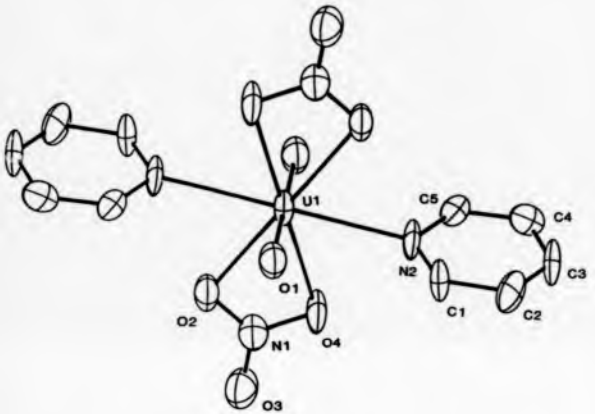

FIGURE 4.1 View of the $C_{10}H_{10}N_4O_8U$ molecule [8].

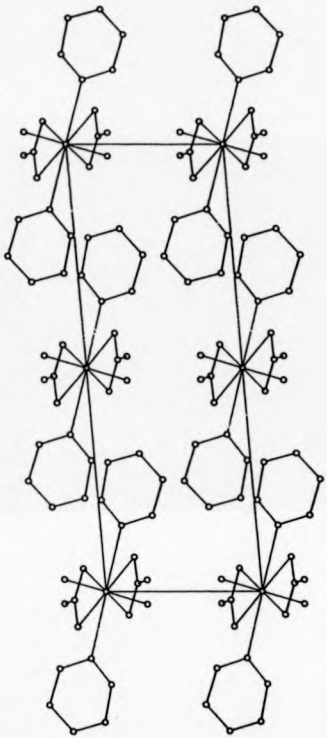

FIGURE 4.2 Packing diagram for $C_{10}H_{10}N_4O_8U$ molecule [8], viewed down *b*.

TABLE 4.1

Atomic coordinates ($\times 10^4$) and equivalent isotropic temperature factors ($\AA^2 \times 10^3$) for [8]
standard deviations in parentheses.

atom	x	y	z	U
U(1)	5000	5000	0	42(1)*
O(1)	5270(8)	5952(22)	-2587(25)	59(5)*
O(2)	5774(7)	7368(18)	2034(24)	55(5)*
O(3)	5261(15)	9853(20)	2731(39)	75(7)*
O(4)	4478(7)	7770(19)	1344(24)	62(5)*
N(1)	5198(10)	8380(24)	2095(26)	52(6)*
N(2)	3522(9)	5634(26)	-1416(33)	52(6)*
C(1)	2936(15)	5109(23)	-183(42)	53(7)*
C(2)	2110(17)	5250(23)	-854(57)	65(10)*
C(3)	1904(11)	6027(36)	-2954(40)	64(9)*
C(4)	2487(12)	6598(34)	-4329(35)	66(8)*
C(5)	3316(11)	6418(29)	-3449(34)	56(7)*

* Equivalent isotropic U defined as one third of the trace of the orthogonalised U_{ij} tensor.

TABLE 4.2

Bond lengths (Å) and angles (°)
(standard deviations in parentheses.

a) Bond lengths

U(1)-O(1)	1.751(15)	U(1)-O(2)	2.486(13)
U(1)-O(4)	2.488(15)	U(1)-N(2)	2.543(15)
U(1)-O(1a)	1.751(15)	U(1)-O(2a)	2.486(13)
U(1)-O(4a)	2.488(15)	U(1)-N(2a)	2.543(15)
O(2)-N(1)	1.251(22)	O(3)-N(1)	1.216(25)
O(4)-N(1)	1.302(20)	N(2)-C(1)	1.318(30)
N(2)-C(5)	1.333(27)	C(1)-C(2)	1.383(37)
C(2)-C(3)	1.363(38)	C(3)-C(4)	1.370(31)
C(4)-C(5)	1.418(27)		

b) Bond angles

O(1)-U(1)-O(2)	85.2(6)	O(1)-U(1)-O(4)	90.4(6)
O(2)-U(1)-O(4)	51.4(4)	O(1)-U(1)-N(2)	87.4(6)
O(2)-U(1)-N(2)	116.0(5)	O(4)-U(1)-N(2)	65.2(5)
O(1)-U(1)-O(1a)	180.0	O(2)-U(1)-O(1a)	94.8(6)
O(4)-U(1)-O(1a)	89.6(6)	N(2)-U(1)-O(1a)	92.6(6)
O(1)-U(1)-O(2a)	94.8(6)	O(2)-U(1)-O(2a)	180.0
O(4)-U(1)-O(2a)	128.6(4)	N(2)-U(1)-O(2a)	64.0(5)
O(1a)-U(1)-O(2a)	85.2(6)	O(1)-U(1)-O(4a)	89.6(6)
O(2)-U(1)-O(4a)	128.6(4)	O(4)-U(1)-O(4a)	180.0
N(2)-U(1)-O(4a)	114.8(5)	O(1a)-U(1)-O(4a)	90.4(6)
O(2a)-U(1)-O(4a)	51.4(4)	O(1)-U(1)-N(2a)	92.6(6)
O(2)-U(1)-N(2a)	64.0(5)	O(4)-U(1)-N(2a)	114.8(5)
N(2)-U(1)-N(2a)	180.0	O(1a)-U(1)-N(2a)	87.4(6)
O(2a)-U(1)-N(2a)	116.0(5)	O(4a)-U(1)-N(2a)	65.2(5)
U(1)-O(2)-N(1)	97.2(10)	U(1)-O(4)-N(1)	95.7(11)
O(2)-N(1)-O(3)	124.1(19)	O(2)-N(1)-O(4)	115.3(17)
O(3)-N(1)-O(4)	120.6(19)	U(1)-N(2)-C(1)	113.7(14)
U(1)-N(2)-C(5)	122.0(13)	C(1)-N(2)-C(5)	118.2(17)
N(2)-C(1)-C(2)	125.3(23)	C(1)-C(2)-C(3)	116.2(25)
C(2)-C(3)-C(4)	121.4(20)	C(3)-C(4)-C(5)	117.7(19)
N(2)-C(5)-C(4)	121.2(18)		

TABLE 4.3

Deviations (Å) from mean planes
starred atoms define planes, e.s.d's +/- 0.05Å).

Plane 1
N(1)* 0.01; O(2)* 0.00; O(3)* 0.00; O(4)* 0.00

Plane 2
N(2)* -0.01; C(1)* 0.00; C(2)* 0.00; C(3)* 0.01; C(4)* -0.01; C(5)* -0.02

Plane 3
C(1)* 0.00; N(2)* 0.00; C(5)* 0.00

Line 4
O(11)* ; O(21)*

Angles between plane normals and line (°)

1:2	11.7
1:3	
1:4	
2:3	
2:4	
3:4	

TABLE 4.3

Deviations (Å) from mean planes
starred atoms define planes, e.s.d's +/- 0.05Å).

Plane 1
N(1)* 0.01; O(2)* 0.00; O(3)* 0.00; O(4)* 0.00
Plane 2
N(2)* -0.01; C(1)* 0.00; C(2)* 0.00; C(3)* 0.01; C(4)* -0.01; C(5)* -0.02
Plane 3
C(1)* 0.00; N(2)* 0.00; C(5)* 0.00
Line 4
O(11)* ; O(21)*

Angles between plane normals and line (°)

1:2	10.7
1:3	11.3
1:4	87.8
2:3	1.9
2:4	88.5
3:4	88.1

References

1. E. Glueckauf and H.A.C. McKay, *Nature*, vol. 165, p. 594, 1950.
2. L.I. Katzin and J.C. Sullivan, *J. Phys. Colloid. Chem.*, vol. 55, p. 346, 1951.
3. H. Barr and A. Horton, *J. Amer. Chem. Soc.*, vol. 74, p. 4430, 1952.
4. I.M. Kopashova, I.K. Skutov, D.S Umreiko, and R.I. Shamanovskaya, *Russ. J. Inorg. Chem.*, vol. 12, p. 1748, 1967.
5. G.M. Sheldrick, *in SHELXTL User Manual*, Nicolet Instrument Co., Madison, Wis., 1981.
6. *International Tables for X-Ray Crystallography Vol IV*, Kynoch Press, Birmingham, 1974.
7. R.G. Denning, "Properties of the UO_2^{2+}," *Gmelin Handbuch, URAN suppl. vol. A6*, pp. 31-79.
8. N.W. Alcock, D.J. Flanders, and D. Brown, *Inorg. Chim. Acta*, vol. 94, p. 271, 1984.

CHAPTER 5

The structure of a 1,10-phenanthroline complex of uranyl acetate

5.1 Introduction

Previous work,[1] described complexes of the bidentate *N*-donor ligand 2,2'-dipyridyl with uranyl nitrate and acetate. The ability of this ligand to twist about the 1,1' C-C bond permits it to be accommodated in the equatorial plane of a hexagonal bipyramid. As an extension of this, it was of interest to substitute the more rigid ligand - 1,10-phenanthroline, which has similar geometry to dipyridyl, but is constrained by the benzene ring which joins the two pyridyl rings. This chapter describes the futher refinement of the highly disordered complex with uranyl acetate.

5.2 Experimental

5.2.1 *Preparation*

The compound was prepared by the technique of liquid diffusion, layering a saturated solution of uranyl acetate ($2cm^3$) on top of a saturated solution of 1,10-phenanthroline ($2cm^3$) and carefully sealing the tube. When the two solutions had completely mixed, the crystals which had formed at the interface were filtered off and washed with ice cold ethanol. The product was found to be an (OH)-bridged dimer from the structure determination.

5.2.2 *Data Collection*

Data were collected with a Syntex $P2_1$ automatic four-circle diffractometer for 2θ in the range 2.5-50° with a scan range of +/- 1.0° (2θ) around K_{α_1}-K_{α_2}. Background intensities were measured at each end of the scan for 0.25 of the scan time. Three standard reflections, monitored every 200 reflections, showed slight changes during data collection; the data were rescaled to correct for this. Unit cell dimensions and standard deviations were obtained by least squares fit to 15 high angle reflections. Of the 2 861 reflections collected, 1 994 were considered to be observed, ($I/\sigma(I) \geq 3.0$), and were corrected for Lorentz, polarisation and absorption effects, the last with ABSCOR.[2] The crystal dimensions were 0.30 x 0.18 x 0.67mm, giving rise to maximum and minimum transmission factors of 0.076 and 0.023 respectively. The density could not be measured because of the solubility of the crystals.

5.2.3 *Crystal Data*

Bis[μ-hydroxymonoacetato(1,10-phenanthroline)dioxouranium(VI) (ethanol solvate); [9]: $C_{28}H_{28}N_4O_{16}U_2$ (n C_2H_5OH), M = 1005.36, monoclinic, space group $C2/c$, a = 23.320(6), b =

9.945(4), c = 15.978(4)Å, β = 119.14(2)°, U = 3237(2)Å^3, Z = 4, D_c = 2.07 g cm^{-3}, μ(Mo - K_α) = 95.27 cm^{-1}

5.2.4 Structure Solution

Systematic absences $hkl: h+k \neq 2n$ and $h0l: l \neq 2n$ indicated a choice of two possible space groups: $C2/c$ and Cc. The position of the uranium atom was found by the Patterson routine of SHELXTL[3] and the remaining lighter atoms by successive Fourier syntheses. Structure solution in $C2/c$ located the phenanthroline ligand (and acetate group) and indicated that the molecule was a centrosymmetric dimer. However, maps showed two bridging atoms implausibly close to each other; the uranyl oxygen positions were also duplicated. Refinement was continued with both sets of positions included at half occupancy. A group of residual peaks distant from the main complex were interpreted as a partially occupied solvent molecule (presumably ethanol) approximated by 2 carbons with 0.5 occupancy, and in addition a smaller bridging peak was also located (final occupancy for these atoms 0.4, 0.4 and 0.2). A final R=0.060 w R=0.067 was obtained. All of the relatively large residuals on the final difference maps lay close to the uranium atoms. The true structure is presumably a non centrosymmetric dimer with one set of uranyl oxygen atoms on each uranium; this gives reasonable O(axial)-U-O(equatorial) angles. An attempt to refine the structure in space group Cc was however unsuccessful, either because of the high correlations between pseudo-related atoms or because the actual crystal studied was made up of molecules in both orientations.

Anisotropic temperature factors were used for the ordered atoms, and hydrogen atoms were inserted at fixed positions (U=0.07Å^2). Hydroxy hydrogen atoms were not included. Final refinement on F was by cascaded least squares methods. A weighting scheme of the form W = $1/(\sigma^2(F) + g(F^2))$ was applied. Calculations were carried out on a Data General DG30 using the SHELXTL system. Initial calculations were performed on a Data General NOVA 3 computer. Scattering factors in the analytical form and anomalous dispersion factors were taken from the International Tables.[4] Atomic coordinates are given in Table 5.1. Bond lengths and angles around the uranium atom are listed in Table 5.2. Table 5.3 contains details of the least squares planes.

5.3 Discussion

The complex exhibits a distorted hexagonal-bipyramidal geometry about the central uranyl group which is coordinated to two nitrogen atoms and four oxygen atoms (two from the acetate ligand and two from the hydroxy-bridge) in the equatorial plane, and thus is similar to the complexes with 2,2'-dipyridyl and nitrate complexes which the same bite distance (N...N mean of 2.67(2)Å in the four complexes previously described).

Figure 5.1 shows an idealised view of [9], in which one pair of uranyl O atoms is associated with each uranium atom, and in which only one set of bridging OH groups is included. Detailed discussion of the dimensions is hampered by the disorder which leads to abnormal values for U-O(uranyl) distances, whose apparent range is 1.57(2)-1.96(2)Å, compared to the average U-O distance in other hexagonal bipyramidal complexes (1.78(3)Å).[5] However the U-N and U-O(equatorial) bond lengths seem to be less affected, and are broadly similar in value to those previously reported.[6,7] The U-O(bridging) and (acetate) bond lengths have normal values (range 2.34(5)-2.42(4) and 2.46(1)-2.47(2)Å). Again these are similar to values previously observed[1] but there is a possible lengthening of the U-N(ligand) bonds to 2.65(3) and 2.63(2)Å compared to 2.56(2)Å found in the nitrate complex. The phenanthroline ligand is pivoted as a unit about the line from U to the centre of the 5-5' C-C bond producing an O...N (acetate-phenanthroline) contact of (2.97(2)Å) which is slightly longer than the equivalent distance found in the 2,2'-dipyridyl complex (2.96(1)Å). This twist, indicative of steric strain, produces an angle of 12.6(2)° between the plane of the ligand, and the plane containing the uranium and equatorial oxygen atoms. This may be caused by the need to accommodate the more rigid ligand in the equatorial plane, but it should also be borne in mind that one complex has two nitrate ligands and the other has one acetate and two hydroxides. The atoms which form the equatorial plane, are again puckered with deviations in the range -0.18(5) to 0.15(5)Å. The coordinating ligands are substantially displaced out of the equatorial plane (by up to 0.61(5)Å) as seen in Table 5.3. The acetate group is displaced slightly out of the the equatorial plane with a bite, (2.20(1)Å), similar to that found in the 2,2' dipyridyl analogue, (2.16(1) and 2.17(1)Å). The packing diagram, Figure 5.2, again indicates a face to face alignment of the aromatic rings.

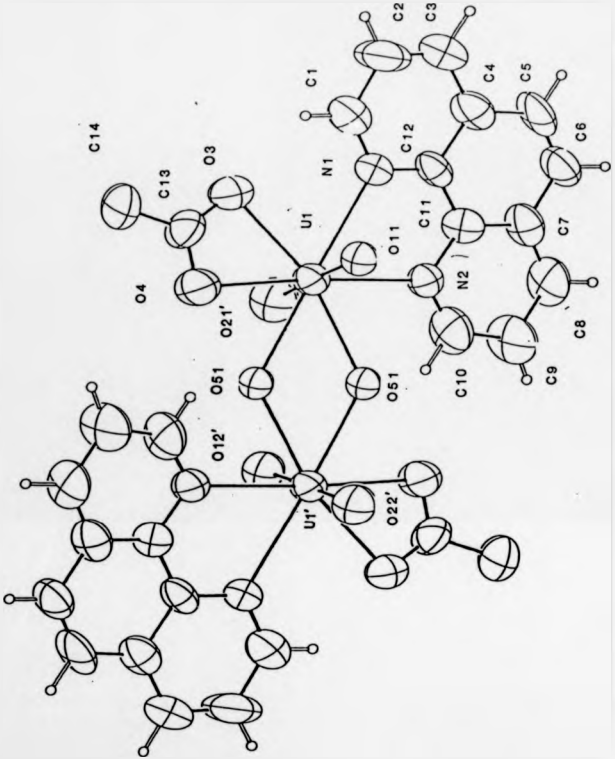

FIGURE 5.1 View of [9], as an idealised noncentrosymmetric dimer, with O(11) and O(21) associated with U(1) and O(12) and O(22) (as the centrosymmetrically related equivalents O(12') and O(22')) associated with U(1'); only O(51) and O(51') are included as bridging hydroxide positions.

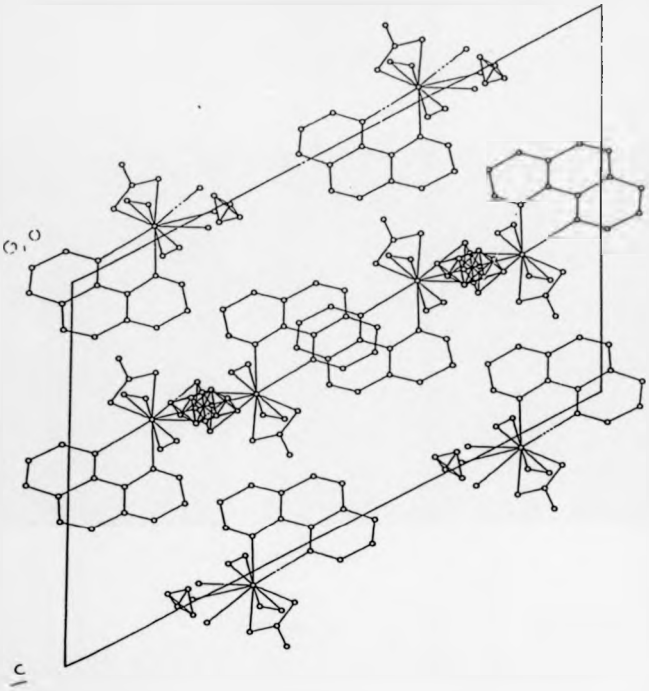

FIGURE 5.2 Packing diagram for [5], viewed down *b*. The alternative positions for the uranyl and bridging oxygen atoms can be seen.

TABLE 5.1

Atomic coordinates (x10⁴) and equivalent isotropic temperature factors (Å²x10³) for [9] standard deviations in parentheses.

Atom	x	y	z	U
O(1)	3477.1(3)	8128.1(6)	5367.0(5)	64(1)*
O(11)	4036(9)	6899(17)	6411(14)	53(5)
O(21)	2933(15)	9085(27)	4461(19)	91(8)
O(12)	3616(12)	6846(20)	6018(17)	67(6)
O(22)	3307(12)	9563(23)	4478(17)	76(6)
O(3)	4273(6)	9850(13)	6381(10)	94(8)*
O(4)	3420(7)	9658(14)	6542(11)	108(9)*
O(51)	2352(12)	8558(22)	4933(18)	48(5)
O(52)	2623(11)	7393(27)	5732(17)	49(6)
O(53)	2464(25)	6993(53)	4592(41)	51(12)
N(1)	4556(6)	7849(12)	5249(10)	66(7)*
N(2)	3442(7)	6525(13)	4059(10)	61(6)*
C(1)	5122(10)	8463(22)	5885(17)	102(13)*
C(2)	5727(10)	8276(23)	5897(18)	105(13)*
C(3)	5768(10)	7400(24)	5286(17)	104(13)*
C(4)	5166(9)	6699(16)	4573(13)	70(9)*
C(5)	5130(11)	5749(19)	3872(15)	90(13)*
C(6)	4590(10)	5132(20)	3306(15)	82(11)*
C(7)	3987(9)	5395(17)	3306(12)	71(9)*
C(8)	3411(10)	4764(18)	2701(13)	91(12)*
C(9)	2830(12)	5026(26)	2718(14)	108(12)*
C(10)	2932(11)	5904(20)	3472(14)	95(13)*
C(11)	3988(7)	6268(15)	3987(9)	53(7)*
C(12)	4561(8)	6965(13)	4615(11)	58(8)*
C(13)	3936(9)	10258(17)	6751(12)	70(9)*
C(14)	4132(11)	11391(22)	7426(18)	115(13)*
C(001)	2081(38)	1426(75)	4939(56)	146(26)
C(002)	2429(41)	2593(83)	5455(56)	153(23)
C(003)	2239(50)	2124(92)	4733(79)	89(24)
C(004)	1876(39)	1378(79)	4440(60)	71(19)

* Equivalent isotropic U defined as one third of the trace of the orthogonalised U_{ij} tensor.

TABLE 5.2

Bond lengths (Å) and angles (°) about the uranium atom

(standard deviations in parentheses. Disorder in the structure introduces inaccuracies in the values).

a) Bond lengths

U(1)-O(1)	1.94(3)
U(1)-O(2)	1.62(4)
U(1)-O(3)	2.50(2)
U(1)-O(4)	2.46(3)
U(1)-O(5)	2.34(5)
U(1)-O(6)	2.41(4)
U(1)-N(1)	2.65(3)
U(1)-N(2)	2.63(2)

b) Bond angles

O(1)-U(1)-O(2)	168.3(24)
O(1)-U(1)-O(3)	85.8(9)
O(2)-U(1)-O(3)	103.4(17)
O(1)-U(1)-O(4)	89.4(13)
O(2)-U(1)-O(4)	90.5(21)
O(1)-U(1)-O(5)	116.1(7)
O(2)-U(1)-O(5)	53.4(26)
O(1)-U(1)-O(6)	81.9(15)
O(2)-U(1)-O(6)	87.1(25)
O(1)-U(1)-N(1)	77.1(15)
O(1)-U(1)-N(2)	93.7(12)
O(2)-U(1)-N(1)	86.1(15)
O(2)-U(1)-N(2)	86.2(13)
O(3)-U(1)-N(1)	70.5(8)
O(3)-U(1)-N(2)	133.0(8)
O(4)-U(1)-N(1)	122.4(7)
O(4)-U(1)-N(2)	173.7(7)
O(3)-U(1)-O(4)	52.6(9)
O(5)-U(1)-O(6)	34.5(12)
N(1)-U(1)-N(2)	63.8(7)

TABLE 5.3

Deviations (Å) from mean planes
starred atoms define planes. e.s.d's +/- 0.05Å).

Plane 1
U(1)* -0.01; O(3)* 0.02; O(4)* 0.02; C(13)* -0.03
Plane 2
N(1)* -0.03; N(2)* 0.01; C(1)* 0.02; C(10)* 0.00; C(11)* 0.01; C(12)* -0.01
Plane 3
O(3)* 0.02; O(4)* 0.02; C(13)* -0.01; C(14)* 0.00
Line 4
O(11)* ; O(21)*

Angles between plane normals and line (°)

1:2	14.5
1:3	3.4
1:4	7.6
2:3	16.2
2:4	21.1
3:4	6.5

References

1. N.W. Alcock, D.J. Flanders, and D. Brown, *Inorg. Chim. Acta*, vol. 94, p. 271, 1984.
2. N.W. Alcock, *Crystallographic Computing*, pp. p271-278, Copenhagen, Munksgaard.
3. G.M. Sheldrick, *in SHELXTL User Manual*, Nicolet Instrument Co., Madison, Wis., 1981.
4. *International Tables for X-Ray Crystallography Vol IV*, Kynoch Press, Birmingham, 1974.
5. R.G. Denning, "Properties of the UO_2^{+}," *Gmelin Handbuch, URAN suppl. vol. A6*, pp. 31-79.
6. G. Bandoli, D.A. Clemente, G. Maragoni, and G. Paolucci, *J. Chem. Soc., Chem. Commun.*, p. 235, 1978.
7. G. Bandoli, D.A. Clemente, G. Maragoni, and G. Paolucci, *J. Chem. Soc., Dalton Trans.*, p. 1304, 1980.

CHAPTER 6

Some Unexpected Side Reactions - Three Further Structures

6.1. Introduction.

It was stated earlier (Chapters 1 and 2) that the preparation of complexes containing U-S bonds is difficult; a result of hard and soft acid and base interactions. This problem is further compounded by the fact that the uranyl ion will complex preferentially with other donors which are present in solution. This chapter describes three complexes obtained during attempts to prepare U-S bonded species. Two of these, [10] and [11], involve S-S bonds formed by the oxidation of the ligand. The third complex [12], illustrates this preferred complexation of donors other than sulphur.

6.2. Experimental

6.2.1 *Preparation*

Bis (tetraphenylarsonium) *cis - cis* (1,2-dicyanoethylene-1,2-dithiolate) dimer, [10]; was isolated during an attempt to prepare the 1,2-dicyanoethylene-1,2-dithiol salt of uranium (VI). The thiol ligand was prepared using the method described by Davison and Holm.[1] 0.50g of this ligand in methanol was then added to a solution of uranyl acetate (0.58g) producing an olive green coloured solution. When addition was complete, the mixture was heated at reflux for 2hrs. When cool, the volume of solvent was reduced until the first sign of precipitation. The solution was then filtered and tetraphenylarsonium chloride (1.0g) in methanol added. After further cooling, yellow needle-like crystals had formed, which were shown by structure determination to be the *cis - cis* disulphide.

Dimethylthiopyrimidine dimer [11], was formed in an attempt to prepare the dimethylthiopyrimidine product of uranyl nitrate described by Baghlaf *et. al.*.[2] Dimethylmercaptopyrimidine (0.71g) dissolved in methanol (doped with dimethylsulphoxide) was added to a solution of uranyl nitrate (1.0g) in methanol. The colour of the solution became yellow-orange. The volume of solvent was reduced by 50%, and the solution allowed to stand. After 48hrs, small well-defined block-like crystals were observed. Structural study showed these to be the dimeric, oxidised form of the ligand.

Bis(N,N-dimethylformamide)dinitratodioxouranium(VI) [12], was isolated during a further attempt to prepare the dimethyl thiopyrimidine complex with uranyl nitrate. The ligand (0.7g) in acetonitrile was added to uranyl nitrate in acetonitrile. The mixture was warmed gently under

conditions of reflux, then allowed to cool. When cool, the volume of solvent was reduced slightly, and the solution stored at 0° C for 7 days. Orange-red pyramid-like crystals were filtered off, and recrystallised from acetonitrile. These became opaque when left in the open for several days, but were stable for weeks if contained in a vial. As a result of this, suitable crystals were immediately encapsulated in a Lindemann capillary for the purposes of structure determination.

6.2.2 *Data Collection and Structural Solution*

For all three compounds, data were collected with a Syntex $P2_1$ automatic four-circle diffractometer. Maximum 2θ was 50° for all three complexes. Scan range of +/- 1.1° (2θ) around K_{α_1}-K_{α_2}, scan speed 2.5-29.3° min^{-1} depending on the intensity of a 2s preacan. Background intensities were measured at each end of the scan for 0.25 of the scan time. Three standard reflections were monitored every 200 reflections These showed slight changes during data collection for [10] and [11]; the data was rescaled to correct for this, but were stable for [12]. Unit cell dimensions and standard deviations were obtained by least squares fit to 15 high angle reflections. In each case, of the reflections collected, the criterion ($I/\sigma(I)\geq 3.0$) was used to deem whether or not they were observed. If so, they were corrected for Lorentz, polarisation and absorption effects, the last with ABSCOR.[3]

All three complexes were solved using SHELXTL[4] on a Data General DG30 computer. The position of the uranium atom in compound [12] was determined from a three dimensional Patterson map. Lighter non-hydrogen atoms for all three complexes were located by subsequent Fourier syntheses and refined anisotropically. Hydrogen atoms were inserted at calculated positions with isotropic temperature factors U=0.07Å^2.

6.2.3 *Crystal Data*

$C_{36}H_{40}N_4S_4As_2$, [10]; M=1047.04, monoclinic, $P2_1/n$, a=13.629(3), b=9.647(3), c=19.872(5), β=102.71(2). U=2560.5(1.0)Å^3, Z=2, D_c=1.36g cm^{-3}, μ(Mo - K_α)=14.98cm^{-1}, F(000)=1 076, R=4.53, Rw=4.70, g=0.0005. Crystal dimensions were 0.47 x 0.14 x 0.28mm giving rise to maximum and minimum transmission factors of 0.87 and 0.72.

$(C_6H_7N_2S_2)_2$, M=342.51, [11]; monoclinic, $P2_1/c$, a=13.284(3), b=9.078(4), c=12.287(5), β=107.74(2),U=1417(1)Å^3, Z=4, D_c=1.60g cm^{-3}, μ(Mo -K_α)=3.49cm^{-1}, F(000)=592, R=5.43, Rw=6.41, g=0.0017. Crystal dimensions were 0.43 x 0.31 x 0.52mm giving rise to maximum and minimum transmission factors of 0.39 and 0.23.

$C_8H_{14}O_{10}U$, [12]; M=540.23, monoclinic, $P2_1/n$, a=5.616(2), b=8.458(3), c=15.984(5)Å, β=98.21(2)°, U=751.4(4)Å^3 Z=2, D_c=2.39g cm^{-3}, μ(Mo-K_α)=103.0 cm^{-1}, F(000)=559.91,

R=2.72, Rw=2.75, g=0.00062. Crystal dimensions were 0.57 x 0.45 x 0.46 giving rise to maximum and minimum transmission factors of 0.18 and 0.11

6.3 Discussion

Complexes [10] and [11] should be viewed as oxidation products. Such oxidations are reported to occur in reactions of thiols with a number of one-electron oxidising agents, producing in the first instance with 1,2-dicyanoethylene-1,2-dithiol the *cis-cis* disulphide [10].

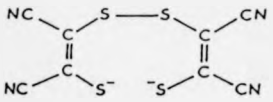

[10]

The uranyl ion in the reactions producing [10] and [11] presumably serves as this one electron oxidant, and is itself reduced to uranium(V). However, this species is relatively unstable (See 1.1) and disproportionates to give uranium(IV) and uranium(VI), which could then be used in further oxidation reactions. Spectroscopic characterisation of the final solutions to identify the uranium species present were not performed, these species would be expected to be predominantly uranium(VI), since any uranium(IV) species produced would be oxidised by the reaction conditions to uranium(VI).

The crystal structure identified [12] not as the desired thio complex, but as the dimethylformamide adduct $UO_2(CON(CH_3)_2(NO_3)_2$. This was apparently formed by the preferential coordination of dimethylformamide impurity present in the acetonitrile. The structure of [12] has recently been reported by Martin-Gil *et. al.*.[5] Our redetermination is of comparable accuracy and shows no differences from the published structure. Further information is therefore not included.

Atomic coordinates, bond lengths and angles for [10] - [11] are given in Tables 6.1 - 6.2. The anion of [10] is illustrated in Figure 6.1. Figure 6.2 shows the packing diagram for this. Complex [11] is illustrated in Figure 6.3, with its packing diagram in Figure 6.4.

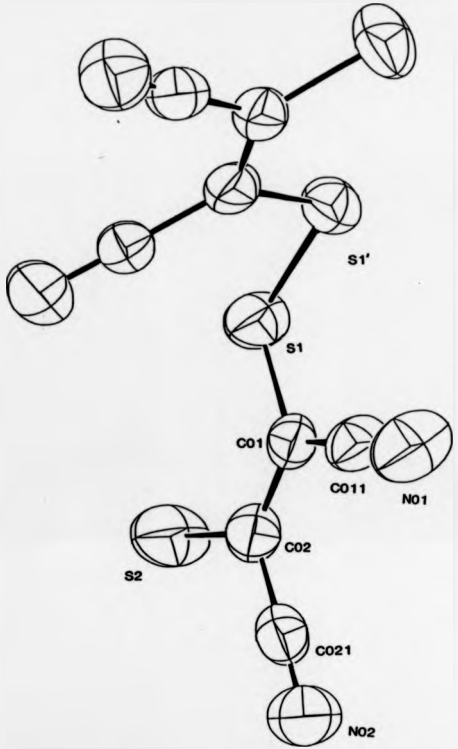

Figure 6.1 View of [10] showing atomic numbering scheme

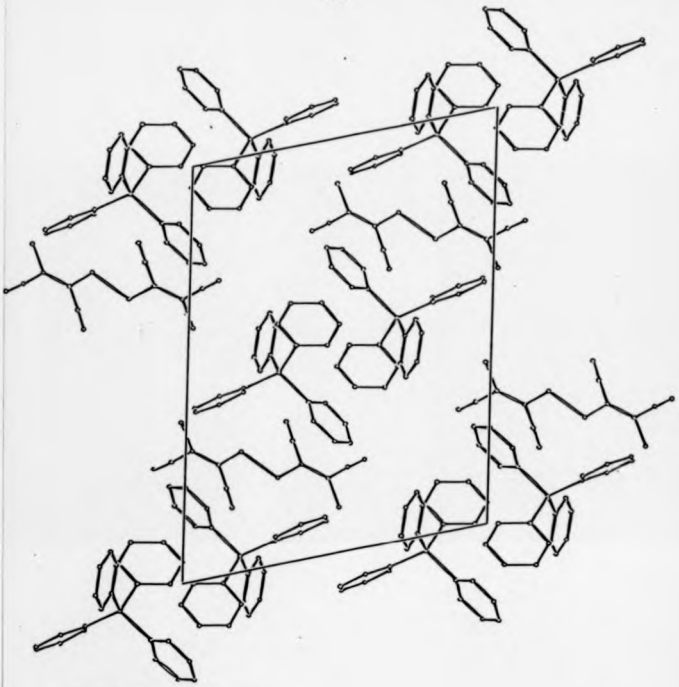

Figure 6.2 Packing diagram for [10]

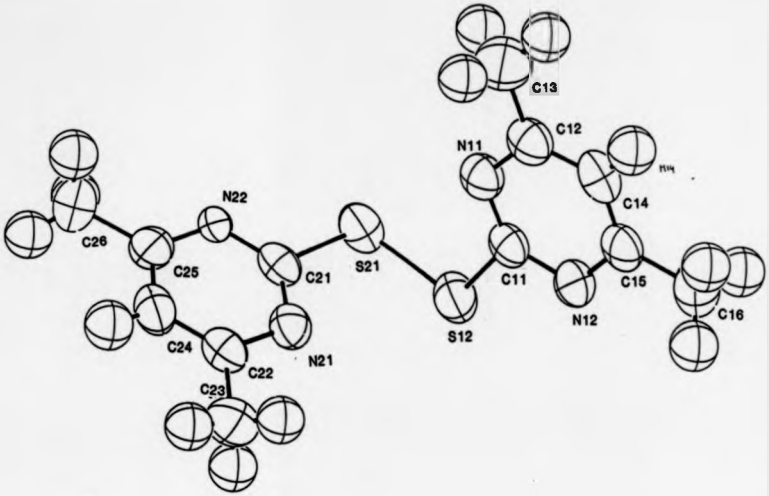

Figure 6.3 View of [11] showing atomic numbering scheme

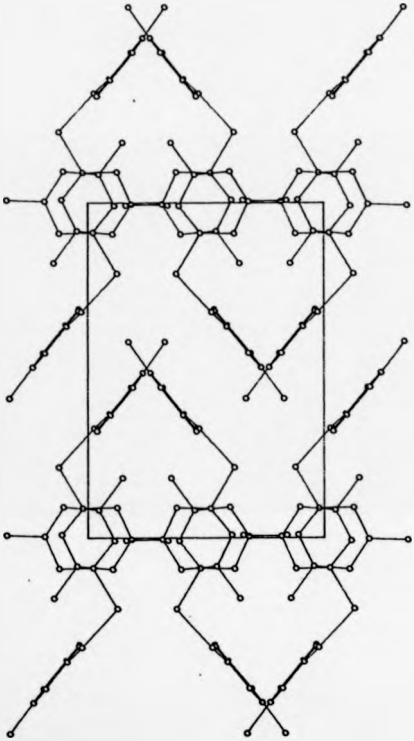

Figure 6.4 Packing diagram for [11]

TABLE 6.1

Atomic coordinates (Å x10⁴) bond lengths(Å) and angles(°) for for [10] (standard deviations in parentheses)

a) Atomic coordinates

	x	y	z	U
As(1)	1926(1)	6289(1)	-383(1)	48(1)*
N(01)	6643(4)	9026(6)	3410(3)	86(2)*
N(02)	4028(4)	9690(6)	2121(3)	78(2)*
S(1)	6886(1)	6289(2)	2097(1)	59(1)*
S(2)	4842(1)	6944(2)	1105(1)	78(1)*
C(01)	6122(4)	7619(6)	2302(3)	48(2)*
C(02)	5236(4)	7848(6)	1851(3)	52(2)*
C(011)	6424(4)	8409(7)	2917(3)	55(2)*
C(021)	4577(4)	8888(7)	2012(3)	56(2)*
C(11)	1387(4)	7494(6)	197(3)	46(2)*
C(12)	2017(4)	8027(7)	787(3)	55(2)*
C(13)	1623(4)	8822(7)	1237(3)	61(2)*
C(14)	618(5)	9098(7)	1094(3)	62(3)*
C(15)	-10(4)	8599(6)	510(3)	60(2)*
C(16)	374(4)	7787(6)	54(3)	50(2)*
C(21)	3098(8)	7136(12)	-587(5)	50(4)*
C(22)	3907(4)	6324(6)	-661(3)	56(2)*
C(23)	4723(5)	6988(7)	-832(3)	68(3)*
C(24)	4691(5)	8403(7)	-924(3)	82(3)*
C(25)	3913(5)	9141(7)	-857(4)	83(3)*
C(26)	3093(5)	8544(7)	-687(4)	69(3)*
C(31)	935(4)	6000(6)	-1220(3)	53(2)*
C(32)	396(5)	4774(7)	-1324(3)	59(2)*
C(33)	-306(5)	4595(8)	-1922(3)	73(3)*
C(34)	-484(5)	5616(9)	-2409(3)	89(3)*
C(35)	59(8)	6822(10)	-2302(4)	110(4)*
C(36)	772(6)	7035(7)	-1708(3)	88(3)*
C(41)	2212(4)	4557(6)	86(3)	46(2)*
C(42)	2071(5)	4416(7)	744(3)	61(3)*
C(43)	2278(5)	3188(7)	1085(3)	73(3)*
C(44)	2626(5)	2101(7)	774(3)	76(3)*
C(45)	2755(5)	2213(7)	111(3)	77(3)*
C(46)	2549(5)	3459(7)	-242(4)	63(3)*

* Equivalent isotropic U defined as one third of the trace of the orthogonalised U_{ij} tensor.

TABLE 6.1 cont.

a) Bond lengths

As(1)-C(11)	1.898(6)	As(1)-C(21)	1.922(11)
As(1)-C(31)	1.921(5)	As(1)-C(41)	1.912(5)
N(01)-C(011)	1.129(8)	N(02)-C(021)	1.137(9)
S(1)-C(01)	1.759(6)	S(1)-S(1a)	2.051(3)
S(2)-C(02)	1.704(5)	C(01)-C(02)	1.359(7)
C(01)-C(011)	1.422(8)	C(02)-C(021)	1.426(9)
C(11)-C(12)	1.392(7)	C(11)-C(16)	1.382(8)
C(12)-C(13)	1.376(9)	C(13)-C(14)	1.379(9)
C(14)-C(15)	1.366(8)	C(15)-C(16)	1.385(9)
C(21)-C(22)	1.389(13)	C(21)-C(26)	1.372(13)
C(22)-C(23)	1.393(9)	C(23)-C(24)	1.376(10)
C(24)-C(25)	1.311(10)	C(25)-C(26)	1.369(11)
C(31)-C(32)	1.385(9)	C(31)-C(36)	1.376(8)
C(32)-C(33)	1.366(8)	C(33)-C(34)	1.364(10)
C(34)-C(35)	1.372(13)	C(35)-C(36)	1.372(10)
C(41)-C(42)	1.370(8)	C(41)-C(46)	1.375(9)
C(42)-C(43)	1.363(9)	C(43)-C(44)	1.356(10)
C(44)-C(45)	1.372(10)	C(45)-C(46)	1.389(9)

b) Bond angles

C(11)-As(1)-C(21)	108.8(4)	C(11)-As(1)-C(31)	108.6(2)
C(21)-As(1)-C(31)	110.0(3)	C(11)-As(1)-C(41)	107.7(2)
C(21)-As(1)-C(41)	112.6(4)	C(31)-As(1)-C(41)	109.0(2)
C(01)-S(1)-S(1a)	104.2(2)	S(1)-C(01)-C(02)	117.1(4)
S(1)-C(01)-C(011)	121.0(4)	C(02)-C(01)-C(011)	121.9(5)
S(2)-C(02)-C(01)	123.8(5)	S(2)-C(02)-C(021)	117.2(4)
C(01)-C(02)-C(021)	118.9(5)	N(01)-C(011)-C(01)	178.4(6)
N(02)-C(021)-C(02)	177.7(5)	As(1)-C(11)-C(12)	119.1(4)
As(1)-C(11)-C(16)	120.5(4)	C(12)-C(11)-C(16)	120.3(5)
C(11)-C(12)-C(13)	119.6(5)	C(12)-C(13)-C(14)	119.6(5)
C(13)-C(14)-C(15)	121.0(6)	C(14)-C(15)-C(16)	120.1(6)
C(11)-C(16)-C(15)	119.3(5)	As(1)-C(21)-C(22)	120.3(8)
As(1)-C(21)-C(26)	118.2(8)	C(22)-C(21)-C(26)	121.4(9)
C(21)-C(22)-C(23)	117.8(7)	C(22)-C(23)-C(24)	119.0(6)
C(23)-C(24)-C(25)	121.9(7)	C(24)-C(25)-C(26)	121.6(7)
C(21)-C(26)-C(25)	118.3(8)	Hs(1)-C(31)-C(32)	120.3(4)
As(1)-C(31)-C(36)	118.6(4)	C(32)-C(31)-C(36)	121.0(5)
C(31)-C(32)-C(33)	119.2(6)	C(32)-C(33)-C(34)	120.5(7)
C(33)-C(34)-C(35)	119.7(6)	C(34)-C(35)-C(36)	121.3(7)
C(31)-C(36)-C(35)	118.2(7)	As(1)-C(41)-C(42)	119.7(4)
As(1)-C(41)-C(46)	119.7(4)	C(42)-C(41)-C(46)	120.6(6)
C(41)-C(42)-C(43)	120.2(6)	C(42)-C(43)-C(44)	120.1(6)
C(43)-C(44)-C(45)	120.7(6)	C(44)-C(45)-C(46)	119.9(6)
C(41)-C(46)-C(45)	118.6(6)		

TABLE 6.2

Atomic coordinates (Å x10⁴), bond lengths (Å) and angles (°) for [11] (standard deviations in parentheses)

a) Atomic coordinates

	x	y	z	U
S(11)	7585(1)	6219(1)	2796(1)	70(1)Å
C(11)	9104(3)	5217(5)	5250(3)	58(2)Å
N(11)	9856(2)	3787(4)	3515(3)	58(1)Å
N(12)	5908(3)	6163(4)	3403(3)	45(1)Å
C(12)	10046(3)	3172(5)	3305(3)	59(2)Å
C(13)	10881(4)	1586(5)	4243(5)	80(2)Å
C(14)	10939(3)	3972(5)	4617(4)	66(2)Å
C(15)	10343(4)	5455(6)	3781(4)	66(3)Å
C(16)	11798(4)	6441(7)	3950(5)	94(3)Å
S(21)	6731(1)	4733(2)	2716(1)	71(1)Å
N(21)	6761(2)	4608(4)	537(3)	59(1)Å
N(22)	5510(2)	3183(4)	1125(3)	63(1)Å
C(21)	6387(3)	4109(4)	1262(3)	54(1)Å
C(22)	6340(3)	4072(5)	-538(4)	63(2)Å
C(23)	6817(4)	4624(7)	-1411(5)	96(3)Å
C(24)	5513(3)	3118(5)	-799(4)	66(2)Å
C(25)	5087(3)	2669(5)	39(4)	63(2)Å
C(26)	4156(4)	1702(6)	-164(5)	85(2)Å

* Equivalent isotropic U defined as one third of the trace of the orthogonalised U_{ij} tensor.

b) Bond lengths

S(11)-C(11)	1.800(4)	S(11)-S(21)	2.023(2)
C(11)-N(11)	1.329(6)	C(11)-N(12)	1.312(6)
N(11)-C(12)	1.346(5)	N(12)-C(15)	1.331(6)
C(12)-C(13)	1.495(6)	C(12)-C(14)	1.364(6)
C(14)-C(15)	1.374(7)	C(15)-C(16)	1.515(7)
S(21)-C(21)	1.778(4)	N(21)-C(21)	1.316(6)
N(21)-C(22)	1.365(5)	N(22)-C(21)	1.317(5)
N(22)-C(25)	1.371(6)	C(22)-C(23)	1.483(8)
C(22)-C(24)	1.367(6)	C(24)-C(25)	1.372(8)
C(25)-C(26)	1.477(7)		

c) Bond angles

C(11)-S(11)-S(21)	105.9(2)	S(11)-C(11)-N(11)	119.6(3)
S(11)-C(11)-N(12)	118.5(3)	N(11)-C(11)-N(12)	129.9(4)
C(11)-N(11)-C(12)	114.8(3)	C(11)-N(12)-C(15)	114.5(4)
N(11)-C(12)-C(13)	116.6(4)	N(11)-C(12)-C(14)	121.4(4)
C(13)-C(12)-C(14)	122.0(4)	C(12)-C(14)-C(15)	118.5(4)
N(12)-C(15)-C(14)	121.7(4)	N(12)-C(15)-C(16)	116.4(4)
C(14)-C(15)-C(16)	121.9(4)	S(11)-S(21)-C(21)	106.1(2)
C(21)-N(21)-C(22)	114.2(3)	C(21)-N(22)-C(25)	116.4(4)
S(21)-C(21)-N(21)	120.1(3)	S(21)-C(21)-N(22)	110.8(3)
N(21)-C(21)-N(22)	129.0(4)	N(21)-C(22)-C(23)	116.0(4)
N(21)-C(22)-C(24)	121.9(5)	C(23)-C(22)-C(24)	122.0(4)
C(22)-C(24)-C(25)	115.4(4)	N(22)-C(25)-C(24)	119.2(4)
N(22)-C(25)-C(26)	117.0(5)	C(24)-C(25)-C(26)	123.7(5)

References

1. A. Davison and R.H. Holm, *Inorg. Synth.*, vol. X, McGraw Hill Book Co., 1967.
2. A.O. Baghlaf, M. Ishaq, O.A.S. Ahmed, and M.A. Al-Julani, *Polyhedron*, vol. 4, p. 853, 1985.
3. N.W. Alcock, *Crystallographic Computing*, pp. p271-278, Copenhagen, Munksgaard.
4. G.M. Sheldrick, *SHELXTL User Manual*, Nicolet Instrument Co., 1981.
5. J. Martin-Gil, F.J. Martin-Gil, A. Pearles, J. Fayos, and M. Martinez Ripoll, *Acta Cryst.*, vol. C39, p. 44, 1983.

CHAPTER 7

EXPERIMENTAL SECTION

7.1. The Collection of X-ray Diffraction Data.

7.1.1 *Crystal Selection*

The first and perhaps most important stage in the collection of X-ray data is crystal selection since a poor crystal would generate a poor data set. For a crystal to be suitable, two main requirements must be met: (a) it must be of proper size (and shape); and (b) it must possess uniform internal structure. The choice of size is a balance of two contradictory factors, though 0.5 x0.5 x 0.5mm is generally a good compromise. This arises from the fact on the instrument used, indeed on most instruments, a plateau of uniform intensity in the primary beam of dimensions 0.5 x 0.5mm can be obtained, so if a crystal were to exceed this size, not all parts of it would be exposed to the same radiation intensity. The second effect which is important in determining crystal size is absorption of X-rays by the crystal, which follows the usual Lambert-Beer law, such that the intensity I of a beam after passing through a thickness t of absorber is given by:

$$I = I_o e^{-\mu t}$$

where I_o is the intensity of the incident beam and μ is the linear absorption coefficient. Since the intensities of the diffracted rays from a given crystal are proportional to its volume *i.e.* the amount of material present, there is an advantage in selecting as large a crystal as possible. Because of absorption however, there is an optimum thickness. For any greater thickness diffracted rays which have passed through the crystal will show a decrease in intensity. This optimum thickness is a function of the linear absorption coefficient, and is given by

$$t_{opt} = \frac{2}{\mu}$$

A second serious problem associated with absorption arises from crystal shape, and manifests itself in the fact that the incident and diffracted rays may have different average path lengths in the crystal for different reflections. As a result, these reflections will suffer to varying extents from absorption, and a systematic error will be introduced into the observed intensities. This is particularly apparent in plate-like and needle-like crystals. One way to overcome this is to shape the crystal, though this has many disadvantages. A second, much better and more accurate, method which is appplicable to all crystals is to measure the crystal precisely, so that the exact shape is known, hence the beam path length can be computed, and the data corrected for

absorption effects.

To meet the second reqirement above, the crystal must be pure and single, *i.e.* not twinned or composed of microscopic subcrystals. As a first test for twinning, the crystal may be viewed under a polarising microscope. If rotated about an axis normal to the polarising material, the crystals should either appear uniformly dark in all positions or be bright and extinguish once every 90°. Crystals which are made up of two or more fragments with different orientations (*i.e.* are twinned) will reveal themselves by displaying both dark and light regions at one time. If the crystals are "small" and single, several are selected and mounted.

7.1.2 *Crystal Mounting and Proceedure*

Crystals are most readily mounted under a binocular wide-field dissecting microscope. A suitable crystal which fulfills the criteria above is placed on a microscope slide and pushed gently with a needle until one end projects beyond the edge of the slide. A small quantity of Araldite is then mixed, and a small amount placed on the end of a thin quartz fibre, (the other end having first been secured in wax in a grub screw). Then the (free) end of the fibre is then aligned with the end of the crystal and the two gently pushed together and allowed to set. Araldite is used since it is fairly rapid setting, but affords enough time to orient the crystal should this be required, and is amorphous, a fact which is most important since the portion of the mounting immediately adjacent to the crystal often protrudes into the X-ray beam. The pin which holds the quartz fibre is then screwed into a goniometer head and the crystal is accurately measured[1] ensuring that the orientation of each face relative to the angular ϕ-scale is known and can be kept constant during the data collection.

The crystal is then transferred to a Syntex $P2_1$ diffractometer (Figure 7.1) which is operated via a series of computer programs described in detail by Sparks,[2] who has has also outlined the procedures for centering and subsequent data collection.[3] The position of the crystal on the goniometer head, G, is adjusted through a series of translational movements until it is visually centred in the path of the X-ray beam, at the intersection of the ϕ and χ axes (C in Figure 7.1). This is accomplished with the aid of an accurately aligned telescope with a cross-wire attached to the ϕ circle.

Once manually centered in the X-ray beam, a rotation photograph can be taken. The χ and 2θ circles are positioned at 0° and the ϕ circle is rotated as the crystal is bathed in the X-ray beam for 10-15 minutes. The diffraction pattern obtained (recorded on polaroid film) has *mm* symmetry. This is illustrated in Figure 7.2. The $2x$ and $2y$ coordinates of these are measured and input to a program which sets χ and 2θ for each reflection corresponding to the equations:-

$$\chi = \tan^{-1}\frac{y}{x}$$

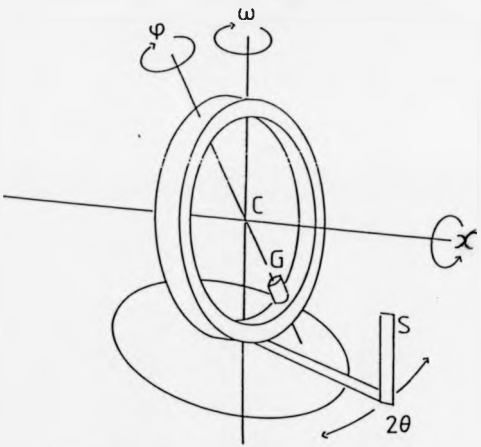

FIGURE 7.1. The four circles of the diffractometer

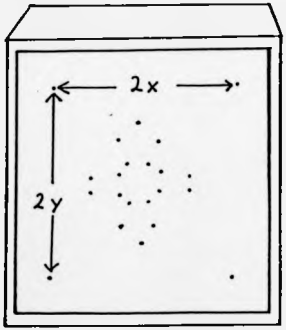

FIGURE 7.2. The pattern of spots on film from a rotation photograph.

$$2\theta=\cos^{-1}\frac{2d}{\sqrt{x^2+y^2+4d^2}}$$

where d is the distance from the crystal to the centre of the Polaroid film. With the 2θ and χ circles set for the calculated position of a reflection, the ϕ circle is rotated until the reflection enters the detector aperture. Once the position of the reflection is found , its position is refined by the determination of positions of half-height peak intensity, proceding through a series of iterations until any variations lie within the tolerances 0.02°, 0.01° and 0.04° for 2θ, ω and χ respectively. In the half-height method, the intensity at the estimated peak centre is first measured. The program then steps in negative and positive directions to determine the position where half that intensity is found. Half the distance between these two point is then taken as a better estimate of the peak centre. The position of the reflection will only be refined if its intensity is greater than a preset minimum value, which is normally set to 1000 c.p.s.

A minimum of 5 reflections should be centered in this way, (a maximum of 15 is permitted by the program). From the refined angular parameters, the auto-indexing program generates 30 possible axial solutions for a unit cell, printing out their lengths(Å) and the cosines of the angles between them. The solutions of shortest length compatible with any apparently orthogonal sets of axes are selected. This is then tested for the correct lattice symmetry.[4] In some cases the true unit cell may not be readily apparent in the solutions due to crystal twinning or the presence of satellite subcrystals. For this reason the maximum number of reflections possible should be used, and through trial and error, one or more of these may be omitted leaving only those from one component for use in the determination of the unit cell.

The selected cell is then examined by taking Polaroid photographs of each axis in turn, thus confirming the true symmetry of the cell. An axis of symmetry for example would be revealed by the axial photograph containing diffraction spots related by a mirror plane. Such an axis would correspond to the unique axis of a monoclinic cell, the c-axis of a hexagonal cell or any axis of a unit cell of higher symmetry. The photographs will also show any fainter interleaving layers of spots at fractions $\left(\frac{1}{n}\right)$ between the major layers indicating the order, n, by which the axis length needs to be multiplied. A disordered array of diffraction spots on the photograph is indicative of twinning and another crystal should be chosen and the procedure repeated.

More precise unit cell parameters with the hkl indices and refined angles of the reflections used in their calculation are derived from a least squares program. This program will also calculate the indices of any omitted reflections (above), and if these are integer values they can be included in the least squares calculation to give unit cell parameters of greater precision.

Unit cell parameters of much greater precision are obtained by running the least squares program based on a set of centered reflections of higher 2θ values. The 15 high angle reflections are selected by running a rapid data collection program through a section of the 2θ range 20°-30°,

depending on how strongly diffracting the crystal is. This preliminary data collection can also be used to determine if the unit cell is primitive or centred and if it is described in the correct Bravais lattice. If the lattice chosen is incorrect the use of a transformation matrix to produce the correct lattice at this point will save a great deal of computer time at a later date. The strongest 15 high-angle reflections from the data set are input in the program and the original centering program used to refine their positions. The final least squares calculations will be based on these reflections and the standard deviations of the unit cell parameters may also be calculated.

The computer now has the information specifying the orientation of the unit cell axes and a data collection program can now be started using this information to set the appropriate azimuthal angle for each reflection. Before this is done, it is useful to plot a profile of one or more of the stronger reflections to determine the shape of the peak. If a doublet is obtained, then it is a likely indication that the crystal is twinned and the crystal should be discarded. From the shape of the peak, it is possible to select the angular range of each reflection that has to be covered in the data collection.

The full data collection is carried out. The procedure is programmed to scan systematically and sequentially each reflection in reciprocal space bounded by the limiting sphere. The θ-2θ scan technique is used in which the ω-circle, which controls the rotation of the reflecting crystallographic plane, moves at half the angular rate of the detector as the profile of the reflection is recorded. A preliminary scan of 2 seconds is used to determine a suitable scan rate for each reflection within the limits of 2.0-29.3 $^{\circ}$ min^{-1} depending on the intensity of this pre-scan. The background counts on either side of the reflection are also measured to give a true estimate of the integrated intensity through their profiles. Throughout the data collection, a number of standard reflections (usually three) are monitored every 200 reflections so that any decay of the crystal induced by exposure to X-rays can be ascertained and the data rescaled if necessary. The data obtained from each reflection is written onto a 9-track magnetic tape which is on-line during the running of the data collection program. The data is then transferred to Data General DG30 computer for structure solution, and the structure solved by use of the heavy-atom method incorporated into a package of package programs in the SHELXTL[5] system, or if no one atom is significantly heavier than the others, direct methods[6] can be used, a truly "black box" technique involving the calculation of a combination of phases for a sub-set of reflection data until a possible solution is reached. The use of this technique was not required in this work.

In some cases the precision of the data collected may be enhanced by carrying out the data collection at low temperatures (typically -120°C to -100°C), and in others the use of low temperatures may stabilise the compound under study enabling the data collection to be carried out. The low temperatures in the region of the crystal are achieved by using the Syntex LT-1 low temperature attachment on the diffractometer. This attachment plays a stream of cooled, dry nitrogen gas

over the crystal, the gas being first cooled by a heat exchanger in a Dewar of liquid nitrogen and then heated to the required temperature.

7.2. Techniques used in handling Neptunium-237

The neptunium 237 used was supplied as the dioxide. This was oxidised to NpO_2^+ by prolonged boiling in concentrated nitric acid[7] (with the addition of fluoride ion to aid dissolution). The neptunium(V) could then be oxidised to neptunium(VI). The oxidant, partially ozonised oxygen, is produced by the passage of oxygen through an electrical discharge. The gas mixture is passed through the Np(V) solution in diluted (4M) nitric acid, (or ethanol) which is heated in a water bath maintained at 60°C. The Np(V) → Np(VI) oxidation, proceeded rapidly and was accompanied by a colour change from dark-green to brown. This oxidation and that of Np(VI) are thermodynamically favoured by the potential of the O_2/O_3 couple,[8] which is greater than those for Np(VI)/Np(V) and Np(VI)/Np(IV) :-

$$NpO_2^{2+} + e^- \rightleftarrows NpO_2^+ \; ; \; E^o = 1.236 \text{ V}$$

$$NpO_2^{2+} + 4H^+ + 2e^- \rightleftarrows Np^{4+} + 2H_2O; \; E^o = 0.938 \text{ V}$$

$$O_3 + 2H^+ + 2e^- \rightleftarrows O_2 + H_2O \; ; \; E^o = 2.07 \text{ V}$$

If the neptunium is impure, it can be precipitated as the hydroxy species $NpO_2(OH)_2$ by the careful addition of dilute aqueous ammonia. This precipitate can then be centrifuged, followed by successive washing with water and acetone to remove the impurities. The hydroxide can then be redissolved in dilute nitric acid.

In some cases the neptunium as supplied contains some plutonium which would account for a significant proportion of its α-activity. For example, the activity of a sample of neptunium which is chemically fairly pure but contains some plutonium (ie 99% ^{237}Np ; 1% ^{238}Pu) would be almost solely due to the ^{238}Pu contamination because of its shorter half life, ^{237}Np: $t_{1/2}$=2.14×10^6 years ; ^{238}Pu : $t_{1/2}$=2.0×10^4 years).

To reduce the hazards introduced by any such contamination, this element must be removed. This is achieved by anion exchange chromatography following the precipitation of the neptunium and plutonium hydroxides by ammonia. The addition of a saturated solution of ammonium iodide in concentrated hydrochloric acid brings about the reduction of Np(VI) → Np(V) and Pu(IV) → Pu(III). This solution is then put onto a column of AG 1-X4 resin, followed by a sufficient volume of 0.2M ammonium iodide in concentrated hydrochloric acid to elute through the blue Pu(III), which is not retained on anion exchangers at any acid concentration. Np(VI), conversely, has a high distribution coefficient in anion exchange resins at this acid concentration as Figure 7.3 shows.[9]

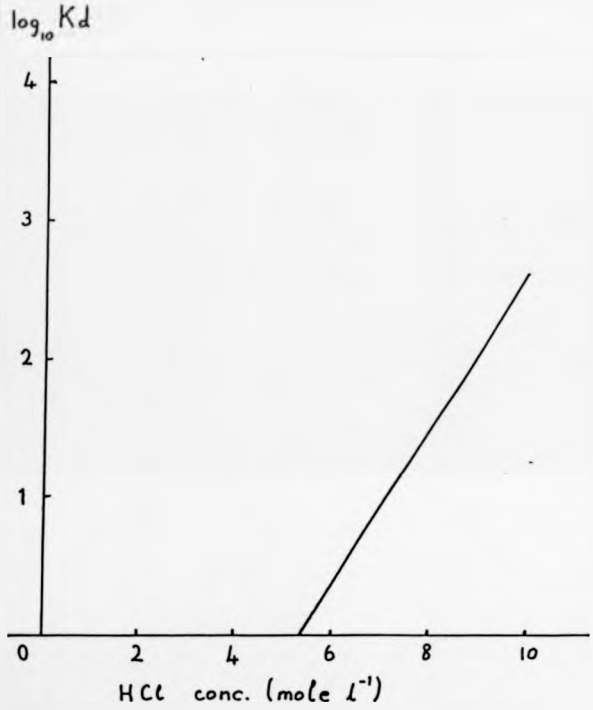

FIGURE 7.3. A plot of the distribution coefficient (Kd) of Np(VI) in hydrochloric acid on the anion exchange resin Amberlite IRA 400 (adapted from ref. 8)

The distribution coefficient,[10] K_d of an ionic species on the resin is given by

$$K_d = \frac{m_s}{m_e} \times \frac{Volume\ of\ solution}{Mass\ of\ resin}$$

where m_s and m_e are the fractions of the ion on the resin and in solution respectively. Thus the Np(VI) remains adsorbed at the top of the column and can be eluted as a separate fraction with 2M hydrochloric acid. Such a separation typically reduces the α-activity due to plutonium-238 to 2-3%, (i.e. 0.02-0.03% ^{238}Pu by mass). This made the material sufficiently safe for it to be handled in a fumehood in solution. Over a relatively short period of time, the NpO_2^{2+} ions in solution reduce to NpO_2^+. Consequently, the Np(VI) solution must be prepared freshly before each complex preparation.

All operations, including the usual crystal mounting techniques, on solid neptunium compounds were carried out in a depressurised glove box to eliminate the risk of contamination. Crystals were mounted on quartz fibres with Araldite and were then encapsulated with Lindemann glass capillaries. The mounted crystals were then transferred to a fume hood and monitored carefully to confirm the absence of any radioactive contamination. The capillaries were coated with a solution of Bostik in acetone to ensure that any residual contamination was safely fixed to the glass and to strengthen the capillary.

The quantities of ^{237}Np handled in each preparation did not exceed 30mg, obtained as a mixture of 5 and 6 oxidation states from an aqueous nitric acid stock solution. A more accurate estimate of the neptunium content may be obtained by radiometric analysis of an active source. The source is prepared by diluting 10 μl of the stock solution to 100 μl with water using micropipettes and transferring a 10 μl aliquot to a prepared tantalum disc. The disc is about 35 mm in diameter and is prepared by careful washing and the application of a thin coating of 'Zapon' lacquer around the edge. The active solution is spread to the perimeter bounded by the lacquer aided by the addition of two drops of a surfactant. The evenly-spread layer of neptunium solution is then evaporated gently under an infra-red lamp and then roasted in a bunsen flame. This produces a coating of tantalum oxide impregnated with about 30 μg of neptunium (i.e. fixed activity).

Using a Simpson counter, the α-counts on the source can be determined by averaging a series of 2 minute readings. Greater precision can be obtained by extending the counting period.

References

1. N.W. Alcock, *Acta Cryst.*, vol. A26, p. 437, 1970.
2. R.A. Sparks, *Abstracts of the American Crystallographic Association*, p. 20, Ottawa, Canada, 1970.
3. R.A. Sparks, in *Crystallographic Computing Techniques*, ed. F.R. Ahmed, pp. 452-467, Munksgaard, Copenhagen, 1976.
4. W. Clegg, *Acta Cryst.*, vol. A36, p. 321, 1980.
5. G.M. Sheldrick, *SHELXTL User Manual*, Nicolet Instrument Co., 1981.
6. M.M. Woolfson, in *Direct Methods in Crystallography*, Oxford University Press, 1961.
7. "The Actinides," in *Comprehensive Inorganic Chemistry, Vol. 5*, ed. A.F. Trottman-Dickenson, Pergamon, New York, 1973.
8. F.A. Cotton and G. Wilkinson, in *Advanced Inorganic Chemistry (4th Edtn.)*, p. 492, Interciences, 1980.
9. C. Keller, in *The Chemistry of the Transuranium Elements*, pp. 310-311,462-463, Verlag Chemie, 1971.
10. E. Lederer and M. Lederer, in *Chromatography: A review of principles and applications; Ch. 11*, Elsevier Publishing Company, 1957.

CHAPTER 8

Conclusions and Areas of Further Study

8.1 Conclusions

In Chapter 1, it was stated that the nature and number of equatorial donor ligands has little or no effect on the length of the U-O(uranyl) bond.[1] Table 8.1, in which these bond lengths are given with the relevant equatorial donor ligand for each compound studied, confirms this. The results of this thesis also show the predicted gradation in the equatorial U-L(ligand) bonds, with U-S being longest, U-N intermediate, and U-O shortest. This is illustrated in Table 8.2. The difference between the mean bond lengths is greater than can be attributed to a simple difference in the covalent radius of sulphur (1.85Å) nitrogen (1.55Å) and oxygen (1.40Å), and must be due to some inherent packing effects.

TABLE 8.1

Effect of equatorial coordination number and donor atom on the mean length of the U-O(UO_2^{2+}) bond (Å)

Compound	E.C.N.	Donor Atoms	U-O bond
[1]	6	6 S	1.755(5)
[2]	6	6 S	1.755(11)
[3]	6	6 S	1.768(13)
[4]	6	6 S	1.798(11)
[5]	5	N, 4 O	1.751(5)
[6]	5	N, 4 O	1.747(6)
[8]	6	2 N, 4 O	1.751(15)
[9]*	6	2 N, 4 O	1.62(4)-1.93(3)

* Severely disordered structure

TABLE 8.2

Range of uranium - ligand bond lengths (Å)

Compound	U - S	U - N	U - O
[1]	2.911(2)-3.021(2)	-	-
[2]	2.900(7)-2.981(6)	-	-
[3]	2.985(6)-2.962(6)	-	-
[4]	2.909(5)-2.960(5)	-	-
[5]	-	2.575(6)	2.294(6)-2.367(5)
[6]	-	2.595(24)	2.281(15)-2.440(14)
[8]	-	2.543(15)	2.486(13)-2.588(15)
[9]*	-	2.63(2)-2.65(3)	2.34(5)-2.50(2)
Mean	2.946(2)	2.571(7)	2.335(10)

Δ	S	O
N	0.375	0.236
O	0.611	

* Severely disorder in this molecule. These results not used to calculate mean and Δ values.

8.2 Areas of further study

It was one of our initial aims to extend this work by replacing the central metal atom in these complexes by neptunium, and plutonium. This was largely prevented by administrative problems. Although some synthetic work was done - the neptunium analogues of [5] and [6] were isolated - no single crystals were obtained. This needs further investigation. Previous work[2,3] has accomplished such a substitution (using neptunium) and confirmed the presence of an actinide contraction of 0.037 and 0.034Å repectively. Such a contraction is greater than the difference in the metallic radii of these two atoms (0.02Å),[4] and between the covalent bond lengths found in CH_3OH (C-O : 1.43(3)Å)[5] and CH_3NH_2 (C-N : 1.48(1)Å).[6] It has not yet been established what effect occurs for plutonium. For the dithiocarbamate complexes described in Chapter 2, it would probably be necessary to use neptunium(V), NpO_2^+, rather than neptunium(VI). This is a result of the mild reducing tendency of dithiocarbamates coupled with the relative instability towards reduction of neptunium(VI) (see Chapter 1).

Finally, the effect of varying the donor atoms in the dithiocarbamate complexes described in Chapter 2 could be studied. A series of complexes with R-COS (monothiocarbamates) and R-CSe_2 (diselenocarbamates) donors using the same R- groups as found in Chapter 2, could be investigated to monitor how steric crowding and equatorial puckering affect the uranyl bond angle. In relation to this area of chemistry, one curious and unexpected observation was made. In an initial attempt to synthesise tris(N,N-diethyldithiocarbamato)dioxouranium(VI) ([4], Chapter 2) the product isolated was a dimer, apparently containing a peroxide bridge. It has not been possible to confirm or disprove this by chemical means. The true character of this compound, and if a peroxide, the formation route will also be of great interest.

References

1. R.G. Denning, "Properties of the UO_2^{n+} (n=1,2) Ions," in *Gmelin Handbuch URAN Suppl. Vol A6*, pp. 31-79, 1983.
2. M.M. Roberts, *"Structural Studies of Uranyl and Neptunyl Complexes"*, *Thesis for Ph.D. Degree*, University of Warwick, 1981.
3. D.J. Flanders, *"Structural Studies of Actinide Compounds"*, *Thesis for Ph.D. Degree*, University of Warwick, 1985.
4. W. Muller, *A.C.S. Symp. Series 131: Lanthanide and Actinide Chemistry and Spectroscopy, Chapter 9.*, 1980.
5. K.J. Tauer and W.N. Lipscomb, *Acta. Cryst.*, vol. 5, p. 660, 1952.
6. M. Atoji and W.M. Lipscomb, *Acta. Cryst.*, vol. 6, p. 770, 1953.

APPENDIX A

Structure Solution and Crystallographic Theory.

A1.1 Diffraction of X-Rays

The fundamental characteristic of crystals is a very high degree of internal order, i.e. the atoms of which the crystal is composed are arranged periodically in three dimensions. The regularity of the external faces of well developed crystals led to the idea that they were built from blocks of a regularly repeating unit - the *unit cell*. The *lattice* formed by these infinitely repeating unit cells is essentially the same as a three dimensional diffraction grating and can be shown to behave as one for radiation that has a wavelength comparable to the interatomic distances within the cell. This was first shown by von Laue in 1912[1] who proved the wavelike character of X-rays. The diffraction pattern obtained can be shown to arise from reinforcing reflections which occur as shown in Figure A.1. when the angle θ is such that the path length ($2x$) between the coincident rays is λ, the X-ray wavelength, or an integral multiple of λ. This condition is satisfied the the Bragg equation:

$$2d\sin\theta = n\lambda \qquad \text{(A.1)}$$

where d is the interplanar spacing defined by the atoms in the planes and n is an integer. The process of diffraction is generally described as arising from a fixed set of planes by adjusting the position of the incident ray until Bragg's law is satisfied. It may also be viewed as involving a fixed incident beam in which case "reflection" occurs from planes set at the correct Bragg angle, θ, with respect to the beam, and generates a reflected ray deviating through 2θ. This is the case experimentally. The family of planes which give rise to reflections in this way are described by the Miller indices (hkl). As shown in Figure A.2, each plane intersects the a,b and c axes of the unit cell at fractions a/h, b/k and c/l respectively.

A1.2 Symmetry and Space Groups

To assign hkl values to a particular reflection, it is obviously necessary to locate and characterise the unit cell. Diffraction of X-rays by a crystal produces a pattern of spots (on a film) which contains information about the relative positions and types of atoms in the unit cell. In general, the unit cell is characterised by six parameters - three axial lengths, and three interaxial angles, and must belong to one of the crystal systems listed in Table A.1. Also listed are the unit cell parameters that characterise each.[2] As shown in Table A.1, it is also possible for certain types of lattice point centering to be present. Combination of the seven crystal systems with the possible centering produces a total of 14 Bravais lattices. Figure A.3 shows the various forms of lattice centering found. The lattice may exist in the following forms P (primitive), R (rhombohedral), I (body centered), C (centered on one face-denoted A,B,or C accordingly) or F

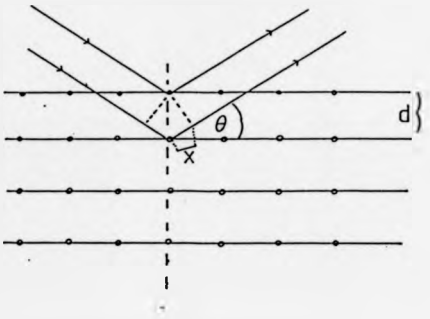

A.1. The diffraction of X-rays from crystal planes.

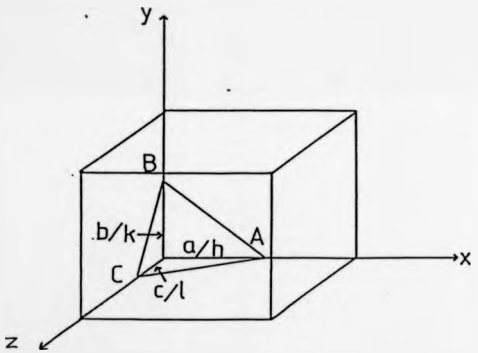

A.2. The derivation of Miller indices (hkl) for any planes of reflection (ABC) within the unit cell.

System	Number of lattices in system	Lattice symbols	Nature of unit-cell axes and angles[1]	Lengths and angles to be specified	Symmetry of lattice[2]
Triclinic	1	P	$a\neq b\neq c$ $\alpha\neq\beta\neq\gamma$	a, b, c α, β, γ	$\bar{1}$
Monoclinic[3]	2	1st setting $\begin{vmatrix} P \\ B \end{vmatrix}$	$a\neq b\neq c$ $\alpha=\beta=90°\neq\gamma$	a, b, c γ	$2/m$
		2nd setting $\begin{vmatrix} P \\ C \end{vmatrix}$	$a\neq b\neq c$ $\alpha=\gamma=90°\neq\beta$	a, b, c β	
Orthorhombic	4	P C[4] I F	$a\neq b\neq c$ $\alpha=\beta=\gamma=90°$	a, b, c	mmm
Tetragonal	2	P[5] I	$a=b\neq c$ $\alpha=\beta=\gamma=90°$	a, c	$4/mmm$
Cubic	3	P I F	$a=b=c$ $\alpha=\beta=\gamma=90°$	a	$m\bar{3}m$
Trigonal	1	R[6]	$a=b=c$ $\alpha=\beta=\gamma$ $<120°, \neq 90°$	a α	$\bar{3}m$
Hexagonal	1	P[7]	$a=b\neq c$ $\alpha=\beta=90°$ $\gamma=120°$	a, c	$6/mmm$

TABLE A.1. The 14 Bravais lattices and conventional unit cells.

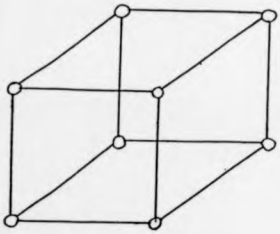

P

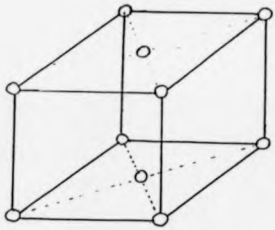

C

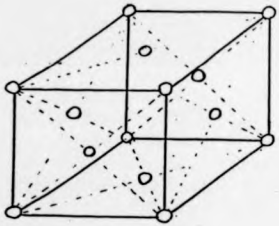

F

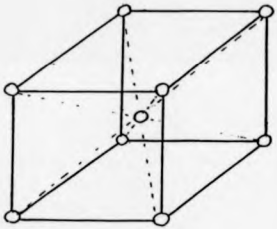

I

A.3. The possible types of lattice centering.

(centered on all faces) forms. The correct choice can be deduced from the general systematic absences in the reflection data:

P	No absence
I	$h+k+l \neq 2n$
C	$h+k \neq 2n$
F	$h+k \neq 2n$, $k+l \neq 2n$
	$h+l \neq 2n$
R	$-h+k+l \neq 2n$

Although the lattice as found may be centered on any face, it is usually preferable to reorient the axes to the conventional setting: *e.g.* C- in monoclinic, *C*2/*c*; or A- in orthorhombic, *Ama*2. However a B-centered monoclinic cell should be transformed to a primitive P cell. form. One exception is in the orthorhombic system where *Ama*2 (No.40) occurs as a standard setting.

The assignment of the correct Bravais lattice is the first stage in the determination of the space group to which the crystal belongs. Each space group contains a unique set of symmetry elements that describe the arrangement of atoms within the unit cell. These symmetry operations may be divided into two types, the first involving point symmetry, *i.e.* rotation axes, rotation-inversion axes, and mirror planes; and the second which involves space symmetry or translation, namely screw axes and glide planes. There are 230 space groups,[3] many of which can be uniquely determined from the systematic absences. Operations of the first type of symmetry elements do not create systematic absences, whereas the presence of operations of the second type can be deduced from the systematic absences.

A *screw axis* (n/m) describes the distributions of a set of atoms (the asymmetric unit) rotated relative to one another through (360/n)° about an axis and a fractional shift (m/n) along the unit cell axis to which the screw axis is parallel. Thus 2_1 designates a 2-fold screw axis with a translation between successive points of 1/2 (m/n) of a unit translation. If for example such an axis were parallel to the *b*-axis of the unit cell, the systematic absence for the 0*k*0 reflections would be $0k0: k \neq 2n$. It is characteristic of an n-fold screw axis that the position of the n^{th} point laid down differs from the initial point only by an integral number of unit translations; *i.e.* the positions of these points within their respective unit cells are identical.

The combination of a mirror plane and a translation parallel to the reflecting plane produces a *glide plane*. The translation in such a plane is along an edge or face diagonal of the unit cell, and in most cases, of magnitude half the axial or diagonal length. A *c*-glide for example has a translation 1/2 along *c* and reflection normal to the *b* direction. This glide plane is recognised by the systematic absence $h0l: h \neq 2n$

Thus the space group $P2_1/c$, for example, would contain a primitive cell (P), with a 2_1 screw axis running along the *b* direction perpendicular to the *c*-glide plane. The systematic absences, and their related symmetry operations are summarised in Table A.2 (ref:2)

A1.3. Data Reduction

Once all the reflection data are stored on disk (Chapter 7), the integrated intensities for each reflection (I_{hkl}) are converted to their corresponding structure factors (F_{hkl}), since it is these quantities which are used in the calculation of electron density maps, from which the atomic positions are determined. This is accomplished using the data reduction program in SHELXTL[4] The two parameters are related by the equation:

$$|F_{hkl}| = \sqrt{\frac{KI_{hkl}}{Lp}} \qquad \text{(A.2)}$$

where K is a scale factor which depends upon crystal size, beam intensity, and can be regarded as being constant for any given set of measurements, and L and p are the Lorentz and polarisation factors. The Lorentz factor , L, depends upon the measurement technique used, and for diffractometer data is given by:

$$L = \frac{1}{\sin 2\theta} \qquad \text{(A.3)}$$

It is important because the time required for a reciprocal lattice point to pass through the *sphere of reflection* is not constant, but varies with its position in reciprocal space and direction of approach. The polarisation factor, P, arises because of the nature of the X-ray beam and the manner in which its reflection efficiency varies with the reflection angle, and is given by:

$$p = \frac{1+\cos^2 2\theta}{2} \qquad \text{(A.4)}$$

The derivation of these equations can be found in ref (5).

One of the major functions of the output from the data reduction program is to serve as input for the structure factor program which calculates structure factors on the basis of some assumed arrangement of atoms, and compares these with those actually observed[3]. The data reduction program therefore generates a list of h,k,l,F and $\sigma(F)$ values after correction for any loss in intensity due to crystal decomposition. Variation in the intensities obtained for a set of check reflections (monitored every 200 reflections) is used to calculate this correction. Reflections with faulty backgrounds are eliminated from the data. These are identified by: with faulty backgrounds are identified by

$$B_l - B_r > 10\sqrt{B_l + B_r} + 0.002(P - B_l - B_r) \qquad \text{(A.5)}$$

where B_l and B_r are the left and right backgrounds on each side of P the peak. Reflections with intensities $I/\sigma(I)<3.0$ are also eliminated from the output file. The exclusion of these low intensity

Type of reflection	Condition for possible reflection[1]	Glide plane ( ) or { } or screw axis [ ] or ⟨ ⟩			Systems of axes involved
		Orientation	Component	Symbol[1]	
*hk*0	$h=2n$	(001)	$a/2$	a	Monoclinic (1st setting), tetragonal; Orthorhombic
	$k=2n$		$b/2$	b	
	$h+k=2n$		$a/2+b/2$	n	
	$h+k=4n$ ($h,k=2n$)		$a/4\pm b/4$	d	
0*kl*	$k=2n$	{100}	$b/2$	b	Orthorhombic, tetragonal, cubic
	$l=2n$		$c/2$	c	
	$k+l=2n$		$b/2+c/2$	n	
	$k+l=4n$ ($k,l=2n$)		$b/4\pm c/4$	d	
*h*0*l*	$l=2n$	(010)	$c/2$	c	Monoclinic (2nd setting); Orthorhombic
	$h=2n$		$a/2$	a	
	$l+h=2n$		$c/2+a/2$	n	
	$l+h=4n$ ($l,h=2n$)		$c/4\pm a/4$	d	
*hh*2$\bar{h}$*l*	$l=2n$	{1$\bar{1}$00}	$c/2$	c	Hexagonal
h$\bar{h}$0*l*	$l=2n$	{11$\bar{2}$0}	$c/2$	c	
hhl	$(2h+)l=2n$	{1$\bar{1}$0}	$(a/2+b/2+)c/2$	(n) c	Rhombohedral[2]; Tetragonal, cubic[2]
	$2h+l=4n$		$a/4+b/4+c/4$	d	
*h*00	$h=2n$	⟨100⟩	$a/2$	2_1	Orthorhombic, tetragonal; Cubic
				4_2	
	$h=4n$		$a/4$	$4_1, 4_3$	
0*k*0	$k=2n$	[010]	$b/2$	2_1	Monoclinic (2nd setting), orthorhombi
00*l*	$l=2n$	[001]	$c/2$	2_1	Monoclinic (1st setting), orthorhombi
				4_2	Tetragonal
	$l=4n$		$c/4$	$4_1, 4_3$	
000*l*	$l=2n$	*z*-axis	$c/2$	6_3	Hexagonal
	$l=3n$		$c/3$	$3_1, 3_2, 6_2, 6_4$	
	$l=6n$		$c/6$	$6_1, 6_5$	

TABLE A.2. Determination of translation elements of symmetry from special reflections.

reflections will usually result in a lower R-factor for the refined structure and will save significantly on computation times.

After this initial processing, an absorption correction should always be applied unless the material under consideration has a very low linear absorption coefficient. This absorption correction is now usually performed using the Gaussian integration method in SHELXTL[4]. The incident radiation of intensity I_o is therefore attenuated by an amount which can be calculated from the equation:

$$I = I_o e^{-\mu T} \qquad \text{(A.6)}$$

where I is the measured intensity and μ is the linear absorption coefficient given by the equation:

$$\mu = \sum(\sigma_i n_i) \times Z / U \qquad \text{(A.7)}$$

where σ_i is the linear absorption coefficient of atom i for the X-ray wavelength being used and n_i is the number of such atoms in the molecule.

A1.4 The Structure Factor and Patterson Function

The structure factor F_{hkl} is the resultant of j waves scattered in the direction of the reflection hkl by the j atoms in the unit cell. Each of these waves will have an associated amplitude which is proportional to the scattering factor of the atom, f_j, and a phase α with respect to the wave scattered by the hypothetical origin. In order to calculate the structure factor, the phase problem needs to be solved. To get an estimate of the phase, it is necessary to calculate a set of structure factors, F_c, based on an approximate model of the actual structure. The phase α associated with each of the observed structure factor moduli, is given by:

$$F_o = |F_o| \cos\alpha + i |F_o| \sin\alpha \qquad \text{(A.8)}$$

and the best estimate of the phases can be obtained by calculating a set of structure factors, F_c, based on an approximate model of the actual structure to be determined and a calculation of an approximation of the true electron density from the observed structure factor amplitudes, $|F_o|$, with the calculated phases. The structure factor is the Fourier transform of the scattering density (electrons in the molecule) sampled at the reciprocal lattice point hkl.

The expression describing the distribution of electron density, ρ_{xyz}, in the unit cell is:

$$\rho_{xyz} = \frac{1}{V}\sum_{h=-\infty}^{h=\infty}\sum_{k=-\infty}^{k=\infty}\sum_{l=-\infty}^{l=\infty} F_{hkl}\Big[\cos 2\pi(hx+ky+lz) - i\sin 2\pi(hx+ky+lz)\Big] \qquad (A.9)$$

where F_{hkl} contains the phase information and can represent either F_o or F_c and V is the unit cell volume. The cosine and sine terms result from the consideration of the phase differences between the hypothetical origin and the point x,y,z.

The majority of the compounds contained in this thesis contain one (or more) heavy atoms - uranium - in the asymmetric unit. As such, they constitute a special case since the heavy atom will dominate the scattering of X-rays, and the majority of the phase differences are due to this heavy atom. The Patterson function is a Fourier synthesis using only the indices and the $|F|^2$ -value of each diffracted beam. Since the coefficients are squares, they are phaseless. The Patterson function $P(UVW)$ is given by

$$P_{(UVW)} = \frac{1}{V}\sum_{h=-\infty}^{h=\infty}\sum_{k=-\infty}^{k=\infty}\sum_{l=-\infty}^{l=\infty} |F_{hkl}|^2\cos 2\pi(hU+kV+lW) \qquad (A.10)$$

The peaks in the map correspond to the vectors between any two pairs of atoms in the structure at, say, x_1,y_1,z_1 and x_2,y_2,z_2 such that $U=x_2-x_1$, $V=y_2-y_1$ and $W=z_2-z_1$. The weight of the Patterson peak depends on the number of electrons in the atoms between which the vector occurs. If there are only a few heavy atoms present, the highest peaks will correspond to the vectors between the heavy atoms. The positions of the heavy atom can then be found and used to calculate the F_c values.

A1.5. Structure Solution and Refinement

Once the heavy atom has been located, the assumption is then made that it dominates the diffraction pattern, and the phase angle for each diffracted beam for the whole structure is approximated by that for the heavy atom.[6] To locate the lighter atoms, it is necessary to calculate a difference Fourier synthesis based on ΔF values for each reflection, where

$$\Delta F = |F_o| - |F_c| \qquad (A.11)$$

This will produce a map with peaks corresponding to the remaining atom positions and these can be used to obtain a more precise estimation of the phases associated with the F_c values which will approach the true values associated with F_o.

Further refinement in the atomic positions can be made using least squares methods to minimise a function D given by:

$$D = \sum_{r} W_r\Big(|F_o| - |F_c|\Big)^2 \qquad (A.12)$$

where W_r is the weighting function applied to reflection r. The reliability of a structure during the process of refinement is indicated by the closeness in agreement between the values of F_o and F_c

for each reflection. This is monitored by the residual factor R, where

$$R = \frac{\Sigma\left|\left|F_o\right|-\left|F_c\right|\right|}{\Sigma\left|F_o\right|} \qquad \text{(A.13)}$$

and the convergence of F_o and F_c produces a value of about 0.05 for most small structures.

Because atoms are never at rest, but always have an associated *thermal motion* each atom in the structure has an associated temperature factor so that the atomic scattering factor for a hypothetical atom at rest, f, is replaced by

$$f\, e^{-B_{iso}(\sin\theta/\lambda)^2} \qquad \text{(A.14)}$$

where B_{iso} represents the isotropic temperature factor. The variation of f with $\sin\theta/\lambda$ is shown in Figure A.4 for a variety of values of B which is usually between 2.0 and 5.0Å^2. B_{iso} is related to the mean-square amplitude ($\overline{U^2}$) of atomic vibration by

$$B = 8\pi^2\overline{U^2} \qquad \text{(A.15)}$$

An increase in temperature will be accompanied by a more diffuse electron cloud. This is shown by a rise in B, and as Figure A.4 indicates, the X-ray diffraction intensity falls off with increasing $\sin\theta/\lambda$. As a result of this decrease in intensity, the data collected in the higher angle regions will contribute to a greater resolution of the final structure.

A more precise description of the thermal motion of the atoms is given by the use of *anisotropic temperature factors*. These assume that thermal motion is ellipsoidal, producing six additional parameters per atom on which to base the final refinement. They are incorporated into the function above used to modify f (eq. 13):

$$\exp(-2\pi^2(U_{11}h^2a^{*2}+U_{22}k^2b^{*2}+U_{33}l^2c^{*2}+2U_{12}hka^*b^*+2U_{13}hla^*c^*+2U_{23}klb^*c^*)) \qquad \text{(A.16)}$$

where the U^n terms describe the axis lengths of the thermal ellipsoid projected along the crystal axis and the U^{ij} terms relate to the orientation of the crystallographic axes with respect to the ellipsoid principle axes.

There are a number of other errors in the data which require correction during the final refinement. The first of these are the systematic errors in the reflections collected with high F_o and low $\sin\theta$ values. An analysis of the average $(\Delta F)^2$ values for these reflections at regular intervals of F_o and $\sin\theta$ shows a marked increase toward low $\sin\theta$ and toward high F_o ends. A weighting scheme is therefore introduced to give a more even spread of $(\Delta F)^2$ values. Occasionally, depending upon the crystal mosaicity,[3,7] an extinction correction is also required. Figure A.5 shows that X-radiation reflected from an incident beam that has passed through a series of planes will show a gradual loss in intensity with the depth of the reflection in the crystal. There will also be a loss of intensity due to the coincidence of a doubly reflected beam (shown by a broken line)

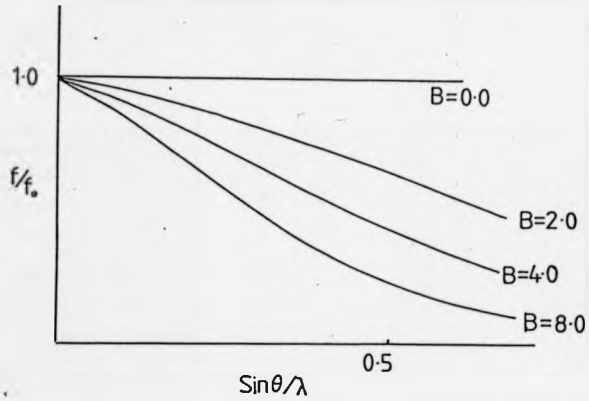

A.4. The variation of the atomic scattering factor (f) with $\sin\theta/\lambda$.

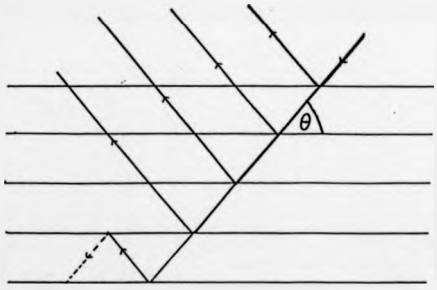

A.5. The effect of extinction.

with the incident beam, the two beams being 180° out of phase.

A correction for extinction[8] can be applied in the last stages of the least squares refinement by converting F_c to the extinction corrected F_c^* where:

$$F_c^* = kF_c\left[1 + g\beta(2\theta)F_c^2\right]^{-\frac{1}{4}} \qquad \text{(A.17)}$$

k is a scale factor, g is the extinction parameter, and $\beta(2\theta)$ depends on the physical constants of the crystal and the geometry of the reflecting position. Thus the function minimised by the least squares refinement is:

$$D = \sum_{hkl} w_r\left(|F_o| - |F_c^*|\right)^2 \qquad \text{(A.18)}$$

PAGINATION
ERROR

References

1. M. von Laue, *Sitzber. Math. Physick. kl. Bayer Akad Wiss Muenchen*, p. 303, 1912.
2. D.J. Flanders, *Ph.D. Thesis, University of Warwick*, 1985.
3. *International Tables for X-ray Crystallography*, D. Reidel Publishing Company, Dordrecht : Holland / Boston : U.S.A., 1983.
4. G.M. Sheldrick, *SHELXTL User Manual*, Nicolet Instrument Co., 1981.
5. G.H. Stout and L.H. Jensen, in *X-Ray Structure Determination*, MacMillan, London, 1968.
6. J.P. Glusker and K.N. Trueblood, *Crystal Structure Analysis*, Oxford University Press, 1985. Second Edition
7. J.D. Dunitz, *X-ray Analysis and the Structure of Organic Molecules*, Cornell University, London, 1979.
8. A.C. Larson, *Acta. Cryst.*, vol. 23, p. 664, 1967.

APPENDIX B

Final Structure Factor Tables

The structure factor tables for compounds [5], [6], and [8] have already been deposited with the editor of *Acta Crystallographica* as these structures have been published or accepted for publication in that journal. The tables for the remaining structures will also be deposited when the structures are published and so have been omitted from this thesis. These tables are available on request.